Brookhaven National Laboratory

Report # 224785

# Field Validation of Innovative Air-Source Heat Pumps for Cold-Climate Heating Applications

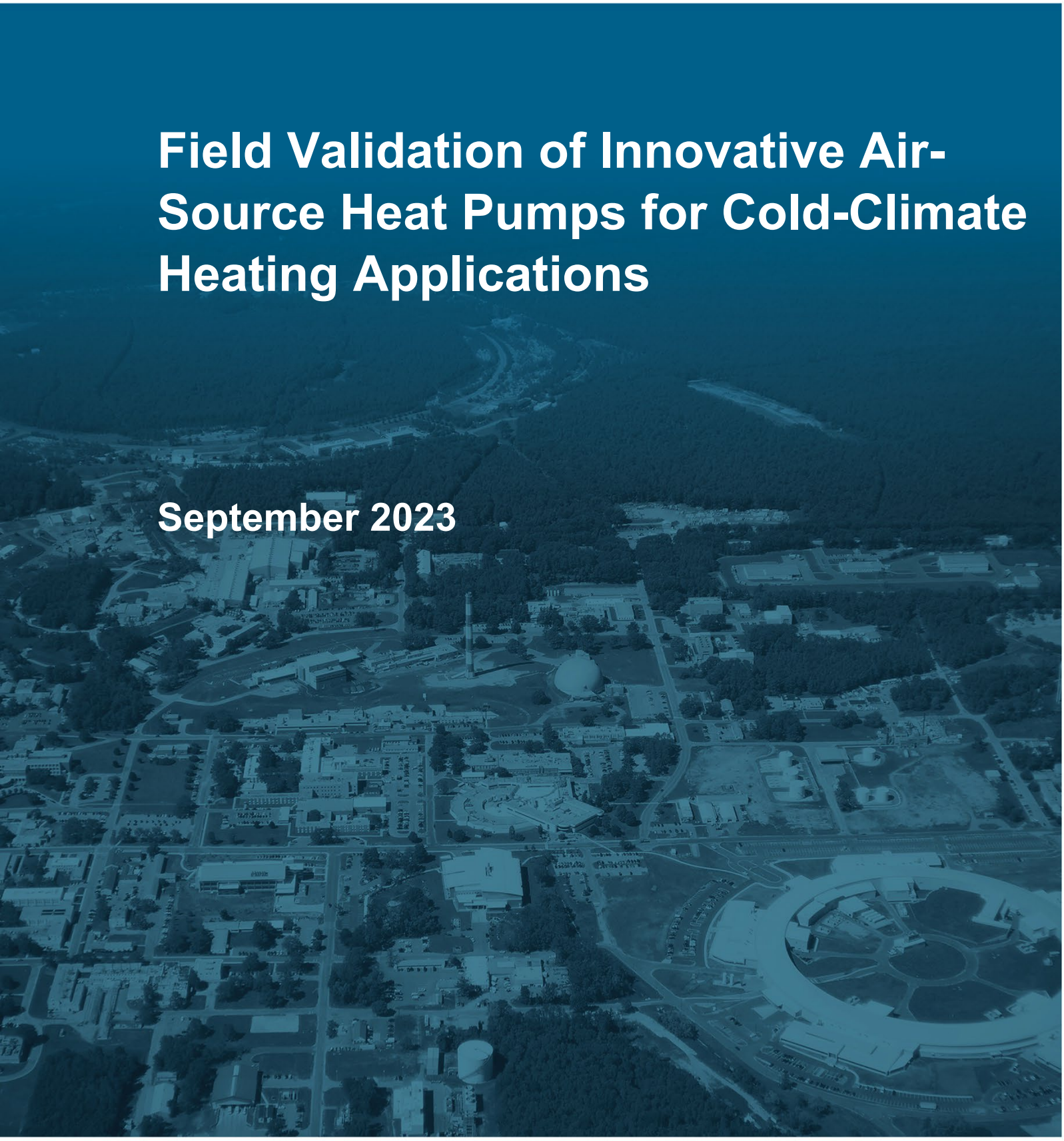

September 2023

managed by Brookhaven Science Associates
on behalf of the U.S. Department of Energy

U.S. DEPARTMENT OF ENERGY

Brookhaven National Laboratory

U.S. DEPARTMENT OF ENERGY

Prepared for:
Dale Hoffmeyer
U.S. Department of Energy's
Building Technologies Office

BNL Contract No. DE-SC0012704

Prepared by:
R. Trojanowski, J. Loprete, J. Lindberg, T. Butcher
**Brookhaven National Laboratory**
Upton, NY 11973

A. Walburger and N. Genzel
**Frontier Energy**
Cazenovia, NY 13035

Corresponding Author
R. Trojanowski
rtrojanowski@bnl.gov
**Interdisciplinary Sciences Dept.**
Building 815
P.O. Box 5000
Upton, NY 11973-5000

www.bnl.gov

# Disclaimer



# Copyright Notices

## Acknowledgments

This work was supported by the US Department of Energy (DOE), Office of Energy Efficiency and Renewable Energy (EERE), Building Technologies Office (BTO), under Contract No. DE-SC0012704 with Brookhaven National Laboratory. The authors would like to acknowledge the support and thank Dale Hoffmeyer and Catherine Rivest at DOE. The authors also appreciate the feedback throughout the project from Tony Bouza (DOE), Marc Lafrance (DOE), Jeff Munk (ORNL), Alexander Rees (DOE), Ed Vineyard (DOE Consultant), and Detlef Westphalen (Guidehouse). The authors would like to thank Lindsay Mott for her assistance with the Institutional Review Board process and especially to the team's subcontractors (Frontier Energy, Energy Futures Group, The Levy Partnership, Center for Energy and Environment, and Taitem Engineering) and their tireless efforts to recruit sites and install the sensors and loggers during COVID-19. Lastly, the authors would like to acknowledge the strong collaboration between Hugh Henderson from Frontier Energy and Jon Winkler and Sugi Ramaraj from NREL over the project's duration.

## Nomenclature

| | |
|---|---|
| ACFM | Actual Cubic Feet per Minute |
| AHU | Air Handling Unit |
| ASHRAE | American Society of Heating, Refrigerating and Air-Conditioning Engineers |
| AWHP | Air to Water Heat Pump |
| BNL | Brookhaven National Laboratory |
| BTO | Building Technologies Office |
| ccASHP | Cold Climate Air Source Heat Pump |
| CDD | Cooling Degree Days |
| CEE | Center of Energy and Environment |
| COP | Coefficient of Performance |
| CDO | Climate Data Online |
| DOE | Department of Energy |
| EERE | Energy Efficiency and Renewable Energy |
| EFG | Energy Futures Group |
| HDD | Heating Degree Days |
| HSPF | Heating Seasonal Performance Factor |
| HVAC | Heating Ventilation Air Conditioning |
| IRB | Internal Review Board |
| NEEP | Northeast Energy Efficiency Partnerships |
| NOAA | National Oceanic and Atmospheric Administration |
| NREL | National Renewable Energy Laboratory |
| NYSERDA | New York State Energy and Research Development Authority |
| ORNL | Oak Ridge National Laboratory |
| RH | Relative Humidity |
| TLP | The Levy Partnership |
| US | United States |
| $\dot{V}_{std}$ | Volume flow rate corrected to standard conditions |
| $A_I$ | Indoor current |
| $C_x$ | Constant polynomial coefficient |
| $T_{supply,avg}$ | Average supply temperature |
| $T_{return}$ | Return temperature |
| $\rho$ | Density of working fluid/gas |
| $c_p$ | Specific heat at constant pressure of working fluid/gas |
| $\dot{Q}_{heating}$ | Heat delivery rate to working fluid/gas |
| $\dot{Q}_{sensible,cooling}$ | Heat removal rate from working fluid/gas responsible for temperature changes |
| $h_{fg}$ | Latent heat of vaporization for water |
| $R_w$ | Estimated gas constant for water |
| $P_{sat,x}$ | Saturation pressure at location x |
| $\varphi$ | Fractional relative humidity |
| $P_{atm}$ | Atmospheric pressure |
| $\omega_x$ | Specific humidity ratio at location x |

| | |
|---|---|
| $\dot{Q}_{latent,cooling}$ | Heat removal rate from working fluid/gas responsible for condensation of water vapor |
| $SHR$ | Sensible Heat Ratio |
| $\dot{Q}_{cooling}$ | Total heat removal rate from working fluid/gas |
| $A_x$ | Current at row x |
| $CWF_x$ | Current-weighting factor for row x using current at row x in the system |
| $P_{Total}$ | Raw power reported from sensor |
| $P_{Weighted,x}$ | Weighted power for data in row x |
| $\sigma$ | Standard deviation |
| $N$ | Number of data points collected |
| $\Delta_{stat}$ | Statistical uncertainty |
| $x_i$ | Raw data of specific column in row i |
| $y_i$ | Filtered data of specific column in row i |
| $\bar{x}$ | Average value of data of specific column in observation interval |
| $m$ | Slope of linear regression fit of data of specific column in observation interval |
| $Var(X)$ | Variance of data of specific column in observation interval |

## Executive Summary

Air-source heat pumps (ASHPs) have historically found application in milder climates in the United States (US). Their application in cold climates has been hindered by reduced performance as outdoor temperatures fall below freezing and the need for backup or auxiliary electric resistance heaters to meet peak heating loads. Recent advances in cold-climate air-source heat pumps (ccASHPs) with features such as variable-speed compressors, multistage systems, and highly optimized thermal design have improved performance by increasing the coefficient of performance (COP), low-ambient-temperature capacity, and heating seasonal performance factor (HSPF) dramatically. Despite their benefits, ccASHPs are still not widely prescribed for cold climate conditions. This is due in part to a lack of verified, demonstrated performance and analysis in cold climates. Ultimately, high-efficiency ccASHPs play a key role in emerging energy/grid renovation efforts in addition to their potential energy savings and avoided carbon emissions, but their actual performance in various cold climate field settings must be better understood.

The *primary objective* of this project was to measure the in-field performance of variable-capacity air-source heat pumps in cold climates with the *goal* of enabling the development of field-based performance maps. Specifically, the study looked at how the heat pumps operated in the field, the frequency of cycling, the frequency of defrost events, and the time spent in each mode of operation. The results are intended to be used by DOE to inform research and development of energy-efficient equipment and to develop guidelines for optimizing primary energy savings when using air-source heat pumps in heating-dominated regions.

This project was executed as a collaboration between Brookhaven National Laboratory (BNL) and the National Renewable Energy Laboratory (NREL) and sponsored by the US Department of Energy (DOE), Office of Energy Efficiency and Renewable Energy (EERE), Buildings Technology Office (BTO). Each of these National Laboratories executed field studies independently but coordinated a uniform measurement and analysis protocol. The studies conducted by NREL are described in a separate report, and this report only covers the research done by BNL and their subcontractors.

To meet the objective and goal of the project, a total of 21 occupied homes were selected for this study, with 18 located in the Northeast and three located in Minnesota. In total, nine (9) 1:1 ductless units (one outdoor compressor unit and one indoor head or air handler), six (6) centrally ducted units, one (1) 1:2 ductless unit, one (1) mixed unit, and four (4) air-to-water systems were studied. The mixed unit involved both a single indoor non-ducted head and a small ducted indoor system. The selected sites included single-family homes, townhouses, and duplexes in regions with greater than 6,000 annual heating degree days (HDD). BNL partnered with Frontier Energy, Energy Futures Group, The Levy Partnership, Taitem Engineering, and Minnesota Center for Energy and Environment to engage and secure the sites as well as help manage the data collection. Data was collected from each site for a year's time or more, with an emphasis on collecting heating data. All site studies concluded in September 2022.

A uniform methodology for data collection and data management was developed for evaluating performance factors such as COP, capacity, and auxiliary power use. Additionally, measurements were taken to determine the energy output from the heat pump and system conditions. All data was

collected at a 5-second interval over the entire duration of the study. An algorithm was developed to determine between operating phases such as heating and cooling steady-state or transient, defrost, off and fan only, provide statistical data, and quantify the heat pump performance factors. The developed algorithm also provided a check for data quality control and assurance.

For all units, the COP was evaluated based simply on the total electric power consumption and the delivered thermal output in either heating or cooling mode. When comparing the steady-state heating COP for all sites, there was a general increase as the outdoor temperature increased, as indicated in ES-1 to ES-3 below, with the exception of a few sites. Some sites did not collect steady-state heating data in particular temperature bins and are therefore not shown. Typically, the ducted sites (CEE-002, CEE-003, CEE-001, EFG-005, TLP-003 and EFG-003) had higher COPs than the ductless 1:1, ductless 1:2, and air-to-water sites. Ductless 1:1 sites had steady-state COPs that ranged from 1.32 to 3.84, as shown in ES-1. Ducted sites had steady-state COPs that ranged from 1.34 to 4.17, as shown in ES-2. ES-3 shows the average steady-state COP values of 1.42 to 2.98 for the air-to-water sites studied, which were all the same unit. The lowest steady-state COP observed was the ductless 1:2 site, EFG-008. Overall, the measured steady-state COP was close to the nominal range, although in some cases notably lower, as described later in the report.

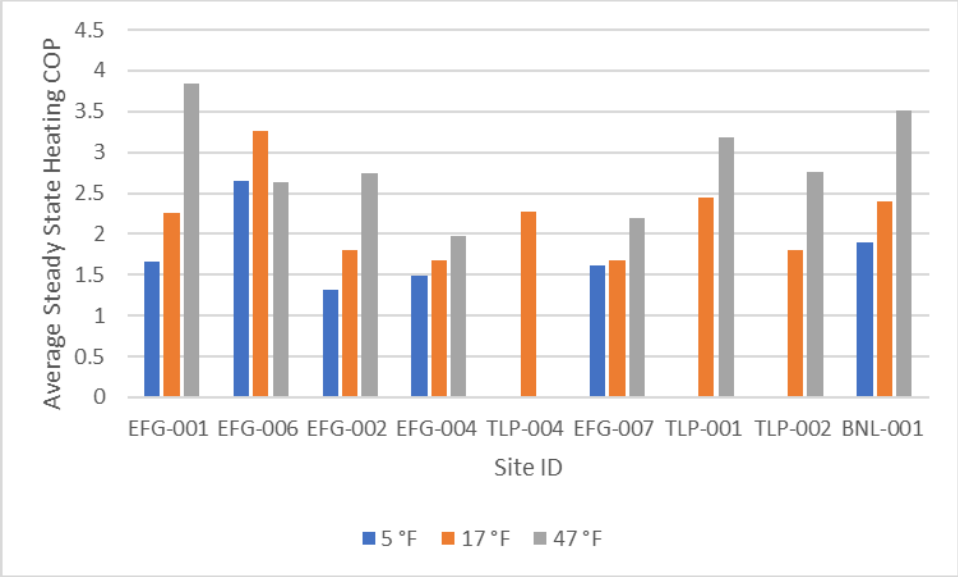


ES-1: Average steady-state heating COP for ductless 1:1 sites

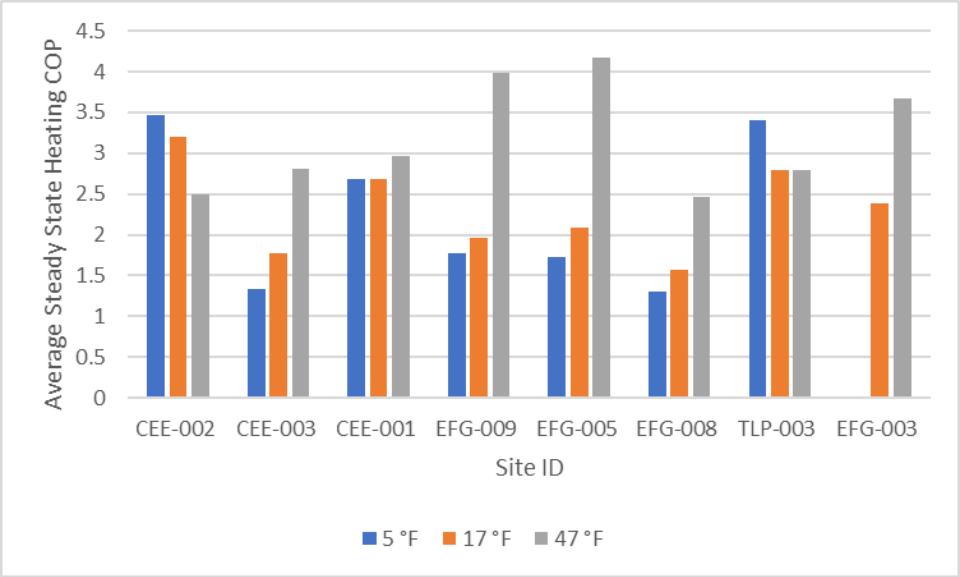


ES-2: Average steady-state heating COP for ducted, ductless 1:2, and mixed sites


ES-3: Average steady-state heating COP for air-to-water sites

ES-4 illustrates the results for the 24-hour average COP in comparison to the steady-state COP for all the ductless 1:1 sites. In this figure, the measured steady-state COP is shown on the horizontal axis, and the measured 24-hour average COP (inclusive of steady-state, transient, and defrost periods) is on the vertical axis. In each of these charts, the solid black line represents perfect agreement. When the data points plotted fall below the black line, this represents the degradation of COP due to cycling and defrost. These results show significant reductions in performance based on the 24-hour averages, particularly at the higher COP levels. These are expected to correlate with higher outdoor air temperatures, and it can be assumed that the units simply cycle more frequently under these warmer conditions.

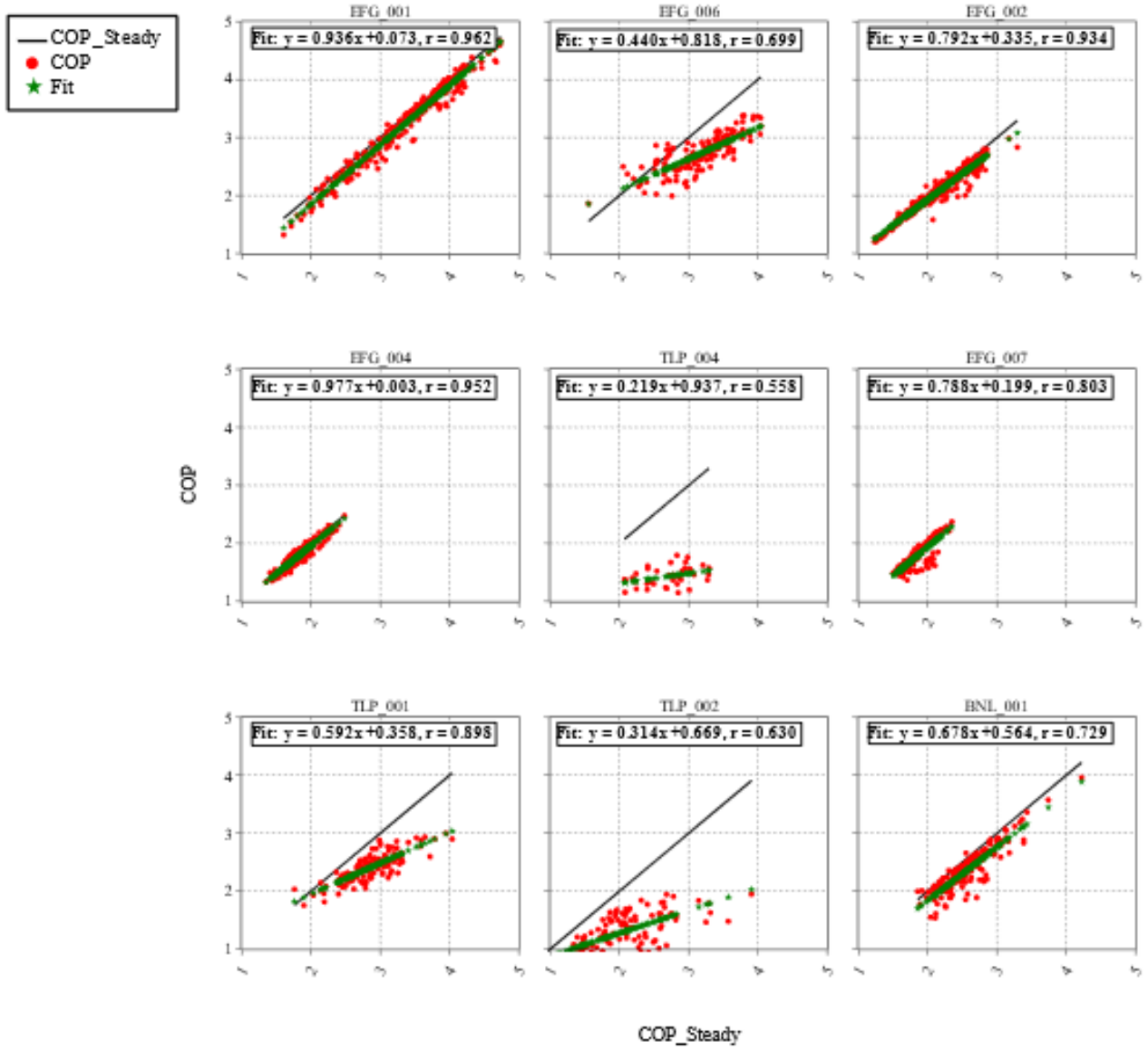


ES-4: Comparison of steady-state COP and 24-hour average COP. Ductless 1:1 units

The overall compressor-based seasonal COP (total heat delivered/total power consumed by the heat pump) was computed for the 2021-2022 heating season for 19 out of 21 sites and is shown in ES-5. Our findings indicate that most units had a seasonal COP between 1.2 and 2.5. Ducted sites with supplemental heating will encounter a lower combined-system seasonal COP when auxiliary heating is accounted for, as electric backup heaters have a COP of 1. Of the types of heat pump installations observed during the study, at least one configuration for each type achieved a seasonal COP of 2 or higher. Site CEE-003 was decommissioned before the 2021-2022 heating season, and instead the 2020-2021 heating season is used in its place. Site TLP-003 had several idle power issues over the course of the study, and as a result a seasonal COP was not computed—however,

this site is discussed later in the report as power issues were teased out during the steady-state analysis.

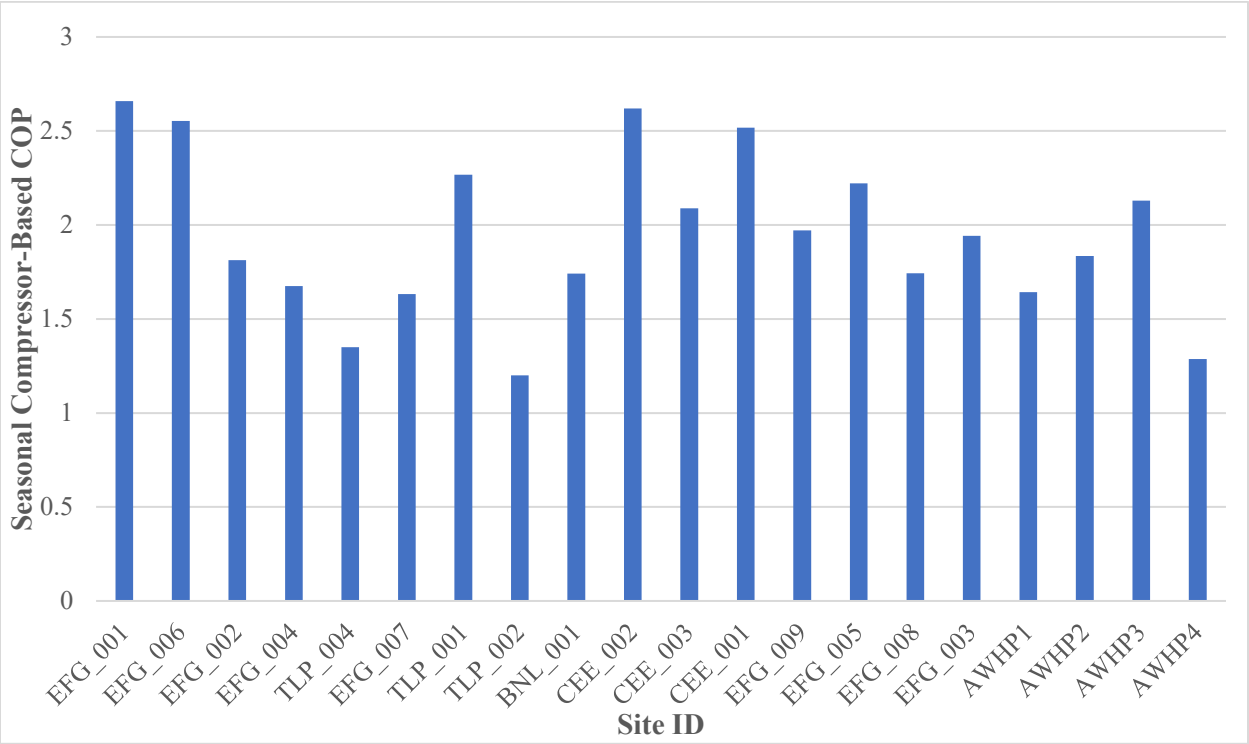


ES-5: Seasonal compressor-based COP during the heating season

A majority of the sites spent much of their time over the study's duration in an off mode. This may be attributed to the ductless systems only heating a portion of the home or unique site-specific reasons such as well insulated energy efficient homes or homeowners preferring the lower cost of their natural gas-fired backup system. Some sites utilized auxiliary heat sources that met 100% of the heating demand or provided supplemental heat on the coldest days. For most of the units tested, nominal output capacity data was available either from the Northeast Energy Efficiency Partnerships (NEEP) database or the manufacturer's literature. A comparison of measured steady-state output and the manufacturer's nominal values may be used to derive a measure of oversizing.

ES-6 below shows the ductless 1:1 units' measured output compared to the rated minimum and maximum capacities. In all cases, the output is consistently near the rated minimum capacity, indicating that the systems are oversized. It is important to note that the rated capacities are established through specific test procedures and conditions, while the measured capacities do not mirror those exact conditions. ES-7 shows a similar trend for the ducted, ductless 1:2, and mixed sites—again indicating oversizing. The NEEP database did not include manufacturer data for TLP_003 and CEE_003, unlike the other values that were present.

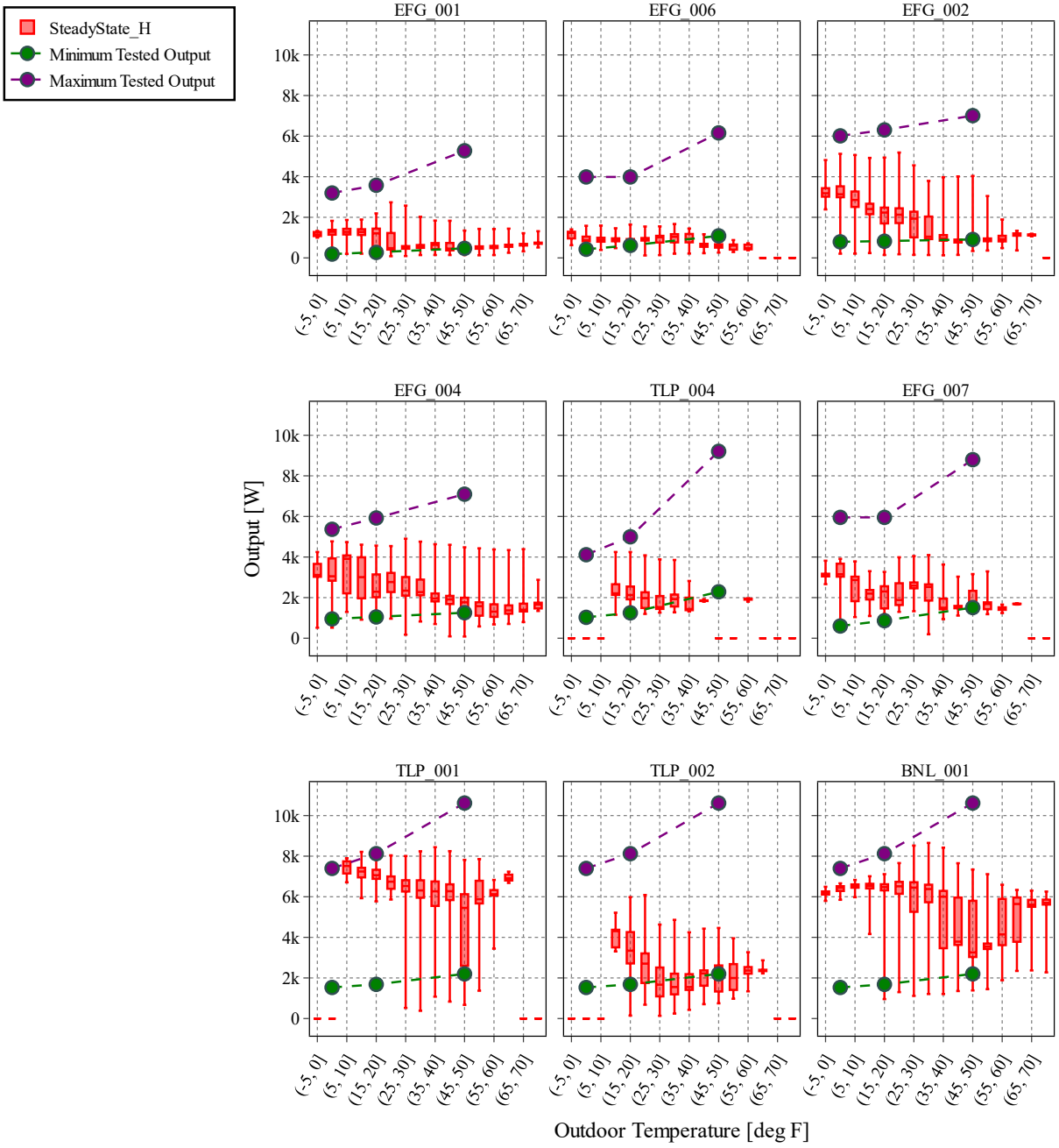


ES-6: Heat output boxplot binned by outdoor temperature compared to available unit performance data for ductless 1:1 sites during steady-state heating

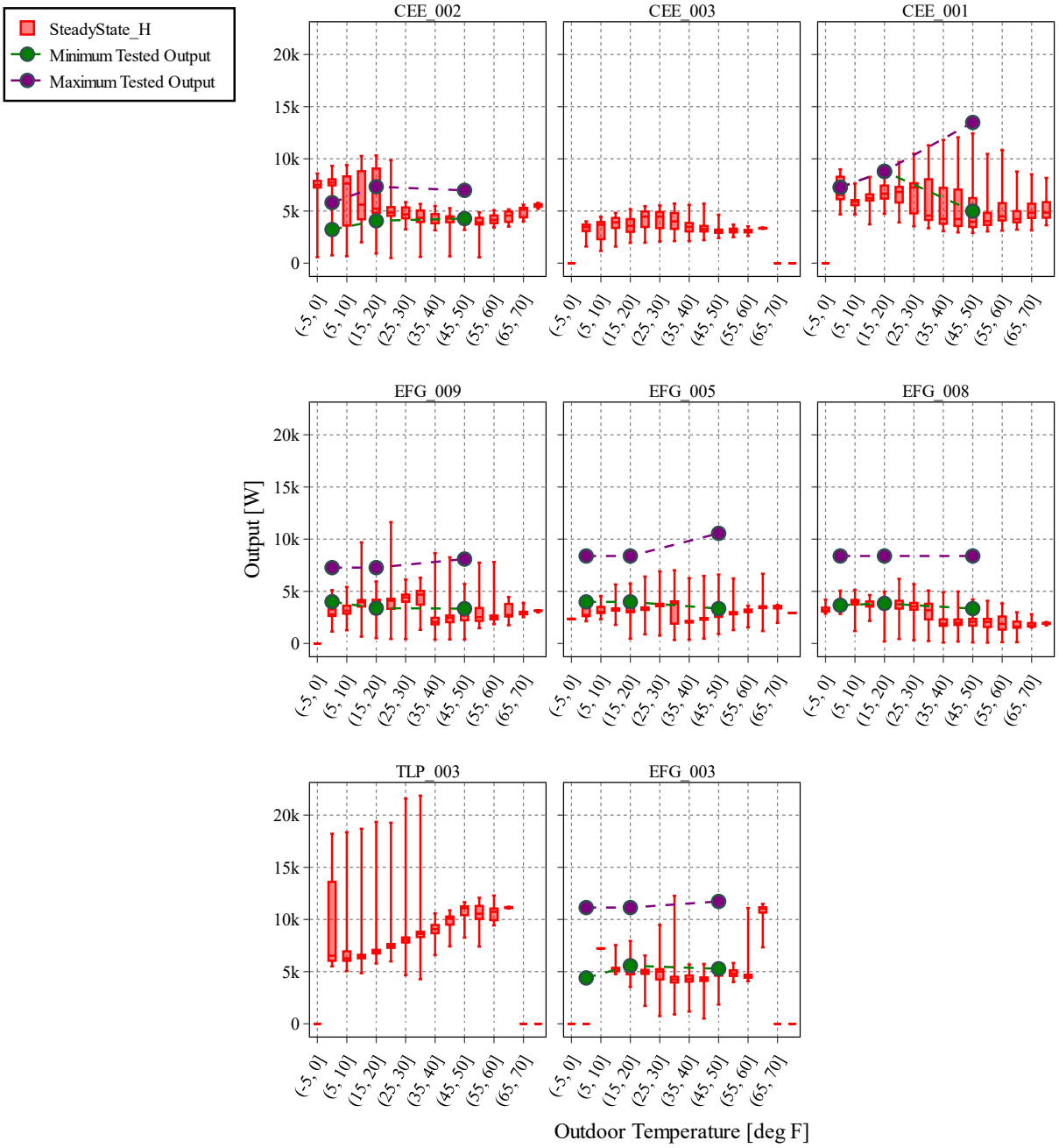


ES-7: Heat output boxplot binned by outdoor temperature compared to available unit performance data for ducted, non-ducted 1:2, and mixed sites

Throughout the study, the sites saw a wide range of delivered thermal energy at different outdoor temperatures. Average output typically increased with building load at decreasing outdoor temperatures for air-to-air heat pumps, but the opposite trend was observed for air-to-water heat pumps, indicating these units may be near their capacity limit. Steady-state output capacity interquartile ranges were often as large as 1 kW, indicating the variable-output devices often settled

at different operating points over the duration of the study. The ability of the devices to modulate their output to account for the variable heating demand is critical as an energy-saving tactic given the variability in demand required during the study, as a constant-output device may result in higher power consumption or unfavorable cycling.

Cycling frequency in heating mode generally followed a trend of decreased number of cycles as outdoor temperatures decreased for all site types, as shown in ES Table 1. This pattern aligns with the observation that the devices maintained minimal off time when operating in colder conditions and further suggests that heating demand might exceed these units' capacity on the coldest days of the year. The run time fraction at the lowest outdoor temperatures indicates the degree of oversizing for the load managed at each site. The results of this analysis were varied, as certain units operated nearly continuously during cold temperatures, indicating correct or undersized equipment, while others continued to cycle, indicating oversized equipment, given that the temperatures during the study year were relatively mild. Sites with supplemental heating equipment utilized supplemental heating most often during the coldest days, as expected, indicating heat pumps can be sized smaller for sites with supplemental heating to increase efficiency.

ES Table 1: Cycling Frequency by Site-Type

| Type | Heating | Shoulder |
|---|---|---|
| Ductless 1:1 | 3.5 | 7.2 |
| Ductless 1:2 | 3.7 | 6.0 |
| Centrally Ducted | 2.1 | 2.9 |
| Mixed | 3.7 | 2.9 |
| Air-to-Water | 1.9 | 3.3 |

Perhaps the most critical trend observed in this study is the prevalence of defrost mode at low outdoor temperatures and its relative power consumption. Most sites saw an increased fraction of runtime operating in defrost mode as outdoor temperatures approached the lower end of the observed range. An analysis of the defrost runtime fraction showed that defrost mode typically contributes a small fraction of total operational time, less than 4 % for ductless 1:1 and air-to-water sites. At one ducted site, defrost times up to 7% were observed, but all other ducted sites had much lower defrost fractional times. The power consumption rate during this mode was generally the same order of magnitude as transient and steady-state heating modes. As a result, a significant amount of energy is consumed at low temperatures purely for the maintenance of the device, as opposed to heating the home. Additionally, defrost mode disrupts the active heating of the home, requiring additional energy to return to the existing heating equilibrium established by the device. Reducing defrost mode frequency and duration is thus a good pathway for increasing heat pump performance in cold climates.

Collectively, the conclusions that can be drawn from this study include:

- Most sites show the heat pumps had variable output but operated near their minimum output for the duration of the study, indicating the systems may have been oversized.

- The achieved output and COP was close to the lower end of the nominal range in many cases. Comparing installation types, centrally ducted sites had the highest COPs at the lowest outdoor temperatures.
- In comparing steady-state COP and 24-hour average COP, which includes effects of cycling and defrost, the extent of the degradation of performance was found to be site-specific but generally significant.
- In some cases, the ductless air-to-air units were found to cycle more than was expected. The location of the indoor units, the location of the controlling thermostat, and the size of the units relative to the space they are expected to condition are parameters that could be used to reduce cycling. Additionally, unique site characteristics such as energy efficiency measures and increased solar gains may contribute to increased cyclic performance.
- At most sites, cycling rates (<5 cycles per hour) were found at temperatures below freezing. However, cycling rates were greater than for more mild and higher temperatures – indicating the units were near constant operation at low temperatures and interrupted by defrost periods and above-freezing temperatures cycling rates increased with temperature, indicating intermittent operation.
- The defrost runtime fraction only accounts for a small fraction of total operational time—less than 4 % for ductless 1:1 and air-to-water sites and less than 10 % for ducted sites, with some caveats.
- The average duration of a defrost cycle is between 30 seconds and 15 minutes. Given that defrost events occur more frequently in colder outdoor temperatures and that these events gradually consume a larger portion of the overall operation time, the system's capacity to provide heating becomes restricted. Consequently, the duration of defrost cycles can significantly influence the overall operation time. Furthermore, since each defrost cycle is succeeded by a phase of transient operation, this cycle-to-cycle transition adversely affects the system's performance over time.
- Heating supply temperatures showed median supply temperatures were between 90 and 130 °F, with ductless sites having a higher supply air temperature than centrally ducted sites, and air-to-water sites had the highest supply temperatures.
- The measurement methodology planned and executed in this project was sound and provided the data needed. While the methodology effectively utilized pre-correlating airflow with the indoor unit current, concerns remain about the accuracy of the airflow measurement and the uniformity of air velocity and temperature across the supply register.
- For the homes in this study, which were well insulated, we observed notably reduced heat pump operating run time fractions. This underscores the substantial influence that building energy efficiency strategies, including enhanced insulation and low-temperature distribution methods, can exert on a heat pump system's overall utilization, operation, and effectiveness. Consequently, heat pumps may emerge as a fitting choice for residences

characterized by lower thermal loads and reduced heat losses. Alternatively, smaller heat pump systems or systems that run at lower compressor speeds can meet space heat demands.

# Table of Contents

# Table of Tables

# Table of Figures

## Preface and Teaming Background

In November 2021, the Department of Energy's Building Technologies Office (BTO) launched the Cold Climate Heat Pump Technology Challenge in partnership with the U.S. Environmental Protection Agency, Natural Resources Canada, and certain residential heat pump manufacturers. The objective of the Challenge was to develop heat pumps that meet a new best-in-class specification of high-efficiency heating performance in cold climates. (https://www.energy.gov/eere/buildings/residential-cold-climate-heat-pump-challenge)

The heat pump field study described in this report and a related report (https://www.osti.gov/biblio/1973090) funded by BTO both started in late 2018 with products that were commercially available at that time. Due to pandemic-related delays, in-field equipment monitoring for the heat pump field study did not start until 2021. These studies investigated the performance of heat pumps available in the market before the Cold Climate Heat Pump Technology Challenge, and therefore, the products monitored in this field study were not designed to meet the new specifications defined in the Cold Climate Heat Pump Technology Challenge. Based on these facts, performance-related conclusions from these studies should not be compared to those resulting from field studies examining heat pumps that have successfully met the specifications as defined by the Cold Climate Heat Pump Technology Challenge.

Two teams collaborated during this project—one was led by the *National Renewable Energy Laboratory* (NREL), and the second was led by *Brookhaven National Laboratory* (BNL). Together, BNL and NREL developed a field test plan to evaluate heat pumps operating in the field. The team defined target site and heat pump characteristics—focused on cold climate air source heat pumps (ccASHPs), with features such as variable-speed compressors and fans, low-temperature capacities, and high-performance factors in cold climates. The team established all instrumentation and sensors to be used for monitoring— documenting the number, location, and minimum accuracy. Additionally, the team detailed data to be documented during the installation of all monitoring equipment to adequately capture general information about the home, equipment, and overall installation to serve as a reference during data analysis and for quality control and quality assurance. Finally, the team worked together to develop data processing scripts for comprehensive data analysis. The NREL team focused on air-to-air ducted heat pumps in the Pacific Northwest, and the BNL project included air-to-air and air-to-water heat pumps in Minnesota, New York, and Vermont. BNL partnered with the following team members:

The *Center for Energy and Environment (CEE)* is a leading energy efficiency agency in Minnesota with prior experience in a field study on ASHP's in Minnesota. CEE contributed to the field measurement protocol development, identified the planned sites in Minnesota, and worked with the installer to plan the system and required sensors, install the sensors, and serve as the local site connection.

The NY office of *Frontier Energy (FE)* (formerly CDH Energy) focuses on the in-field measurement of energy efficiency performance of novel systems and was active in the DOE Building America Program. FE also leads the field efficiency verification effort of the NYSERDA ASHP Demonstration program. Under this project, FE was heavily involved in extending the scope

of the measurement protocol of the NYSERDA program and in helping to plan the measurement and data management plan for the new sites.

*The Levy Partnership (TLP)* is a building energy research and consulting firm located in New York City and was active in the DOE Building America Program. Under the NYSERDA Demonstration program, TLP played a key role in identifying host sites and providing local oversight for the design, installation, and monitoring of the sites. In this project, TLP expanded this role to identify and manage suitable sites in the New York City area.

*Taitem Engineering (TE)* is a consulting firm based in Ithaca, New York that performs mechanical, electrical, and structural design, energy studies, and energy research. In this project, TE worked to identify additional sites in upper New York State, which included air-to-water projects.

*Energy Futures Group (EFG)* is an energy consulting firm headquartered in Vermont with offices in New York and Boston. EFG specializes in the design, implementation, and evaluation of programs and policies to promote investments in efficiency, renewable energy, other distributed resources, and strategic electrification. EFG staff have worked on these issues on behalf of energy regulators, government agencies, utilities, and advocacy organizations in 30 states, 6 Canadian provinces, and several countries in Europe. EFG was a key participant in the NYSERDA ASHP program. EFG was responsible for identifying and managing sites in New York's Hudson Valley and Vermont.

# Introduction

Electric air source heat pumps are established heating and cooling technologies that have been widely adopted in mixed climate zones. There is growing interest in increasing the use of this technology for heating applications in cold and very cold climates. However, their performance in cold climates, at various field conditions, is not well documented, and further lab and field-based research are needed to design and validate the performance of systems in multiple configurations (e.g., central, ducted, multi-zonal). More information about the design, operation, and performance of this technology in cold climates is needed to inform research and development of equipment with higher capacity and less Coefficient of Performance (COP) degradation (i.e., the system's efficiency at delivering heating to the home) at low ambient temperatures. Research to better understand the actual performance of air source heat pumps at various field conditions and how they are operated and sized will inform future Department of Energy (DOE) technology research and industry equipment sizing guidelines.

Recent advances in cold-climate air-source heat pumps (ccASHPs), with features such as variable-speed compressors and fans, multistage systems, and highly optimized thermal design, have increased the COP and low-temperature capacity in cold climates. Under this DOE Building Technologies Office (BTO) project, a field study was conducted of heat pump installations across the central and northeastern United States (US) to better understand performance and building integration challenges in cold climates. In addition, field data about controls and usage will inform solutions to building integration challenges. Specifically, the scope of this study included 1) air-to-air non-ducted, mini-split heat pumps, 2) air-to-air ducted heat pumps, and 3) air-to-water heat pumps for residential-scale applications.

## 1.1 Project Goals

The goal of this project was to map the performance of a range of air-source heat pump equipment that represent innovative systems relevant to heating-dominated regions under actual field conditions. The results are intended to be used by researchers and manufacturers to inform research and development of energy-efficient equipment and to develop guidelines for optimizing primary energy savings when using air-source heat pumps in heating-dominated regions. This information may also enable accelerated adoption of air-source heat pumps by designers, installers, state and regional energy efficiency organizations, and building owners.

## 1.2 Key Research Questions

1. Heat Pump Installed Capacity and COP
    a. What is the measured heating capacity and efficiency of installed, central, variable-capacity heat pump systems, specifically at cold temperatures?
2. Variable-Capacity Modulation and Heat Pump Sizing
    a. How does the cycling rate and runtime of the variable-capacity heat pumps depend on outdoor air temperature?
3. Defrost Mode Energy
    a. How much energy is consumed by the heat pump during defrost mode?

    b. How often do defrost cycles occur, what is the duration, and how does the frequency and duration depend on outdoor air temperature?
4. Supply Air Temperature
    a. What is the heat pump supply air temperature when using compressor-based heating at various outdoor air temperatures?

## 1.3 Approach Overview

Multiple sites in the northern US were used, including new sites and sites from previous and ongoing field studies with air-source heat pumps. A comprehensive field measurement and data management plan for these test sites guided data collection to develop full performance maps of the heat pump systems. These maps can be incorporated into energy modeling software to extend the results to different climate regions, sizing practices, and configurations. Two teams collaborated during this project—one was led by the *National Renewable Energy Laboratory* (NREL), and the second was led by *Brookhaven National Laboratory* (BNL). The NREL team is focused on air-to-air ducted heat pumps in the Pacific Northwest, and the BNL project included air-to-air and air-to-water heat pumps in Minnesota (MN), New York (NY), and Vermont (VT).

Team members from BNL, CEE, EFG, and TLP interacted with homeowners from the selected sites to collect information regarding the heat pump or home characteristics. These questions were detailed in the project protocol, which was approved by the DOE's Institutional Review Board (IRB). This included project recruiting material, planned measurements, test period procedures, and management of host site personal information.

A variety of air-side temperature, current, and power measurements were used to quantify heat pump capacity and calculate the COP over an entire heating season. Two independent, standalone data loggers were used at each site – one located within proximity of the heat pump outdoor unit (ODU) and the other close to the indoor unit (IDU). This approach minimized time on-site by reducing the need to run wires, and data was combined during post-processing. The ODU data logger included a weather station to monitor outdoor air dry-bulb temperature and relative humidity.

During each initial site visit, team members correlated the IDU airflow rate to the indoor current consumption by installing a temporary air handler flow plate or duct blaster to measure the indoor airflow at a range of blower speeds. Blower power was measured throughout the study to estimate the indoor airflow rate during the long-term monitoring. This analysis was later used in calculating the performance metrics.

This report summarizes the sites overseen by BNL in terms of the equipment tested, field study methodologies and approach, research findings, and performance results. While an emphasis in this study was placed on heating performance, the monitoring and data analysis also extended through the cooling season.

## Site Characteristics and Heat Pump Information

Field sites were selected to meet the research objectives of the project. Specifically, test sites in colder climates, such as Zones 5 – 7 (cold – very cold), were preferred, but some sites were located in Zone 4 (mixed-humid). Target sites included single-family homes, townhouses, and duplexes in regions with greater than 6,000 annual heating degree days (HDD). HHD are defined as the number of heating degrees in a day, between 65°F and the daily mean temperature (average of the high and low temperature for a given day). For example, a daily high and low of 45 °F and 35 °F, respectively, would equate to an average of 40 °F, equating to an HDD of 25 (the difference of 65 °F and 40 °F). HDD typically provides some indication of the home's energy demand. Additionally, the heat pumps deemed suitable for the project were those able to produce at least 50% of their nominal (47º F) capacity at 5°F. Many of the study's identified sites were where heat pumps were already installed or identified through local utility rebate programs. Target sites required the heat pump to be the primary source of heat in the home or space.

### 2.1 Site Locations

A total of 21 occupied homes were selected, with 18 located in the Northeast and three located in Minnesota for this study. Nine (9) 1:1 ductless units (note 1:1 indicates one outdoor unit matched with one indoor unit), six (6) centrally ducted units, one (1) 1:2 (one outdoor unit matched with two indoor units) ductless unit, one (1) mixed unit, and four (4) air-to-water systems were studied. In the case of ductless heat pumps with multiple indoor heads, each indoor head was treated as a separate unit and fully instrumented. Table 1 below shows each site's location (city, state), the date of logger installs and removal, and the climate zone. Figure 1 below shows the approximate location of each NY and VT site listed above, while Figure 2 shows the approximate location of the sites in MN.

Table 1: Site Characteristics: Location, Installation and Removal Dates, and IECC Climate Zone

| Site ID | City, State | Monitoring Install Date | Uninstall Date | Monitoring Period | IECC Climate Zone |
|---|---|---|---|---|---|
| | | | | Days | |
| Ductless 1:1 | | | | | |
| BNL-001 | Schenevus, NY | 2/23/2020 | 6/21/2022 | 849 | 6 |
| EFG-002 | Stamford, VT | 2/18/2021 | 9/12/2022 | 571 | 6 |
| TLP-001 | Bronx, NY | 3/19/2021 | 8/31/2022 | 530 | 4 |
| TLP-002 | Bronx, NY | 4/8/2021 | 4/17/2022 | 374 | 4 |
| EFG-001 | New Paltz, NY | 2/4/2021 | 9/12/2022 | 585 | 6 |
| EFG-004 | Germantown, NY | 2/23/2021 | 9/12/2022 | 566 | 5 |
| EFG-006 | Albany, NY | 2/23/2021 | 3/31/2022 | 401 | 5 |
| EFG-007 | Albany, NY | 3/25/2021 | 3/31/2022 | 371 | 5 |
| TLP-004 | Brooklyn, NY | 6/3/2021 | 7/12/2022 | 404 | 4 |
| Centrally Ducted | | | | | |
| EFG-003 | Esopus, NY | 2/18/2021 | 9/12/2022 | 571 | 6 |
| CEE-001 | Big Lake, MN | 9/10/2020 | 8/3/2022 | 692 | 6 |
| CEE-002 | Northfield, MN | 9/18/2020 | 6/1/2022 | 621 | 6 |
| CEE-003 | Northfield, MN | 10/30/2020 | 4/5/2021 | 157 | 6 |
| EFG-005 a | Newburgh, NY [1] | 3/10/2021 | 9/12/2022 | 551 | 5 |
| EFG-005 b | | 3/11/2021 | 9/12/2022 | 550 | |
| TLP-003 | Mohegan Lake, NY | 5/27/2021 | 5/19/2022 | 357 | 4 |
| Ductless 1:2 | | | | | |
| EFG-008 | Cottekill, NY | 4/1/2021 | 9/12/2022 | 529 | 6 |
| Mixed | | | | | |
| EFG-009 | New Paltz, NY[2] | 10/28/2021 | 9/12/2022 | 319 | 6 |
| Air-to-Water | | | | | |
| AWHP1 | Ithaca, NY | 1/21/2021 | 8/28/2022 | 584 | 6 |
| AWHP2 | Holland Patent, NY | 3/26/2021 | 8/28/2022 | 520 | 6 |
| AWHP3 | Chatham, NY | 4/15/2021 | 8/28/2022 | 500 | 5 |
| AWHP4 | Ithaca, NY | 7/14/2021 | 8/28/2022 | 410 | 6 |

[1] Two (2) Distinct Centrally Ducted Systems: 1- Conventional-type AHU and 1-Pancake AHU

[2] Centrally Ducted (Conventional-type AHU) + Indoor Head (Wall Unit) in the basement

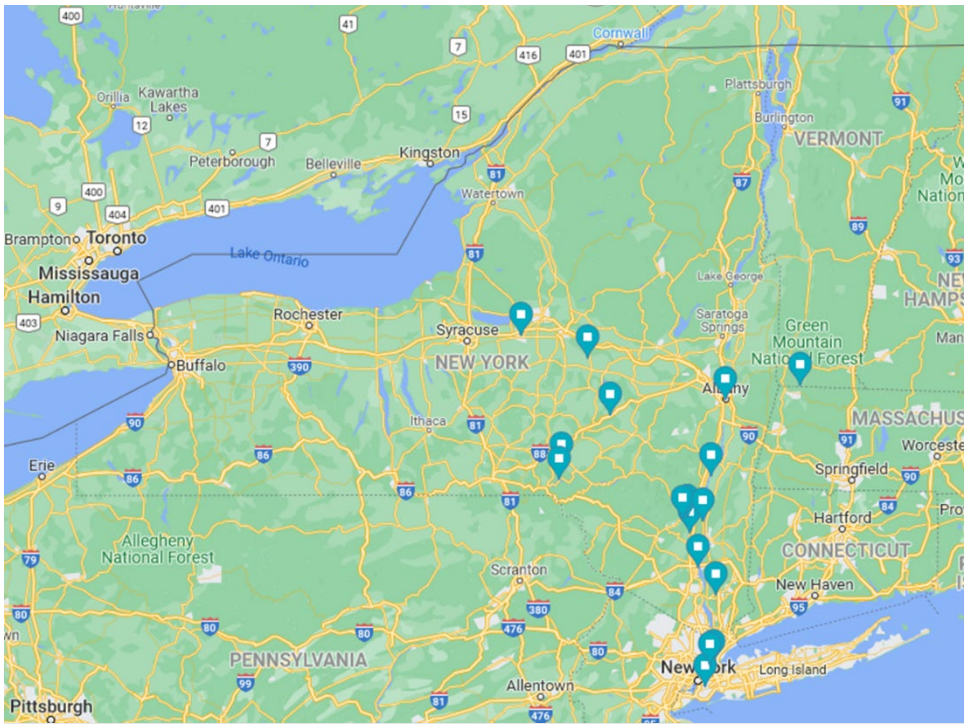


Figure 1: Approximate locations of the 18 sites studied in NY and VT.

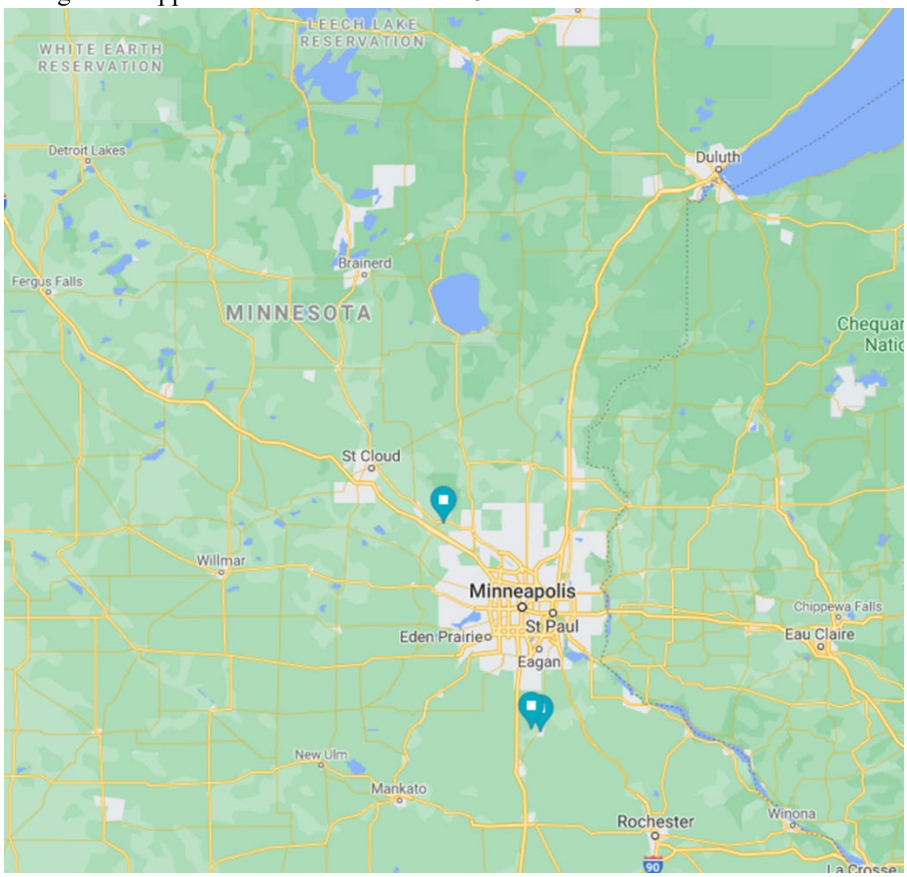


Figure 2: Approximate locations of the three (3) sites studied in MN.

## 2.2 Weather Data

The primary focus of this field study was heating data and quantifying the performance of heat pumps during the heating season. As mentioned above, the selected sites targeted had 6000 or greater HDD. Table 2 provides the HDD, cooling degree days (CDD), design temperatures, and the number of hours data was collected in temperatures colder than the heating design temperature and warmer than the cooling design temperature. The heating design temperature indicates that 99% of the time, based on a 30-year average, the temperature is above that. For instance, a site with a heating design temperature of -4 °F is only colder than that 1% of the time.

As shown in Table 2, with the exception of 3 sites (BNL-001, CEE-001, and AWHP2), all sites had less than 50 hours below the heating design temperature—ranging from 0% to 1.2% of the study's duration. Further, Figure 3, Figure 4, and Figure 5's histograms indicate the amounts of data collected during the entire study period by temperature bins. Overall, a considerable amount of data was collected at most sites, representing the heating, shoulder (milder weather), and cooling seasons. Specifically, 19 out of 21 sites had more than one year's worth of data collected. Of those sites, 12 had more than 10,000 hours. It follows that most sites should have a good representation of at least one heating and cooling season.

Table 2: Site Characteristics: Heating and Cooling Degree Days, Design Temperatures, and Hours Below or Above Design Temperatures

| Site ID | ASHRAE Heating/Cooling Design Day (US Department of Housing and Urban Development, n.d.) | | Design Temperatures (ICC, 2020) (°F) | | Number of hours below/above the design temperature | |
|---|---|---|---|---|---|---|
| | HDD | CDD | 99% Heating | 1% Cooling | Heating | Cooling |
| Ductless 1:1 | | | | | | |
| BNL-001 | 7613 | 233 | -4 | 85 | 68 | 340 |
| EFG-002 | 7880 | 212 | -4 | 86 | 12 | 25 |
| TLP-001 | 5400 | 770 | 9 | 92 | 0 | 50 |
| TLP-002 | 5400 | 770 | 9 | 92 | 0 | 0 |
| EFG-001 | 6377 | 546 | 2 | 89 | 19 | 192 |
| EFG-004 | 6942 | 400 | -3 | 88 | 0 | 160 |
| EFG-006 | 6860 | 544 | -3 | 88 | 6 | 112 |
| EFG-007 | 6860 | 544 | -3 | 88 | 6 | 69 |
| TLP-004 | 4681 | 1123 | 10 | 92 | 0 | 10 |
| Centrally Ducted | | | | | | |
| EFG-003 | 6438 | 550 | 2 | 88 | 9 | 143 |
| CEE-001 | 8429 | 567 | -13 | 89 | 189 | 291 |
| CEE-002 | 7773 | 658 | -10 | 88 | 43 | 603 |
| CEE-003 | 7773 | 658 | -9 | 89 | 0 | 0 |
| EFG-005 a | 5813 | 790 | 2 | 90 | 1 | 196 |
| EFG-005 b | | | | | | |
| TLP-003 | 6103 | 576 | 6 | 92 | 13 | 5 |
| Ductless 1:2 | | | | | | |
| EFG-008 | 6377 | 546 | 2 | 89 | 30 | 170 |
| Mixed | | | | | | |
| EFG-009 | 6377 | 546 | 2 | 89 | 9 | 120 |
| Air-to-Water | | | | | | |
| AWHP1 | 7182 | 312 | 0 | 85 | 22 | 261 |
| AWHP2 | | | 0 | 86 | 154 | 124 |
| AWHP3 | 6556 | 618 | -3 | 88 | 18 | 2 |
| AWHP4 | 7182 | 312 | 0 | 85 | 4 | 102 |

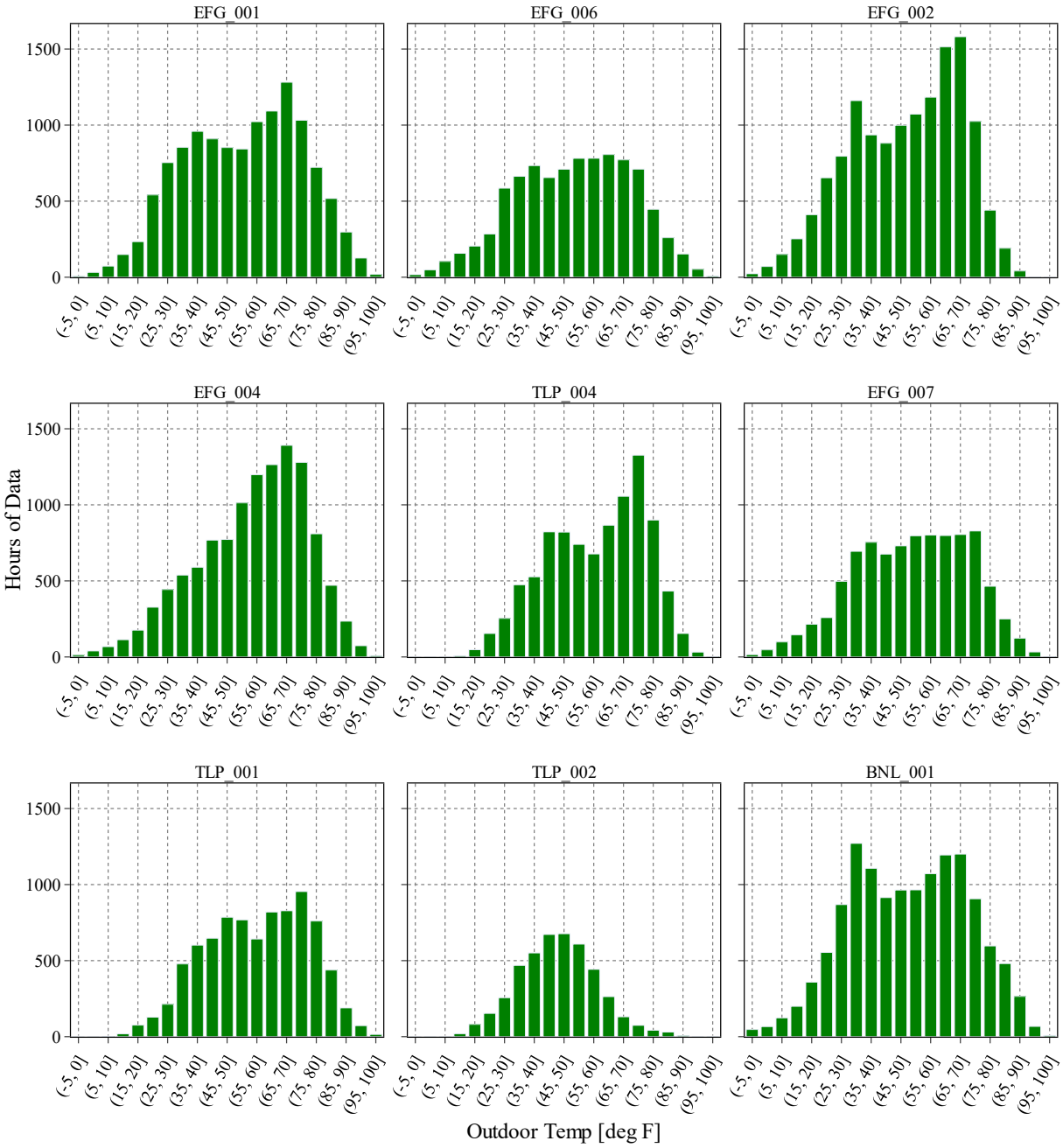


Figure 3: Hours of data collected binned by outdoor temperature for ductless 1:1 sites

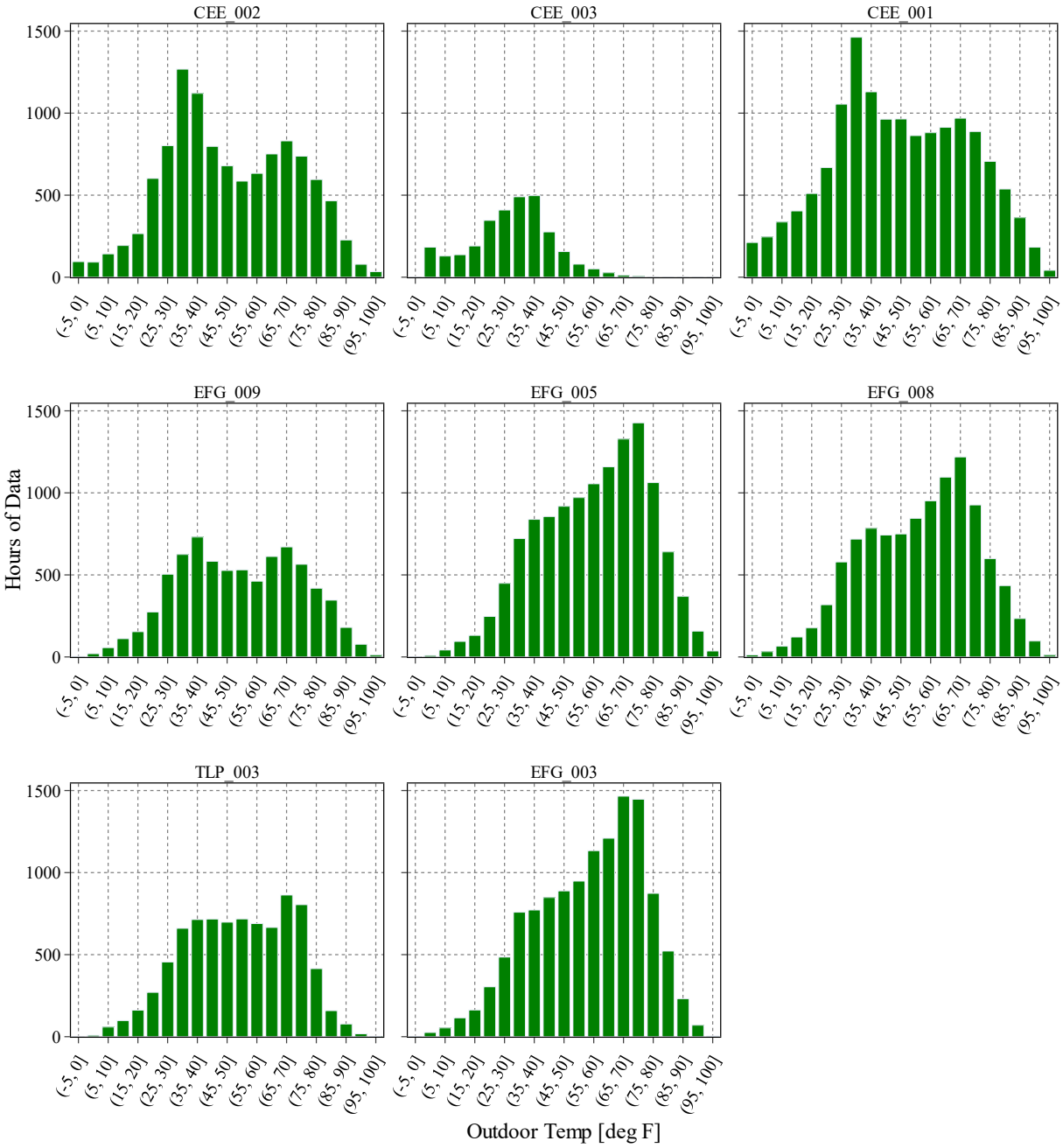


Figure 4: Hours of data collected binned by outdoor temperature for ducted, 1:2 ductless and mixed sites

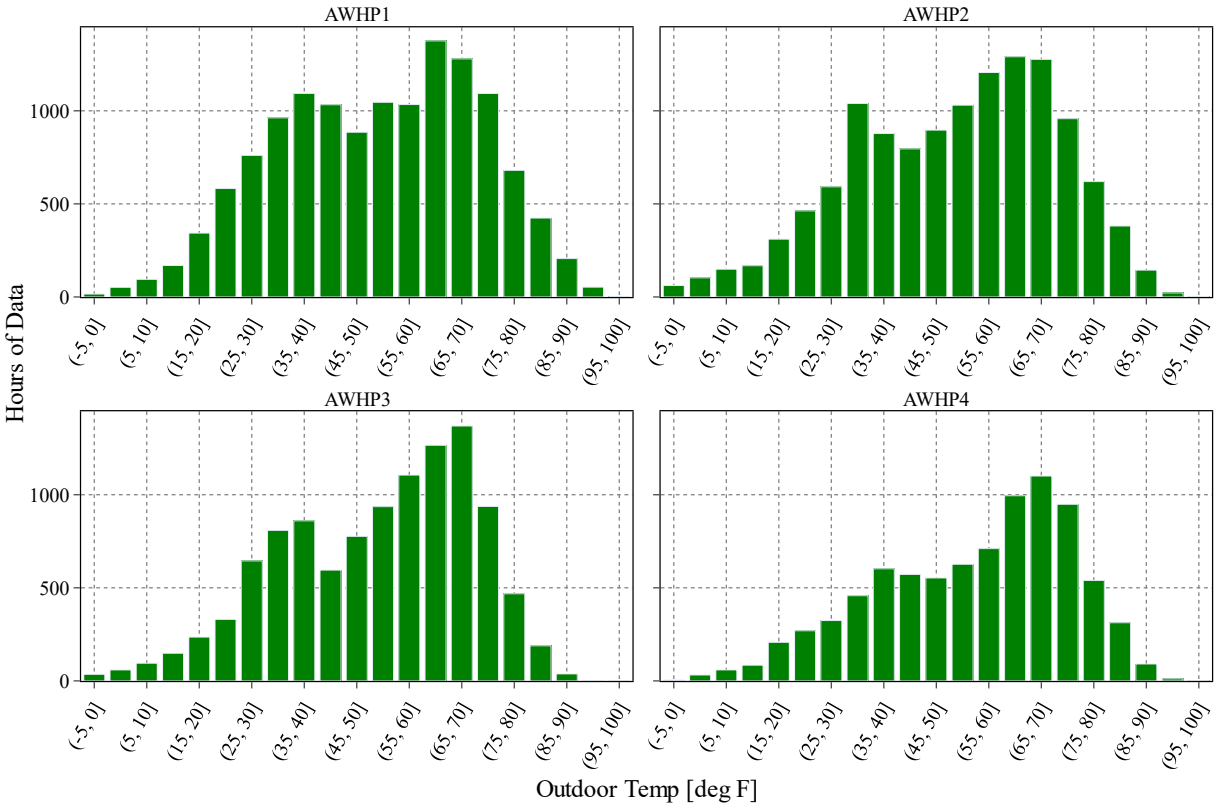


Figure 5: Hours of data collected binned by outdoor temperature for air-to-water sites

## 2.3 Heat Pump and Auxiliary Heat Specifications and Settings

In addition to collecting information about the site's location and climate characteristics, general information about the different units was collected, such as the type and model number for both indoor and outdoor heat pump units (model numbers have been redacted for this report), the heating and cooling capacity of the units, current draw, design temperature range or lockout temperature, and whether or not a pan or crankcase heater existed. Table 3 provides a high-level summary of the heat pumps studied with information about the estimated conditioned space, the nominal capacity of the unit, the minimum operating temperature (lockout), and if the unit was listed on the Northeast Energy Efficiency Partnerships' (NEEP's) ccASHP list. Measurements confirm that all the units chosen for this study operated in heating mode at their lowest design temperature. Additionally, most units were modulating—allowing them to provide variable capacity.

Table 3: Site Heat Pump Specifications Summary

| Site ID | Listed on ccASHP NEEP list? | Estimated area of conditioned space | Nominal Capacity | | Lockout Temperature |
|---|---|---|---|---|---|
| | | | Heating | Cooling | |
| | | sq. ft. | Btu/hr | | °F |
| Ductless 1:1 | | | | | |
| BNL-001 | Yes | 1,700 | 25,200 | 22,000 | -5 |
| EFG-002 | Yes | 1,300 | 18,000 | 14,500 | -15 |
| TLP-001 | Yes | 1,100 | 25,200 | 22,000 | -5 |
| TLP-002 | Yes | 690 | 25,200 | 22,000 | -5 |
| EFG-001 | Yes | 400 | 10,900 | 9,000 | -13 |
| EFG-004 | Yes | 1,115 | 18,000 | 15,000 | -13 |
| EFG-006 | Yes | 300 | 13,600 | 12,000 | -13 |
| EFG-007 | Yes | 700 | 20,300 | 17,200 | -13 |
| TLP-004 | Yes | unknown | 25,400 | 21,500 | -5 |
| Centrally Ducted | | | | | |
| EFG-003 | Yes | 2,792 | 38,000 | 33,000 | -13 |
| CEE-001 | Yes | 5,260 | 48,000 | 47,500 | -4 |
| CEE-002 | Yes | 2,500 | 23,800 | 24,000 | -20 |
| CEE-003 | No | unknown | 25,200 | 36,000 | -20 |
| EFG-005 a | Yes | 2,560 | 27,600 | 27,400 | -13 |
| EFG-005 b | Yes | | | | |
| TLP-003 | No | 1,600 | No published data | 36,000 | No published data* |
| Ductless 1:2 | | | | | |
| EFG-008 | Yes | 1,560 | 28,600 | 28,400 | -13 |
| Mixed | | | | | |
| EFG-009 | Yes | 1,980 | 24,800 | 22,800 | -13 |
| Air-to-Water | | | | | |
| AWHP1 | No | 1,784 | 48,000 | | -22 |
| AWHP2 | No | 1,000 | 48,000 | | -22 |
| AWHP3 | No | 1,989 | 48,000 | | -22 |
| AWHP4 | No | unknown | 48,000 | | -22 |

* This site had auxiliary electric heating that was not used. The system was not configured with a lockout temperature.

The objective of this study was to evaluate the field performance of the heat pump. Therefore, information regarding site characteristics and installation details was collected with an emphasis on the site conditions, control settings of the units, and use of any auxiliary heat. This data was captured to help understand heating/cooling practices that may influence heat pump use and performance. The setpoint temperatures homeowners employed were also documented, as was any use of humidifiers or dehumidifiers. However, this data was captured through a homeowner survey (self-reported) and not monitored or logged throughout the duration of the study. Therefore, if setpoints were changed, this was not captured. Nevertheless, this survey was only recorded to help with data interpretation during data analysis. Unique characteristics of the home were also noted to help better understand the performance of each system.

## Methodology

To capture detailed performance data, site measurements, data acquisition and management, and site control were necessary. Therefore, at all sites, the monitoring included:

- Heat pump system performance
- Operation and performance of backup heat source when used
- Continuous data transfer via the internet or cell phone link, with backup data loggers where necessary
- Continuous data review to improve measurement set and protocol as needed

A uniform methodology for data collection and data management was developed for evaluating performance factors such as COP, auxiliary power use, and capacity. Additionally, the energy output from the heat pump was determined directly from air (or water) mass flow and temperature difference. The comprehensive testing and data management plan included details for data flow, review, quality control, and an operating protocol—each of which is detailed in the following sections.

### 3.1 Field Protocol

The field monitoring protocol was developed with direction from 1) DOE regarding field measurements and test protocols, 2) prior experience with project team members in the field monitoring of air-source heat pumps, 3) recent Vermont, Massachusetts, and Rhode Island ASHP field studies [4], 4) NREL guidelines for field verification of the performance of heat pumps, and 5) published reports from other groups in this area. A uniform measurement protocol was planned for all sites (BNL and NREL) to the greatest degree possible to enable efficient automated data review and performance analysis.

The protocol detailed what data was necessary to collect at each host site. In brief, summary procedures for collecting characteristics about the home, heat pump installation and diagnostic data, and data management information were included in the protocol. The home characteristic data collection section specifically included survey questions regarding general home descriptions, with site photos including the heat pump and any supplemental heating sources, as well as information regarding supplemental heat sources (discussed in 2.3 Heat Pump and Auxiliary Heat Specifications and Settings). The heat pump installation diagnostic data section of the protocol included commissioning data to ensure the heat pump was properly installed and charged and procedures for the airflow and current tests to correlate the two. Finally, the data management section of the protocol included procedures for data collection, including the data to be documented, the sensors and loggers used, the logging period, and quality control/quality assurance checks.

### 3.2 Data Acquisition

Final measurement locations on the heat pump systems were determined based on preliminary tests, discussion amongst the BNL team, NREL, subcontractors, and discussions with Oak Ridge National Laboratory (ORNL). Table 4 below summarizes the measurement points implemented in

both ductless and ducted air source heat pump systems. For uniform data analysis, the sensors at all sites were prescribed a short title, referred to as the Data File Code.

Table 4: Primary Recorded Parameters at Each Site.

| Measurement | Data File Code | Units |
|---|---|---|
| | TIMESTAMP | |
| | RECORD | |
| Total Power | P_Total | Watts |
| Compressor Power Frequency | F_Comp | HZ |
| Outdoor Temperature From RH Probe | T_RHS_OUT | ℃ |
| Outdoor Relative Humidity | RH_OUT | % |
| Indoor Temperature From RH Probe, At Indoor Unit Return | T_RHS_IN | °C |
| Indoor Unit Return Relative Humidity | RH_IN | % |
| Indoor Temperature From RH Probe, At Indoor Unit Outlet | T_RHS_SUP | °C |
| Indoor Unit Outlet Relative Humidity | RH_SUP | % |
| Outdoor Temperature | T_OUT | °C |
| Refrigerant Temperature, Outdoor Coil Mid | T_RO_M | °C |
| Refrigerant Temperature, Outdoor Coil Cooling Mode Exit | T_RO_O | °C |
| Refrigerant Temperature, Indoor Coil Mid | T_RI_M | °C |
| Refrigerant Temperature, Indoor Coil Heating Mode Exit | T_RI_O | °C |
| Indoor Unit Temperature of the Air Inlet | T_AI | °C |
| Indoor Unit-Temperature of the Outlet Air | T_AO1 | °C |
| Indoor Unit-Temperature of the Outlet Air | T_AO2 | °C |
| Indoor Unit-Temperature of the Outlet Air | T_AO3 | °C |
| Inverter and Compressor Current | A_CI | Amps |
| Outdoor Unit Total Current | A_HP_Total | Amps |
| Indoor Unit Current | A_I | Amps |

For the indoor unit inlet (return) air, relative humidity (RH), and inlet (return) air temperature, a single measurement point centrally located in the inlet air stream was used. For the outlet (supply) air in ducted and non-ducted systems, RH was measured at a single point. For outlet (supply) temperature in both systems, a minimum of three (3) temperature sensor points were logged. Most

sites used an Omega Thermistor TH-4408-40-T to measure the temperature. However, some sites used T-type thermocouples. Sensors were not permitted to have a "line-of-sight" to auxiliary heating elements. Careful attention was paid to the location of all three temperature measurements—as even a small difference in temperature can impact COP significantly. Temperature measurements were required to have an error no greater than ±1°F. Temperature measurements located on the outdoor unit were measured using a Watlow Type TTC, AFEC series (1/16" - 4" Probe). Careful attention was paid when mounting the thermocouple and insulating it. A separation barrier was recommended so the junctions remained ungrounded. RH instrumentation required a nominal accuracy of 3.0% RH or better, and all sites used the Campbell Hygro VUES-10-PT in indoor and outdoor locations. All power measurements were made with an accuracy of ±2% and typically used a WattNote WNB-3D-240P & 2-20A CTs.

The unit's current was measured using a low-cost current transducer ACTL-0750-005 Opt 1V, connected to the input pulse counter on the Campbell Scientific logger. Initially, the frequency was measured directly between the inverter and the compressor. However, initial frequency measurements resulted in an unreasonably high frequency. Inspection via an oscilloscope showed that the power to the compressor is a combination of low-frequency power and high-frequency noise. The ACTL-0750-005 Opt 1V was specifically developed for variable-speed motor drives and provided a better raw measure of the unit's current than measuring the frequency directly. This was critical for developing the fan curves to directly correlate current versus airflow. Current measurements of both the indoor and outdoor units typically used a split core current sensor, J&D JC 10F-005A-V (0 - 5 amps) and J&D JC 10F-025A-V (0 - 25 amps), respectively. The field measurements were verified for all sites during installation to ensure each sensor was operating properly. A diagram detailing the location of each sensor for a representative mini-split site is shown in Figure 6.

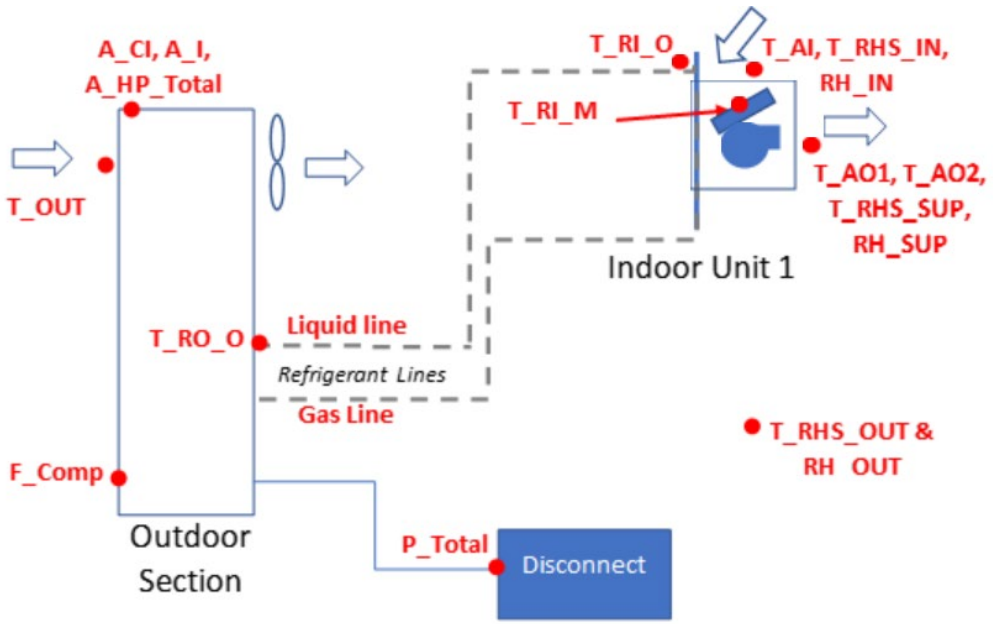

Figure 6: Typical sensor location for a single head, non-ducted heat pump

In addition to the supply temperatures, indoor space temperatures were recorded at some locations away from the indoor unit of the non-ducted system and in selected locations for the ducted system. For each home site with a ducted system, a minimum of three of these measurement locations was selected. For each site with a non-ducted system, a minimum of one space temperature was recorded for each indoor unit. The data from these locations was not easily integrated with the basic heat pump system but rather was logged separately to avoid wiring runs in the home. These measurements were made with independent loggers (HOBO UX-100-001) and not used for any analyses shown directly in this report.

Raw data was sampled with a time period of 5 seconds. A Campbell Scientific CR1000 data logger system was the suggested platform; however, other loggers were used in some cases, as noted in Table 5. Some sites had two loggers (both outdoor and indoor), while other sites used a single logger and ran wires from the outdoor sensors to the indoor logger. A wireless modem was used to transmit data from the home to the team for upload without going through the home Wi-Fi system. Any data that could not be recorded at 5-second intervals was given values of 'NA' for the missing data point. It was recognized that site-specific exceptions to this list may be necessary. Therefore, the use of alternative sensors or instrumentation based on site factors, accuracy, or availability of test equipment was requested by team members and reviewed for approval by BNL or NREL.

Table 5: Data Logger Type and Location for Each Site

| | Data Logger | | | | |
|---|---|---|---|---|---|
| **Site ID** | **CR1000X** | **CR300 w/ Radio** | **CR800 w/ Radio** | **CR3000** | **Obvius AcquiSuite EMB A8810-0** |
| **EFG-001** | Outdoor | Indoor | | | |
| **EFG-002** | Outdoor | Indoor | | | |
| **EFG-003** | Outdoor | Indoor | | | |
| **EFG-004** | Outdoor | Indoor | | | |
| **EFG-005** | Outdoor | | Indoor-1 | | |
| | | | Indoor-2 | | |
| **EFG-006** | Outdoor | Indoor | | | |
| **EFG-007** | Outdoor | Indoor | | | |
| **EFG-008** | Outdoor | Indoor-1 | | | |
| | | Indoor-2 | | | |
| **EFG-009** | Outdoor | | Indoor-1 | | |
| | | Indoor-2 | | | |
| **TLP-001** | Outdoor | Indoor | | | |
| **TLP-002** | Outdoor | Indoor | | | |
| **TLP-003** | Outdoor | | Indoor | | |
| **TLP-004** | Outdoor | Indoor | | | |
| **CEE-001** | | | | Outdoor & Indoor | |
| **CEE-002** | | | | Single logger indoor | |
| **CEE-003** | | | | Single logger indoor | |
| **BNL-001** | Single logger indoor | | | | |
| **AWHP-001** | | | | | Single logger indoor |
| **AWHP-002** | | | | | Single logger indoor |
| **AWHP-003** | | | | | Single logger indoor |
| **AWHP-004** | Single logger indoor | | | | |

A uniform format was specified for all data collected at each site to facilitate the data analysis, and a Python script was developed for mass processing. The first quality control and assurance level began with the weekly data downloads and was managed by each site lead. At this level, minimal data processing occurred. Still, team members identified failures with sensors (no data or data out of reasonable range), data logger communication issues (no data streaming or connection losses), and overall system deficiencies (the heat pump unit itself failed). Early identification of such issues allowed for quick mitigation and restoration of data streaming or the system.

## 3.3 Determining Heat Pump Operating Mode

Operation mode was determined according to the decision tree shown in Figure 7. Files were stored in accordance with the same file folder hierarchy labeled by site name, and the resulting output file utilized the earliest recorded dataset and the most recent dataset in producing the processed filename. The Python script was optimized for parallel processing, wherein each dataset for a site was split up into equal subsets based on the host PC's available physical CPU cores. The subsets were then processed and linked together into a final dataset.

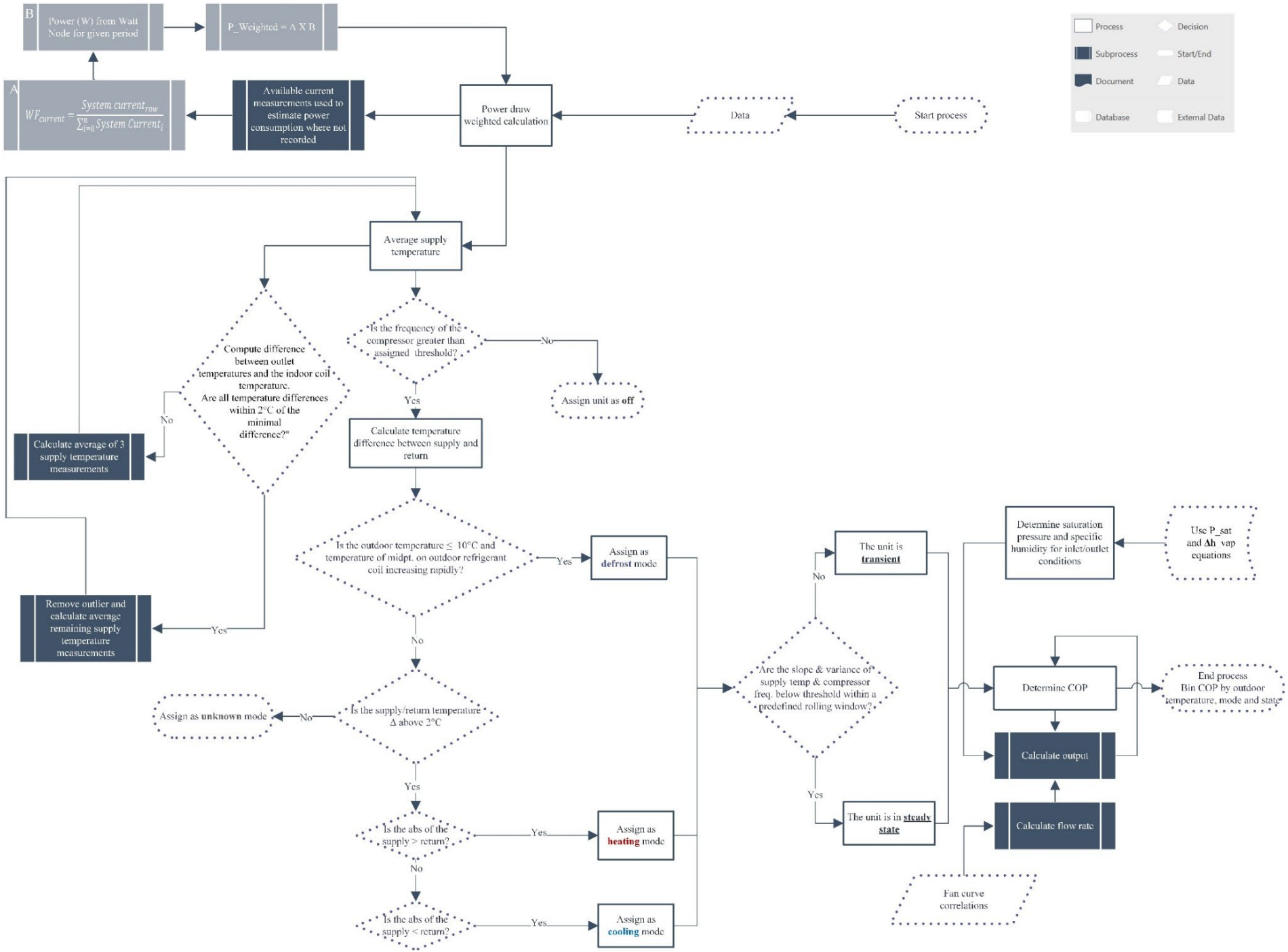


Figure 7: Decision tree for determining state and calculating performance

Quality control (QC) and quality assurance (QA) measures were taken to ensure the data collected was of good quality. With large data sets, abnormal data is inevitable—either due to broken sensors, equipment or the logger, or due to data deviations caused by the logger itself. Once the files were loaded in, the measured parameters were checked against known operational limits to check for any abnormalities. If any abnormalities were found, backup measurements were used to replace logic for those sensors whose data was deemed out of range. Abnormalities were determined through outliers, unexplainable spikes, surpassed threshold values, or other detection algorithms. This was important for the utilization of two parameters, namely the compressor frequency and power consumption. The compressor frequency measurement is utilized mainly for determining whether the compressor was on or off, and the compressor current was utilized in areas where the compressor frequency measurement failed. Additionally, if the power consumption measurement failed, estimates could be made using the current measurements, supply voltage, and the power factor for the site.

After basic corrections were made to the raw data, a weighted averaging procedure was applied to the measured power draw. This was necessary because the pulse-output power measurement, in some cases where the power level was low, only produced an output at time intervals longer than the 5-second logging period. This could result in raw power data with several "0" values followed by a power value assigned to the following data row. Rather than simply average the power over all of these affected rows, the measured current was used to generate a weighted average power over each row in this set. The compressor frequency was checked to determine whether or not compressor-based heating, cooling, or defrost should be assigned.

The supply and return temperatures were compared and used to differentiate between heating and cooling. In heating mode, the supply temperature should exceed the return temperature (Figure 8), and the opposite for cooling. Heating and cooling distinctions were obvious in the dataset, but defrost mode was more complicated to detect. Often, manufacturers' control strategies for the equipment, such as the strategy for initiating and ending a defrost cycle, are proprietary. Therefore, the algorithm focused on two critical temperature measurements to determine defrost. When the outdoor ambient temperature reached a certain threshold temperature, it was compared to the refrigerant temperature at the midpoint of the outdoor coil. During a defrost period, the outdoor refrigerant temperature rises rapidly to a temperature far above the ambient temperature to melt off/discourage ice formation, as shown in Figure 9.

Once the general mode was determined, it was further divided into steady-state and transient operation modes. Once this was established, the relevant performance parameters were computed and reported. A separate Python script was utilized to plot the resulting processed dataset and output individual Excel files for each plot. Further details on the methods and equations utilized are described in the following subsections.

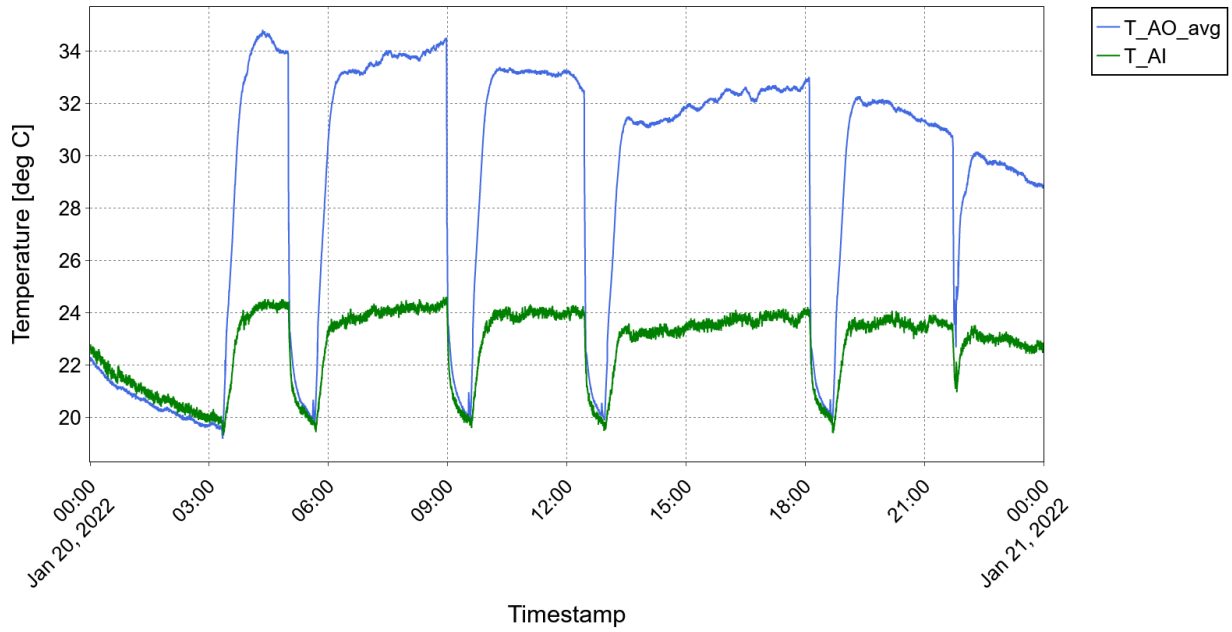


Figure 8: EFG-001 raw time series plot of a typical heating day, with air supply temperature (blue) and air return temperature (green).

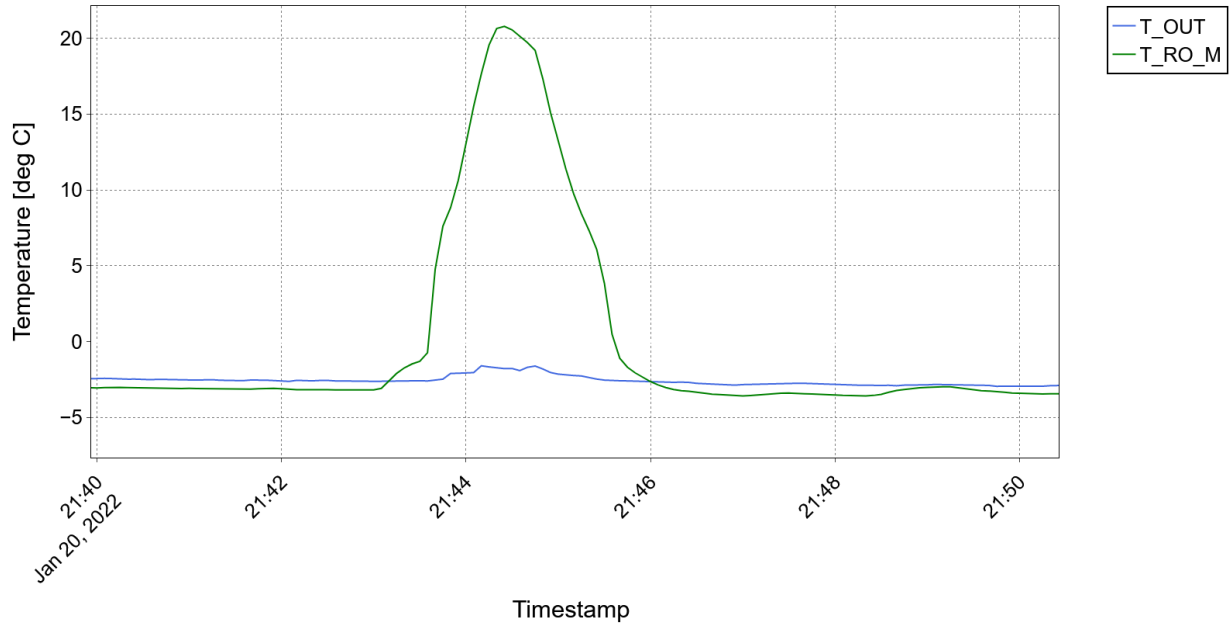


Figure 9: EFG-001 raw time series plot of a typical defrost cycle, with outdoor ambient temperature (blue) and outdoor refrigerant coil temperature at the midpoint of the coil (green).

## 3.4 Performance Calculations

Heat pump performance calculations rely on the determination of several intermediary parameters. The most basic of these parameters was airflow corrected to standard conditions, which was

correlated with indoor current as in Eqn. (1) and was a necessary parameter for computing heat output in Eqns. (2), (3), and (6) for air-to-air sites, while the flow rate was a direct measurement for AWHP sites. The density and specific heat of air at standard conditions were utilized for all air-to-air sites. For AWHP sites, the average density and specific heat at the supply and return were utilized. Heating mode output capacity calculations utilize Eqn. (2) and require fewer intermediary parameters to be calculated. For the cooling mode, the contribution of the latent heat of the water during dehumidification was quantified. The energy required for dehumidification was significant and was quantified using the sensible heat ratio, as in Eqn. (7). To determine the latent heat component, the saturation vapor pressure was computed according to the Clausius-Clapeyron equation (Çengel, Boles, & Kanoğlu, 2019), Eqn. (4) at the supply and return temperatures. This was then utilized with the relative humidity measurement to determine the specific humidity. The latent heat of vaporization of water was then used in conjunction with the difference in specific humidity and air mass flow rate to determine the energy required for dehumidification, as in Eqn. (6). In order to compute COP, the power was weighted according to Eqns. (9) and (10), and finally characterized using Eqn. (11). The error in performance parameters relies on statistical analysis, where the standard error and a 99% confidence interval was utilized, conforming to Eqn. (12). Since the resulting error decreases with the number of samples taken, this error acts as a measure of repeatability. A larger statistical error may indicate that an insufficient amount of data was collected in individual temperature bins to make a definitive statement on the performance characteristic of interest.

$$\dot{V}_{std} = C_2 A_I^2 + C_1 A_I + C_0 \tag{1}$$

$$\dot{Q}_{heating} = \rho \dot{V}_{std} c_p (T_{supply,avg} - T_{return}) \tag{2}$$

$$\dot{Q}_{sensible,cooling} = \rho \dot{V}_{std} c_p (T_{return} - T_{supply,avg}) \tag{3}$$

$$P_{sat,x} = P_0 e^{\left(\frac{h_{fg}}{R_w}\right)\left(\frac{1}{T_0} - \frac{1}{T_x}\right)} \tag{4}$$

$$\omega_x = 0.622 \frac{\varphi P_{sat,x}}{P_{atm} - \varphi P_{sat,x}} \tag{5}$$

$$\dot{Q}_{latent,cooling} = \rho \dot{V}_{std} \left(\omega_{return} - \omega_{supply}\right) h_{fg} \tag{6}$$

$$SHR = \frac{\dot{Q}_{sensible}}{\dot{Q}_{sensible} + \dot{Q}_{latent}} \tag{7}$$

$$\dot{Q}_{cooling} = \dot{Q}_{sensible,cooling} + \dot{Q}_{latent,cooling} \quad (8)$$

$$CWF_x = \frac{A_x}{\sum A} \quad (9)$$

$$P_{Weighted,x} = CWF_x * P_{Total} \quad (10)$$

$$COP = \frac{\dot{Q}}{P_{Weighted}} \quad (11)$$

$$\Delta_{stat} = \pm 2.576 \frac{\sigma}{\sqrt{N}} \text{ (99\% confidence)} \quad (12)$$

## 3.5 Determining Steady State Periods

Steady-state periods were determined utilizing the average supply temperature and compressor frequency as input variables. These parameters were chosen as they are representative of steady device operation and steady satisfaction of heating demand. Due to fluctuations in the dataset, the raw data was first smoothed using a symmetric rolling moving average filter (linear convolution) centered about the data point of interest over one minute of data collection according to Eqn. (13). A moving average filter was selected due to its reduced computational complexity given the overall size of the dataset, which extends to several millions of data points per site. Then, rolling linear regression was performed to obtain the rate of change via Eqn. (14) on the smoothed data over a 3-minute interval to identify the existing trends. If the corresponding slope is less than a pre-defined tolerance, the data was labeled as steady-state and transient otherwise.

Data was first tested against temperature, then compressor frequency. Furthermore, variance in the dataset was considered, and thresholds based on acceptable standard deviations were utilized. The rate of temperature change was limited to a slope less than 0.25 °C/min in a 3-minute interval for the air-to-air sites and a 2 °C/min for the air-to-water sites. This was determined via an iterative process across the sites. Due to the different capabilities of each unit, the compressor frequency slope limit was based on less than 2.5% of the maximum rate of change of the compressor's frequency. The variance thresholds for temperature and compressor frequency correspond to a standard deviation of 0.5 °C and 1 Hz, respectively, computed via Eqn. (15). By incorporating two different approaches and two different input variables representing the device's capabilities, we reduce the possibility of false positives. A time series plot of the supply temperature and compressor frequency as raw data, filtered by our transient label, and filtered by our steady-state label, is shown in Figure 10, Figure 11, and Figure 12, respectively.

$$y_i = \frac{1}{N} \sum_{j\,=\,-\frac{N-1}{2}}^{j\,=\frac{N-1}{2}} x_{i+j} \tag{13}$$

$$m = \frac{n\sum xy - \sum x \sum y}{n\sum x^2 - (\sum x)^2} \tag{14}$$

$$Var(X) = \sigma^2 = \frac{\sum (x_i - \bar{x})^2}{n-1} \tag{15}$$

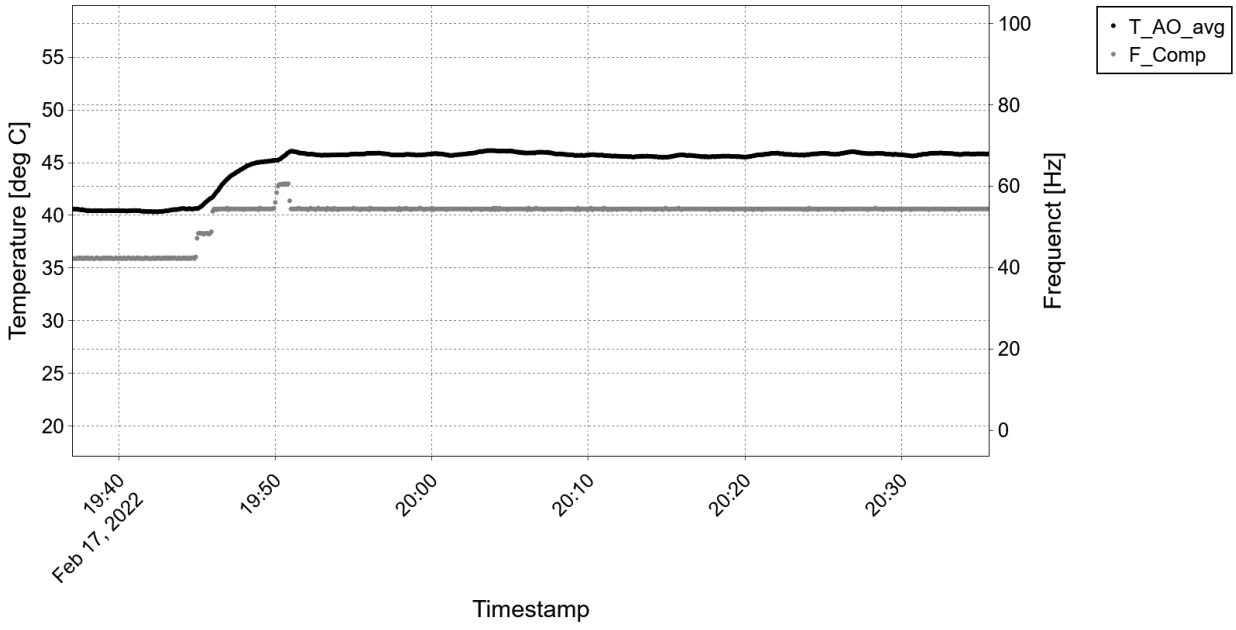


Figure 10: EFG-002 raw time series plot of average supply temperature (black) and compressor frequency (gray) over a specified time window.

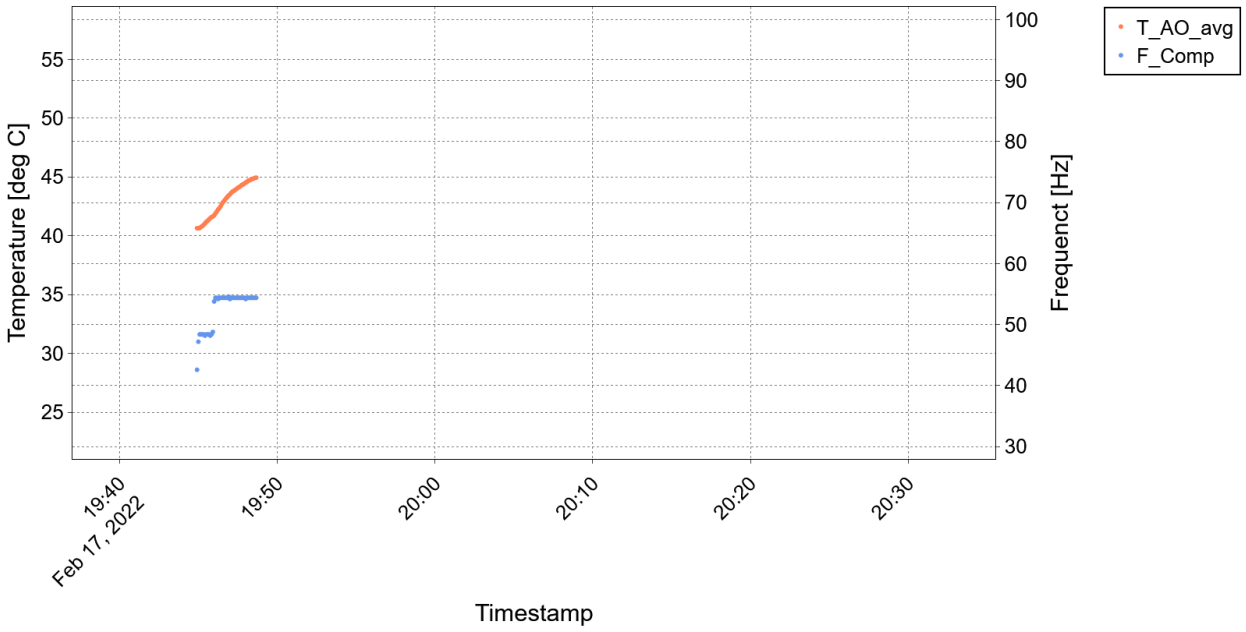


Figure 11: EFG-002 “transient” labeled data time series plot of average supply temperature (orange) and compressor frequency (light blue) over a specified time window.

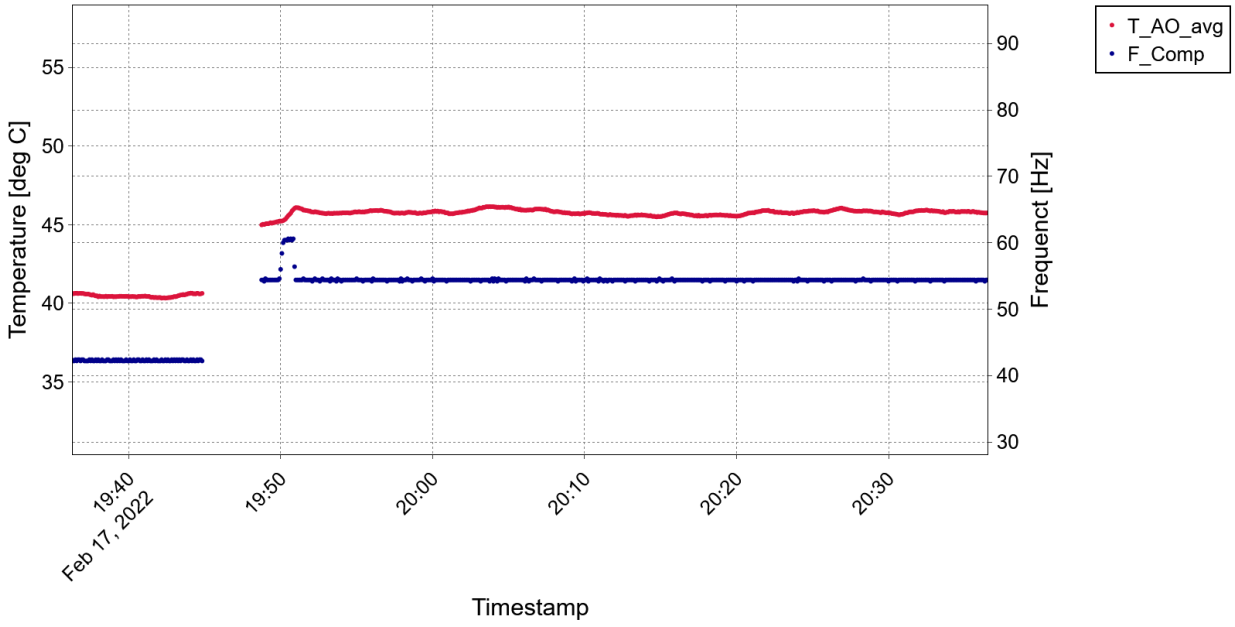


Figure 12: EFG-002 “steady-state” labeled data time series plot of average supply temperature (red) and compressor frequency (blue) over a specified time window.

Note that the resulting performance characteristics for steady-state data are dependent upon the temperature tolerance selected. While this tolerance was deemed sufficient, installations that

incorporate a heat pump with a more gradual heating approach (a slower temperature rise rate) may require stricter tolerances.

## Blower Airflow Data and Correlations

For both ducted and ductless systems, it was necessary to establish a correlation prior to testing between the indoor fan current and the airflow. The indoor unit's current draw was measured throughout the study, while the flow rate of air and fan speed was not. Therefore, prior to the start of the testing period, both the supply airflow rate and indoor fan current will be measured simultaneously to provide a measure of the flow rate of air being supplied to the room or area for each given fan speed and mode (heating versus cooling). The protocols to measure the indoor current and airflow to help build the correlations for ducted and ductless systems are detailed below. The correlation for determining the airflow from the current is discussed above.

### 4.1 Ducted systems

Airflow was measured using a TrueFlow device, which is an array of differential pressure velocity measurement probes that fits into an air handler filter enclosure. The Energy Conservatory produces the TruFlow device and has a nominal accuracy of 7% within the true value. For these tests, differential pressure was measured with a digital instrument with a minimum resolution of 1 Pa and an accuracy of ±2 Pa at the measurement condition.

A new system filter was installed at the start of the test, and additional filters were left at the site for routine changeouts. Fan current was measured using an analog current transducer with a nominal precision of ±2% at the measured condition. Pressure tests were done in both the heating and cooling modes.

### 4.2 Ductless systems

For ductless systems, a rigid enclosure was built around the discharge to capture all airflow. This was connected to a Duct Blaster, available from The Energy Conservatory. The Duct Blaster Fan speed was adjusted for a pressure in the enclosure of 0 ±2.5 Pa to ensure that the flow through the flow sensor on the Duct Blaster was the same as through the ductless heat pump. The Duct Blaster has a nominal flow accuracy of ±3%.

Figure 13 below is a simple sketch of an example system. The rigid enclosure was typically constructed of heavy cardboard, lightweight insulating board, or other rigid material—with all edges of the enclosure properly sealed.

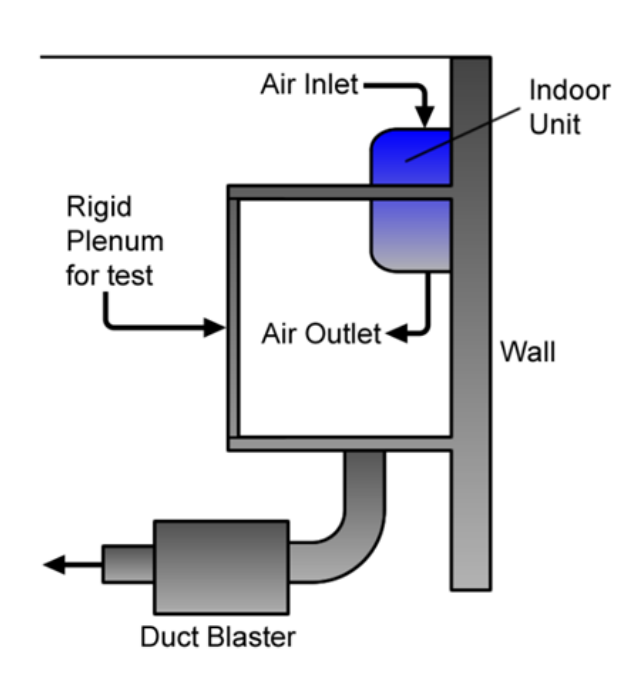


Figure 13: Airflow measurement setup for determining blower correlations.

As with the ducted units, flow and current measurements were made over a wide range of flows. Fan current was measured using an analog current transducer with a nominal precision of ±2% at the measured condition.

## 4.3 In-lab tests

Initial lab tests were conducted with team members from NREL and FE in December 2019. When conducting the duct blaster tests, the pressure at the plenum was set to 0, so the duct blaster was adjusted to match the pressure supplied by the indoor head. The duct blaster flow was also adjusted so the pressure at the plenum was both positive and negative. This allowed a correlation to be built so that when we only know the indoor current measurement, we will be able to calculate a flow rate. Figure 14 and Figure 15 show the indoor unit's current measurement correlation to the volumetric flow rate determined from the duct blaster tests for both heating and cooling, respectively.

In addition, the measurement was taken at very high and low pressures at the plenum to account for cases when the coil becomes wetted in very humid events or if the filters were blocked (in the protocol, we asked homeowners to change the filter every quarter and contractors supplied four filters at the beginning of the test). As seen in Figure 14 and Figure 15, there is some overlap in the correlations, specifically in the extreme cases (tail ends of the plots).

From the current measurement and correlation, the volumetric flow rate is determined. Using this value and the temperature difference between the supply and return (measured parameters), we can then calculate the output from the unit. Similarly, a COP from the unit is calculated by using the calculated output and measured input as described above in 3.4 Performance Calculations.

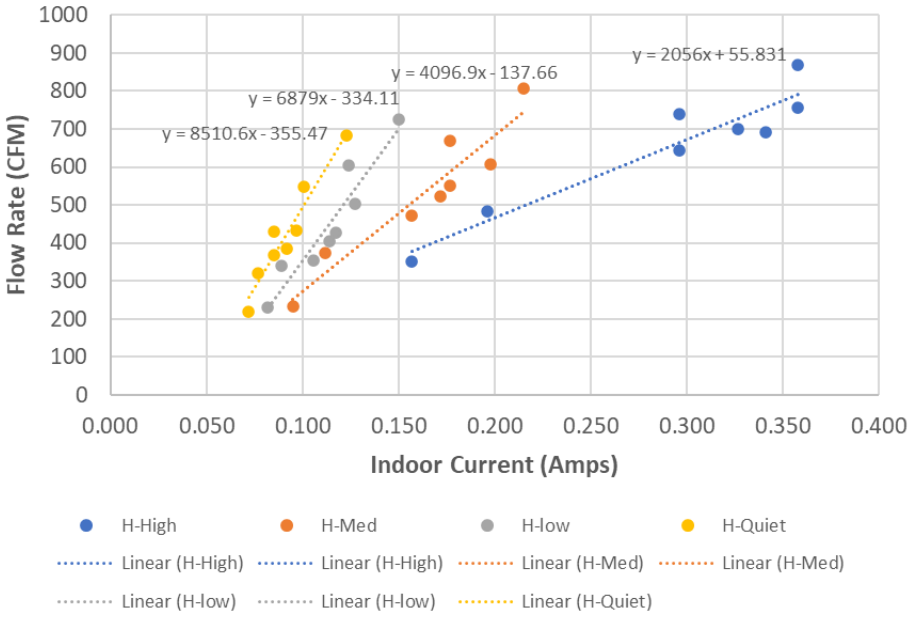


Figure 14: Heating fan curve- current vs flow rate

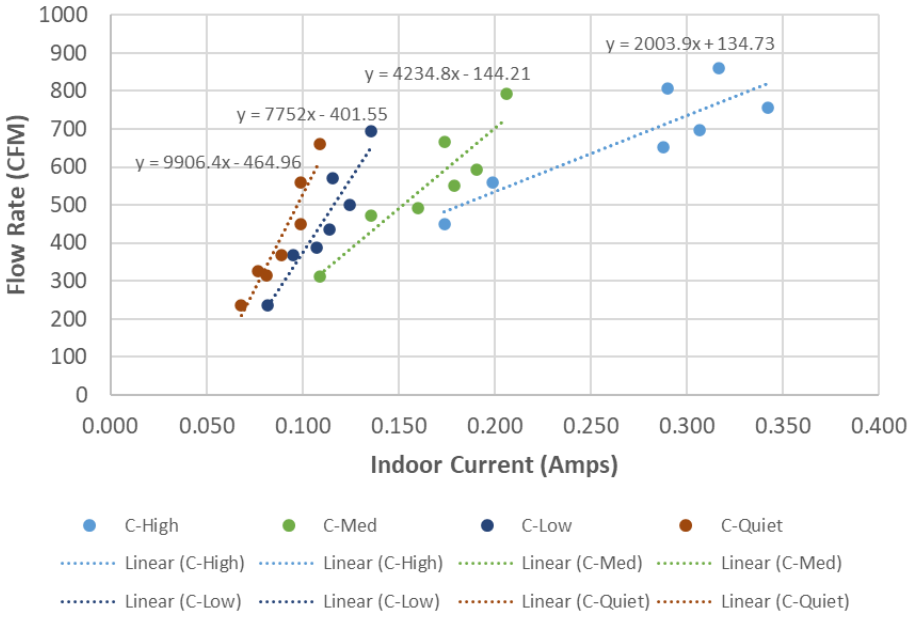


Figure 15: Cooling fan curve- current vs flow rate

## 4.4 In-field tests

Airflow testing on the ductless units raised concerns about the test protocol. The test protocol called for operating the indoor unit in fan-only mode to reduce the impact of air density variation and minimize the correction to standard conditions. Test results from two identical units (both indoor and outdoor components) at sites TLP-001 and TLP-002 indicated that the flow rate achieved for each fan setting was dramatically different in the heating mode versus the fan-only mode where most units were tested.

Both systems were the same outdoor unit paired with a single indoor head. The nominal system size is 2 tons. The only difference between sites was the thermostats—which ultimately impacted the available modes that could be tested and number of fan speeds that could be achieved. Site TLP-001 used an OEM-supplied thermostat that allowed for fan-only operation. The system was tested in all four fan speeds in the fan-only mode. The unit achieved a maximum flow of 305 SCFM (153 SCFM/ton). Site TLP-002 used a non-OEM thermostat that did not support the fan-only mode and only three speeds of operation. The airflow test was performed in the heating mode, and the results were corrected back to standard air conditions of 59°F. This unit reached a maximum of 500 SCFM (250 CFM/ton). These tests indicated that the amperage between the two units is consistent with the flow, and it can be strongly inferred that units directly control fan speed based on the operating mode.

Comparing the results from the two tests showed consistency in an overall flow/current relationship, but the TLP-001 results in fan-only are much lower than the TLP-002 results in heating, as shown in Figure 16.

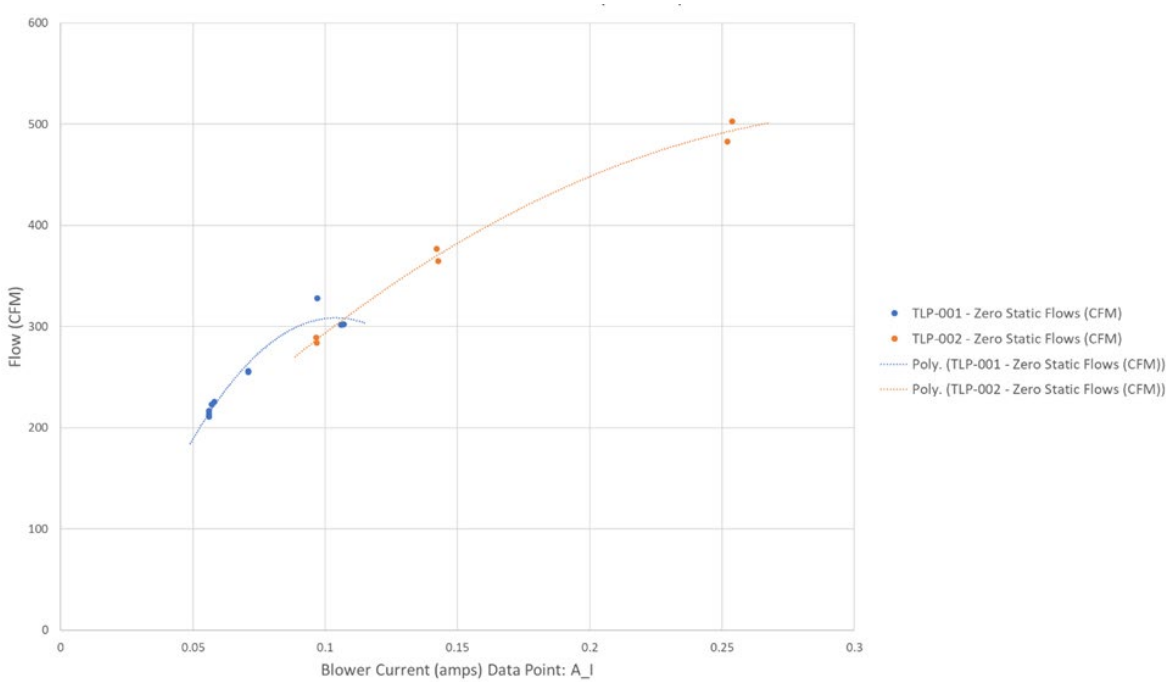


Figure 16: Airflow and current correlation for TLP-001 and TLP-002 comparison

There was concern that this may present a problem for other sites. EFG-007 was identified as a site where indoor fan current during heating mode (compressor Hz > 0) from the monitored data exceeded the maximum observed during the airflow test. This implied that the airflow testing for this site in fan-only does not fully capture the range of flows. EFG-007 reached 275 SCFM (183 SCFM/ton) during airflow testing.

The protocol only suggested looking at fan-only modes to do the airflow correlations; however, building fan curves in both heating and cooling modes may have been necessary. Team members looked further into site EFG-007 as a pilot site for additional airflow correlations to understand how they operate in fan-only mode versus heat loads and if this would lead to a different curve. The results are shown in Figure 17.

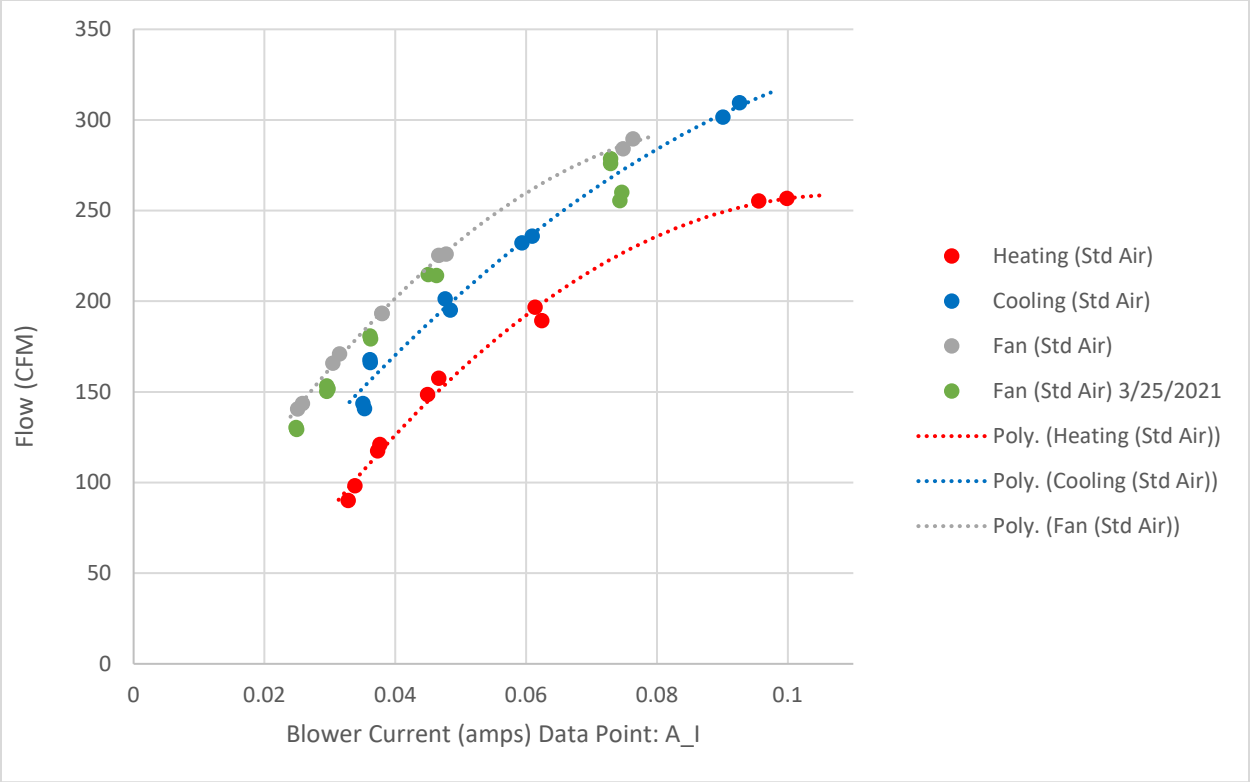


Figure 17: Airflow and current correlation in a fan-only and heating/cooling operation

Upon further testing, the test results showed that non-ducted units control the range of possible flow based on operating mode, and a fan-only characterization may not accurately characterize the flow. Future studies should develop fan curves for all modes tested. In detail:

- There was extreme repeatability between the fan-only test and the original results. This indicated that the testing protocol deployed was sound and repeatable.
- Cooling operation showed **SIMILAR** airflow to both tests – it was anticipated to have higher airflows for cooling.
- Heating operation showed **LOWER** airflow than both tests.
- All results were corrected based on discharge temperature back to 15 °C to account for density differences. The Duct Blaster measures ACFM based on fan pressure, and ACFM is influenced by the density of the air entering the Duct Blaster at high-pressure discharge temperatures.

## General Operating Results

Once the data was processed, it was discretized into 5-degree temperature bins based on the recorded outdoor temperature. The operating modes of the units were then characterized by the amount of time in hours spent in each temperature bin, the percentage of total time spent in each operating mode over the whole data collection period, and the fraction of time spent in each operating mode within that bin. The possible operation modes considered are steady-state compressor-based heating and cooling ('SteadyState_H' and 'SteadyState_C', respectively, and

no auxiliary heating or cooling), transient compressor-based heating and cooling ('Transient_H' and 'Transient_C', respectively, and no auxiliary heating or cooling), 'Defrost', 'Off', 'Fan Only', steady-state and transient combined heating ('SteadyState_Comb_H' and 'Transient_Comb_H'), and steady-state/transient supplemental heating ('SteadyState_Supp_H' and 'Transient_Supp_H'). Combined (denoted as 'SteadyState_Comb_H' or 'Transient_Comb_H') heating includes *both* compressor-based and auxiliary heating sources, whereas supplement heating only considers the auxiliary heating source. The results from the 21 sites are split into 3 subgroups: Ductless 1:1, Miscellaneous (Ducted, Ductless 1:2, and Mixed), and Air-to-Water, and are ordered from lowest maximum output to highest maximum output within the subgroup.

Sufficient data collection is critical in determining a conclusive statement regarding performance. The cumulative hours spent in each operational mode throughout the entire data collection period substantiates the rationale for specific performance parameters within particular temperature ranges. For instance, a computed COP exceeding or falling below expectations in a temperature range gains greater substantiation with several hundred hours of recorded data, as opposed to a solitary hour. Sites with minimal hours collected in a given temperature bin may be subject to artificially high or low calculated COPs. Consequently, greater reliability should be attributed to performance attributes corresponding to temperature ranges with more substantial data volumes.

Moreover, determining how often these devices are on in general is important for evaluating their use as a primary heating/cooling source and oversizing concerns, if any. For example, if the unit is on in a mild-heating bin 100% of the time, it could be undersized for lower outdoor temperatures and higher heating demands. Or, if the unit is only operating ~50% of the time during the heating season, the unit may be oversized, or an auxiliary heat source may be employed.

Figure 18 depicts the hours of data collected for the ductless 1:1 sites and shows a large disparity between the number of heating and cooling hours collected at each site—with the majority of sites having significantly more heating hours recorded. EFG-001, EFG-006, and EFG-004 have more balanced heating and cooling hours, while EFG-002 and EFG-007 almost exclusively collected heating data. Sparse amounts of data were collected relative to the other sites for sites TLP-001 and TLP-004. These units were off for nearly 90% of the observation period, as illustrated by Figure 19. Some site issues were observed during testing that may explain the low-use patterns and are detailed in Section 8.1 Equipment Issues and Underutilized Systems. While most of the heat pumps in this study were capable of modulation, each site spent a significant amount of time in the 'Off' mode. This may be due to the use of auxiliary heat; however, many of the homeowners indicated that the heat pump was their primary source of heat for the given location. Across the ductless 1:1 sites, the relative amounts of time spent in the transient heating mode compared to the steady-state heating mode varied.

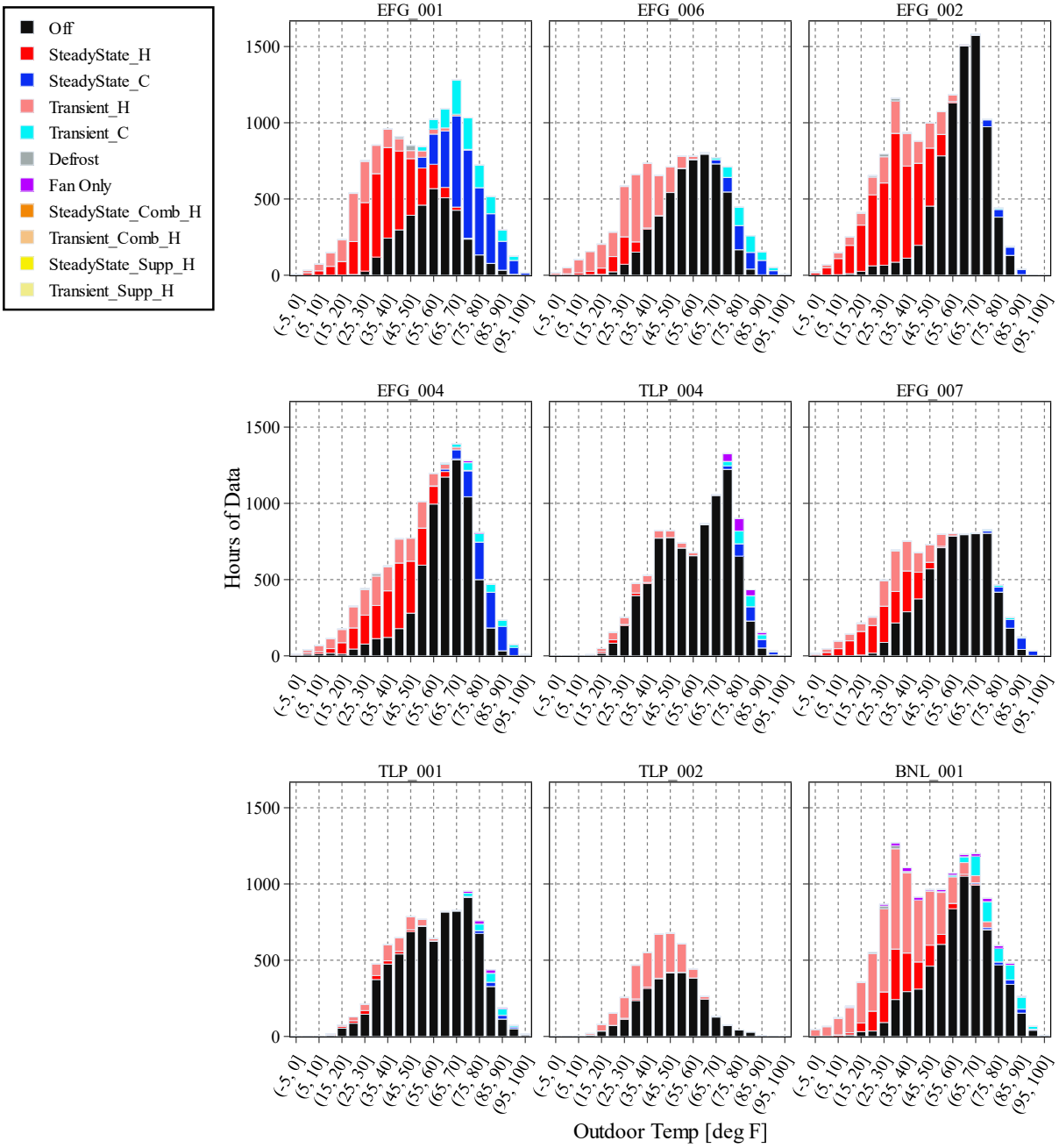


Figure 18: Hours of data collected binned by outdoor temperature colored by operating mode for ductless 1:1 sites.

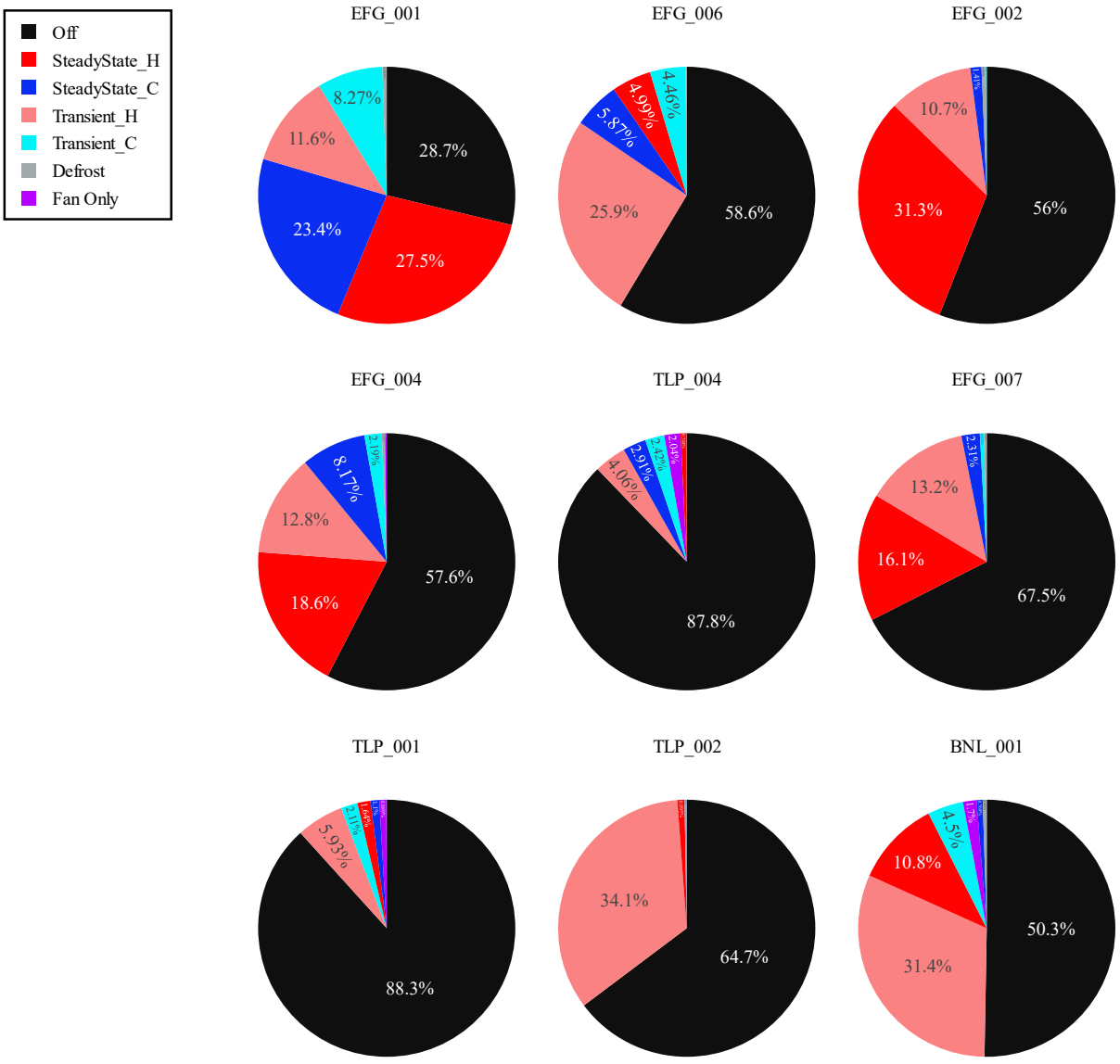


Figure 19: Percentage of total time in each operating mode for ductless 1:1 sites.

The general operating mode information for the ducted, ductless 1:2, and mixed sites is included in Figure 20 and Figure 21. Similar to the non-ducted sites, the ducted, ductless 1:2, and mixed sites also spent a significant amount of time in the 'Off' mode—with all besides CEE_003 spending more than 50% of the monitoring period in an 'Off' mode. Additionally, of the ducted sites with auxiliary heating systems directly monitored, supplemental heating only accounted for

a small percentage of time (< 7%). Overall, the amount of total heating and cooling hours across sites varied, with sites CEE-002, EFG-009, EFG-005, and EFG-003 having balanced heating and cooling hours. Meanwhile, sites TLP-003 and EFG-008 collected more heating hours than cooling.

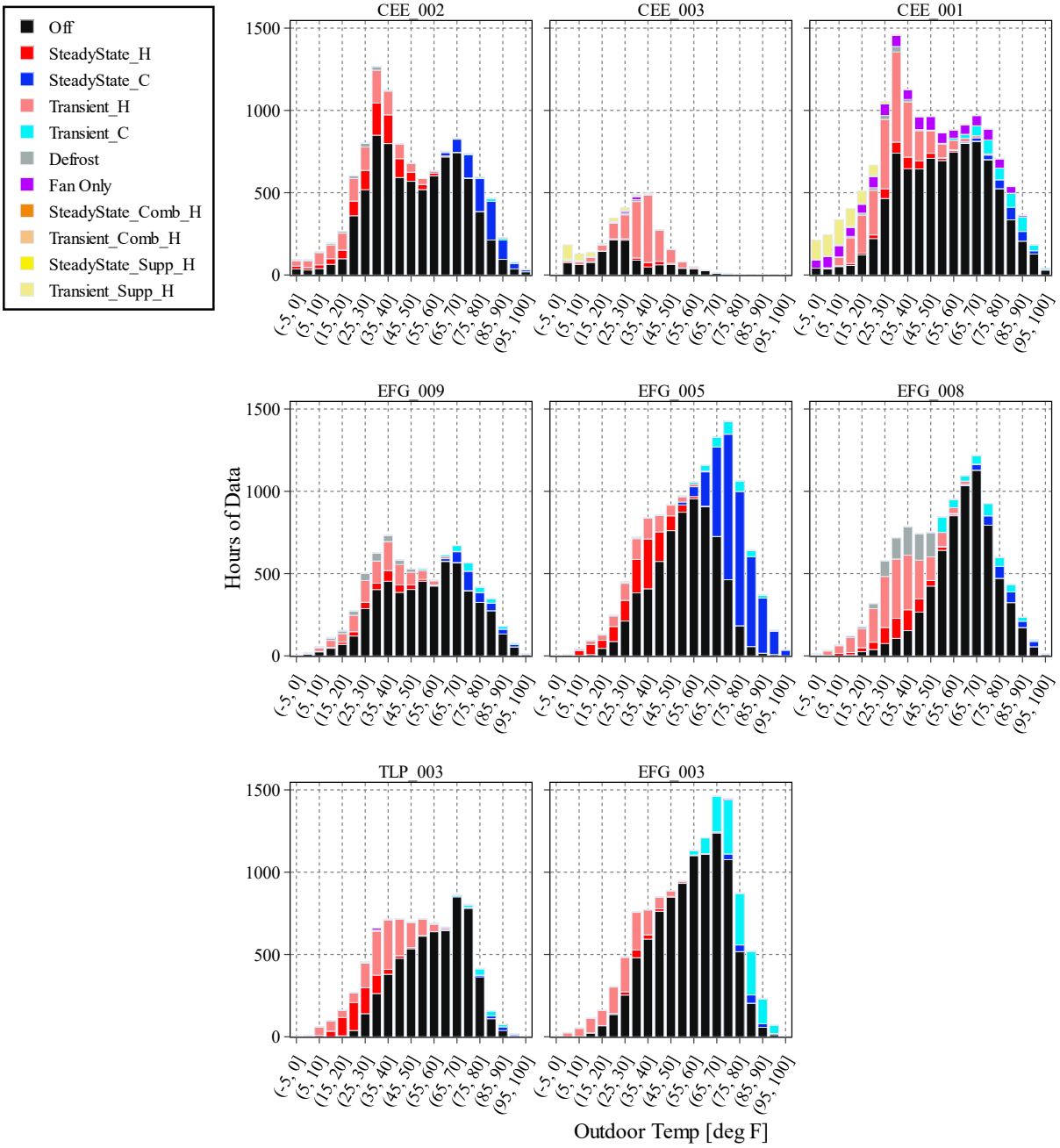


Figure 20: Hours of data collected binned by outdoor temperature colored by operating mode for ducted, non-ducted 1:2, and mixed sites.

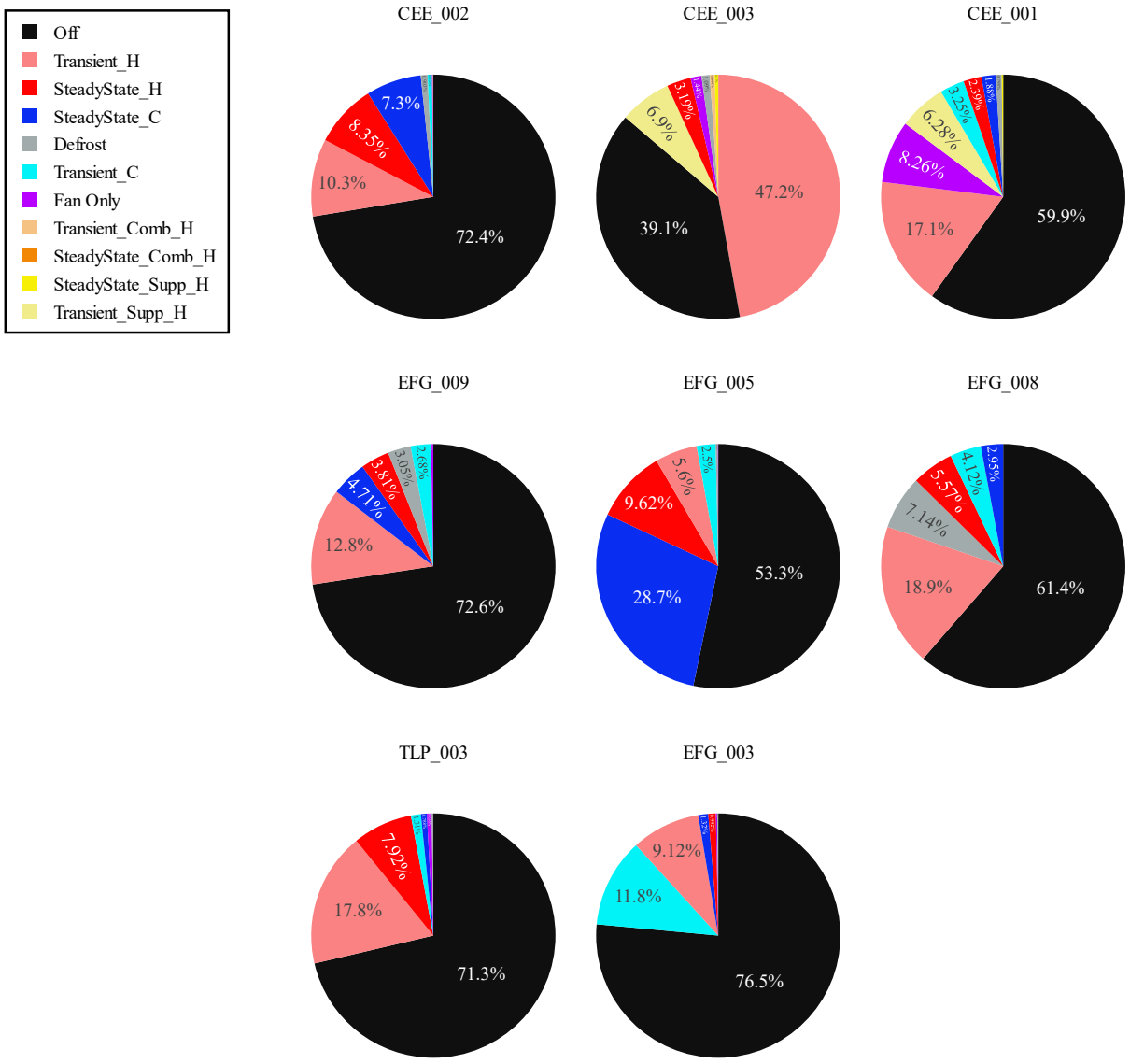


Figure 21: Percentage of total time in each operating mode for ducted, non-ducted 1:2, and mixed sites

Lastly, the overall operating mode divisions during the data collection period for the air-to-water sites are visualized in Figure 22 and Figure 23. For all the air-to-water sites, the majority of time was spent in the 'Off' mode, with some sites showing more supplemental heat use than others. In explanation, the heating capacity for the air-to-water sites compared to the ductless and centrally ducted sites is high, roughly twice the heating capacity. Conversely, the heating area served at

these sites was in the range of the ductless sites and smaller than the centrally ducted sites. Based on these site characteristics, the air-to-water heat pumps may be oversized, resulting in low usage. In detail, the AWHP1 site is not well insulated but standard code compliant. Alternatively, site AWHP3 is well insulated. As seen in Figure 22 and Figure 23, sites AWHP2 and AWHP4 have low utilization. Site AWHP2 provides heat for a 1088 sq. ft. separate home office building. This building is very well insulated with 1.5 inches of foam insulation over 3.5 inches of batt insulation in the wall. The ceiling has 2' X 8' trusses with spray foam over 6 inches of batt insulation. This building has been refitted with all low-temperature hydronic thermal distribution, including panel radiators and in-floor radiant heating. There is a backup heating boiler that is manually controlled by the owner and rarely used. In contrast, site AWHP4 is not well insulated but standard code compliant with baseboard heat that was able to run at low water temperatures. The AWHP4 also had an electric boiler as backup.

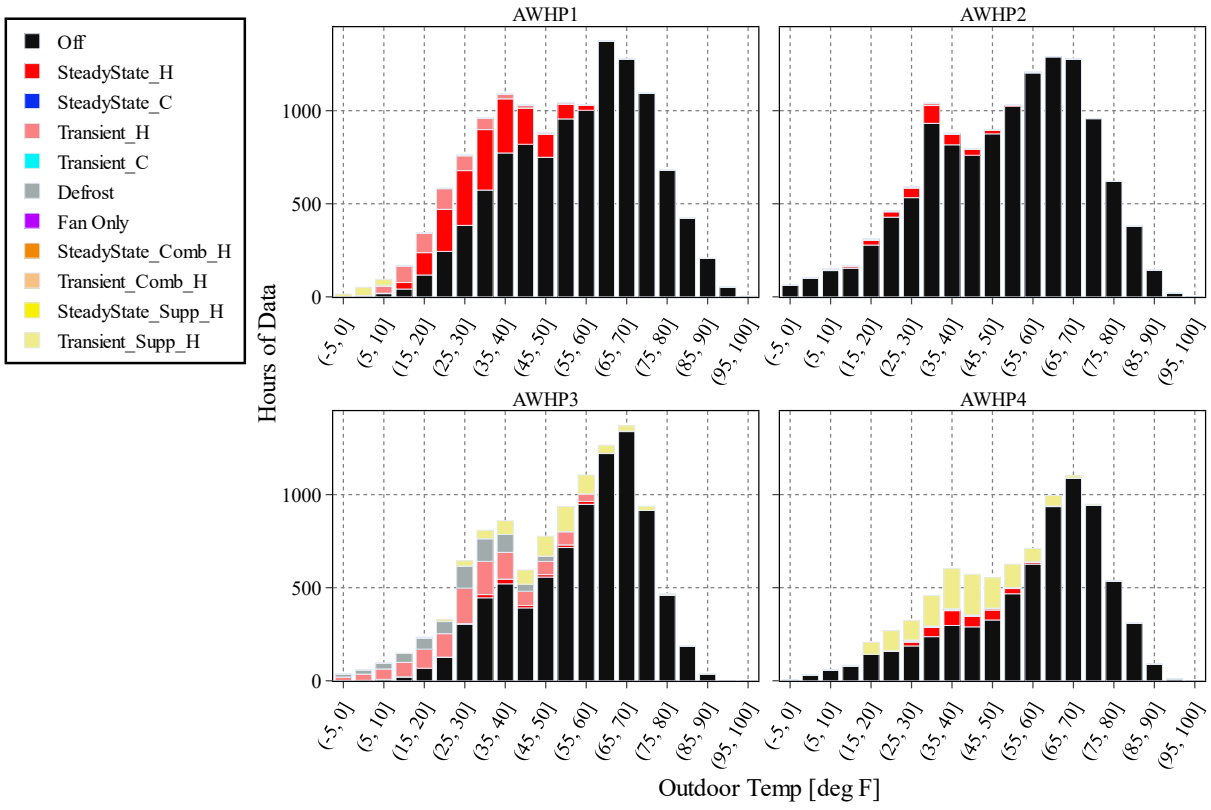


Figure 22: Hours of data collected binned by outdoor temperature colored by operating mode for air-to-water sites

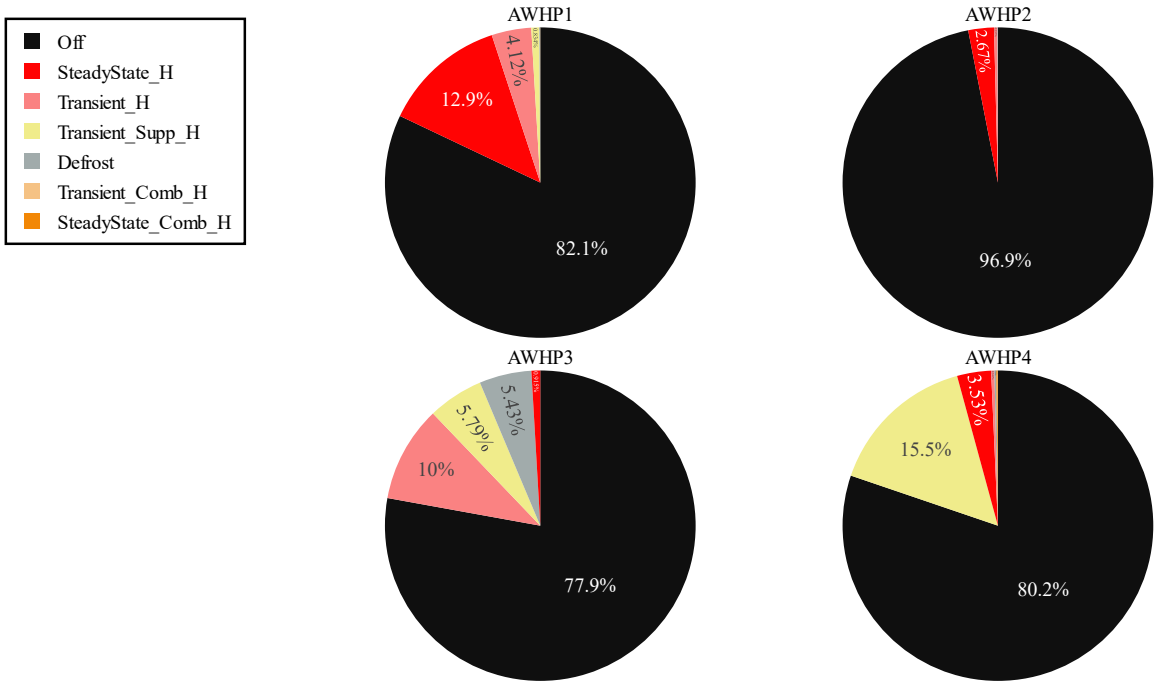


Figure 23: Percentage of total time in each operating mode for air-to-water sites

Further investigations into the impact of outdoor temperature on the operation mode of the heat pumps were performed. A runtime fraction plot, varying from 0 (no occurrence) to 1 (always), summarizes the portion of the data collected at each temperature bin that corresponds to a particular operation mode. Comparing the time spent in a heating mode—steady-state versus transient and off may provide some insight into the sizing factor. Furthermore, the fraction of time spent in defrost mode and the fraction of time supplemental heating is utilized are important to quantify, as these will undoubtedly be relevant in determining how these devices operate in cold climates under real-world operation. Figure 24 shows the runtime fraction for the ductless 1:1 sites, Figure 25 for the ducted, ductless 1:2 and mixed sites, and Figure 26 for the air-to-water sites.

As seen in Figure 24, the ductless 1:1 units spent the majority of time in a heating mode, steady-state or transient, during the lower temperature bins. Sites with a steady-state heating fraction greater than transient or off may be more appropriately sized for the space they are conditioning or have fewer defrost events occur. However, it is difficult to accurately determine the oversizing of ductless units only heating a portion of the home or open area without the ability to isolate the desired conditioned space from the remaining portion of the home.

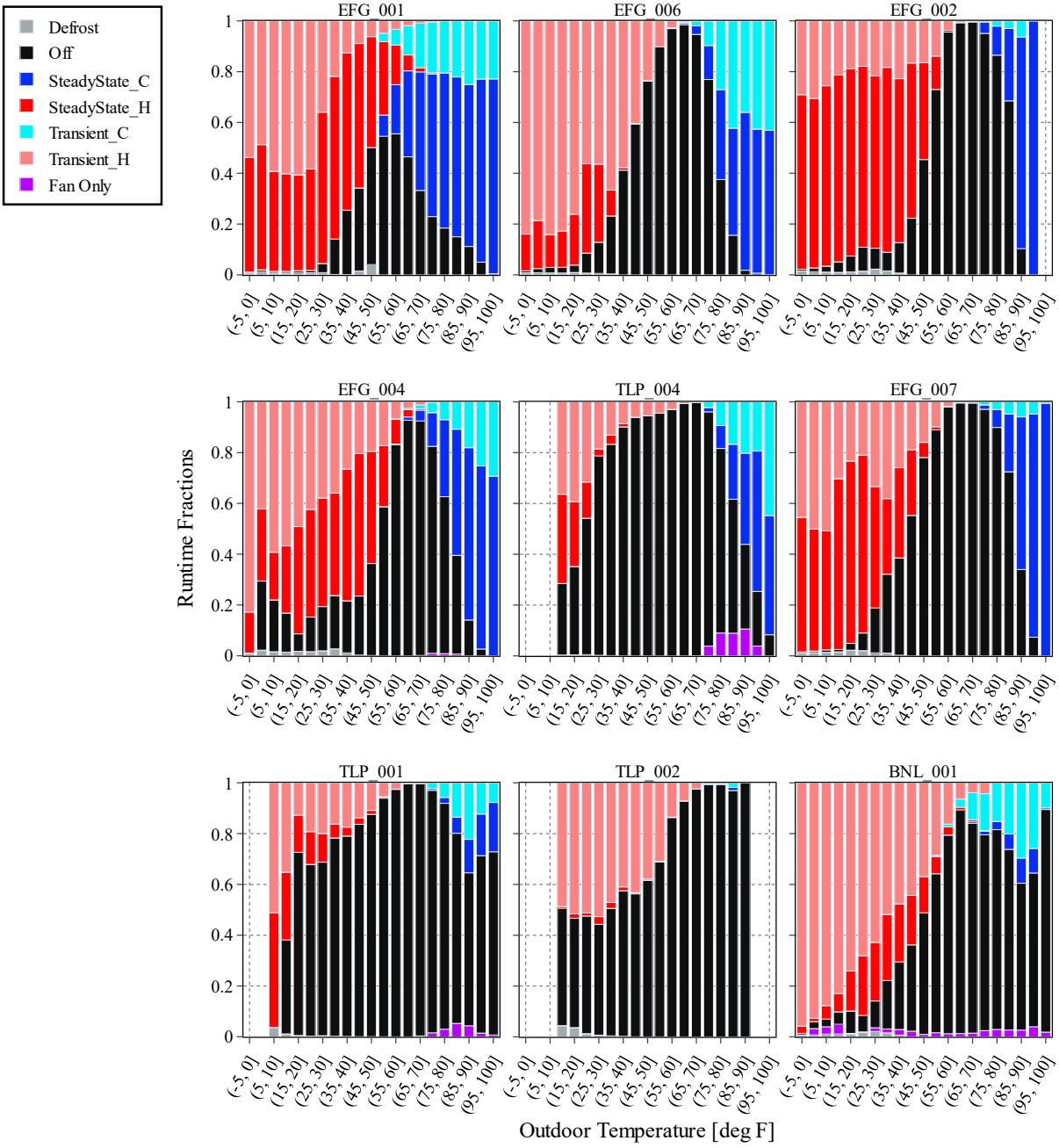


Figure 24: Fraction of time spent in each mode binned by outdoor temperature for ductless 1:1 sites

Some ducted sites showed a significant amount of time spent in the heating (steady-state or transient) mode during lower outdoor temperatures, while other units showed significantly more time spent in the 'Off' mode. Sites such as CEE-001 and CEE-003 indicated notably elevated usage of supplemental heat in colder periods compared to the heat pump's contribution. This suggests that the heat pump's capability to meet demand diminishes at temperatures below 15 °F. Transient modes could be linked to defrost cycles or on/off cycling. Notably, sites with a

substantial share of time spent in transient heating rather than steady-state heating might signify oversizing, as heating demand gets met prior to achieving steady-state operation. Although this observation may not be immediately apparent from the overall percentage (as seen in Figure 23), examining operation modes by outdoor temperature reveals significant transient heating even at the lowest outdoor temperatures considered. However, without an energy audit, determining accurate oversizing becomes challenging. Unfortunately, for ductless units and sometimes ducted units, auxiliary heat sources are often employed, making it necessary to evaluate their loading/oversizing based on their operational patterns. In such cases, an energy audit may not provide insights into understanding oversizing effectively.

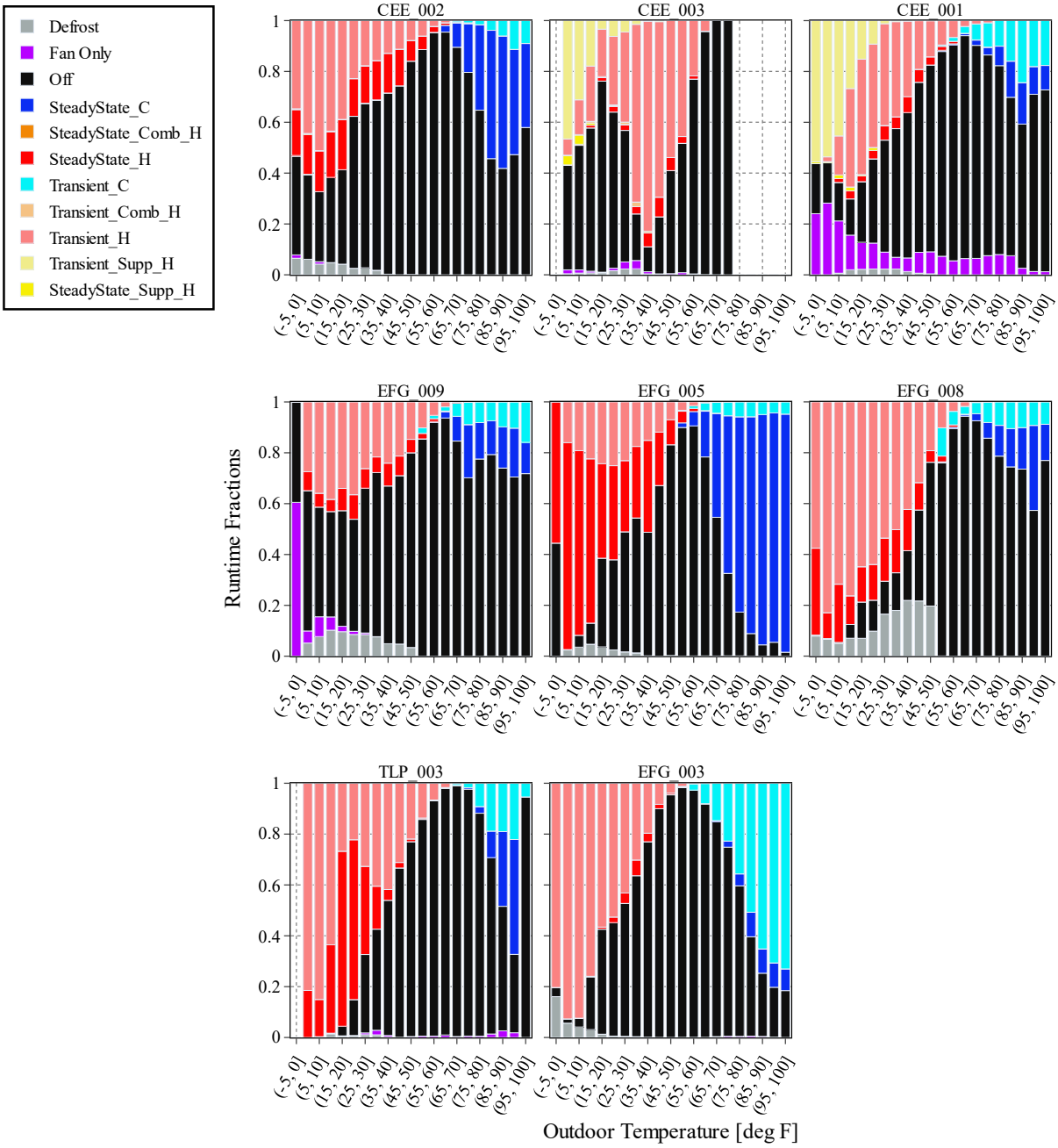


Figure 25: Fraction of time spent in each mode binned by outdoor temperature for ducted, non-ducted 1:2, and mixed sites

The runtime fractions for the air-to-water sites in Figure 26 have wildly different characteristics. Site AWHP1 shows what would be considered the expected operation, exclusively utilizing the heat pump at warmer outdoor temperatures and relying on a mixture of supplemental heating and

compressor-based heating as outdoor temperatures are driven lower. Once the outdoor temperature is subzero, the unit solely relies on supplemental heating. In contrast, site AWHP2 shows no supplemental heating at subzero temperatures, but as stated previously, the auxiliary heat was rarely used, and the home was very well insulated. Site AWHP3 shows a trend of decreased supplemental heating as the outdoor temperature is driven lower and an extremely high defrost percentage. Since our developed algorithm cannot distinguish between defrost and a period of time when supplemental heating is used simultaneously during a defrost event, it is likely that some of the supplemental heating is lumped in with the 'Defrost' periods.

For site AWHP4, the unusually large fraction of 'Off' time may be explained due to the low amount of data collected in colder temperatures. The dataset captured fewer than 200 total hours at the lower end of the temperature spectrum, and the instances of low outdoor temperatures were non-consecutive. Rather than several days at low outdoor temperatures, the site likely saw small dips into the lower temperature bins when there was no operation. If the site had accumulated more data hours under consistently low temperatures, the 'Off' time percentage might have aligned more closely with the trends exhibited by similar sites.

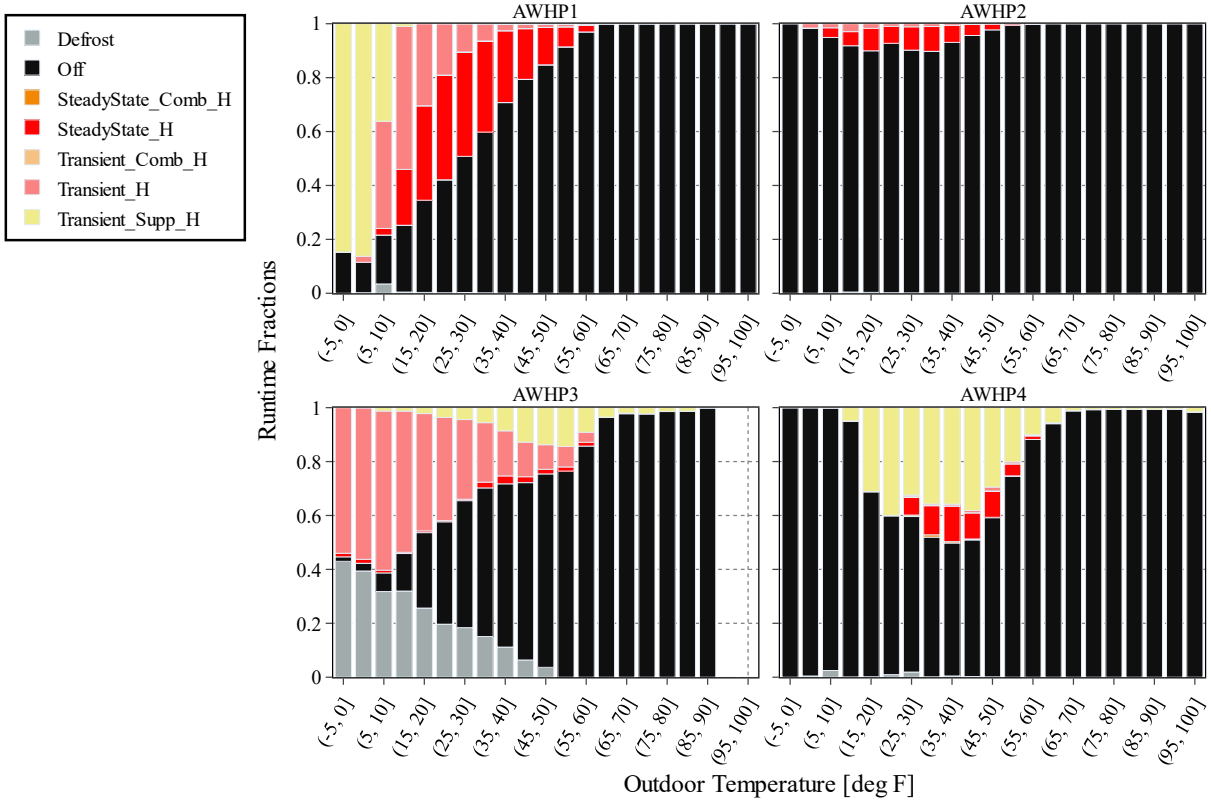


Figure 26: Fraction of time spent in each mode binned by outdoor temperature for air-to-water sites

The most common operation mode at various operation temperatures for all sites is summarized in Table 6. Overall, a significant amount of transient heating (Transient_H) is observed at the

lowest outdoor temperature considered, with 8 out of 21 sites being in this operating mode at 5 °F. As the outdoor temperature increases to mild temperatures, such as at 47 °F, all but two sites were off for most of the data collection period at this outdoor temperature. Steady-state cooling (SteadyState_C) occurred more often than steady-state heating (SteadyState_H) for 4 out of 21 sites at the highest and lowest temperatures, respectively.

The number of cycles within each temperature range is crucial to ascertain the reason behind heightened transient conditions. In particular, it's essential to determine whether the increased cycling operation results from defrost events or is a consequence of oversizing. To determine the latter, the room temperature measurements would provide insight as to whether the conditioned space was increasing in temperature quickly, meeting the demand setpoint, and then cooling quicker, resulting in more frequent, short cycles—and a higher percentage of transient operation. To determine if the transient conditions were a result of defrost events, observing the frequency of defrost cycles (or fraction of time) would shed some insight. Ultimately, if the defrost time or frequency of occurrence was increased at 5 °F, accompanied by minimal on/off cycle counts, this would suggest that transient operation could be attributed to defrost events. Alternatively, if the defrost time or frequency of occurrence decreased at 5 °F, but the number of cycles was substantial, it would suggest that transient operation may result from oversizing. Depending on the site, both of these situations were observed.

For a well-designed home heating system featuring a heat pump with an auxiliary heat source, the supplemental heat source would only be used when the heat pump system cannot meet the required heat demand, i.e., during temperatures below the design day temperature. Our analysis revealed that supplementary heating takes precedence over heat pump-based heating in five out of six sites where supplementary heating was recorded. Sites CEE-001, CEE-003, and AWHP-001 exhibited extended periods of supplementary heating, particularly during the coldest temperature ranges, as anticipated. In the case of Site AWHP3, the supplementary heating operation may have been grouped with the defrost operation, making it challenging to differentiate between supplementary heat used simultaneously during heat pump defrost events and independent defrost periods. As for AWHP4, although there wasn't a consistent data collection at markedly low temperatures to explain performance below 15 °F, an unusually high proportion of supplementary heating was still observed at temperatures exceeding 30 °F. This peculiarity is noteworthy, as it deviates from other homeowner explanations wherein disparate fuel and electricity costs might prompt homeowners to favor supplementary heating. Notably, the supplementary heating employed at this site was an electric boiler, which should theoretically provide no cost advantage over utilizing a heat pump.

Table 6: Dominant Operation Mode at Various Operation Temperatures for All Sites.

| Site Name | Most Common Operation Mode at Rated Outdoor Temperatures | | | | |
|---|---|---|---|---|---|
| | 5 °F | 17 °F | 47 °F | 82 °F | 95 °F |
| Ductless 1:1 | | | | | |
| EFG-001 | SteadyState_H | Transient_H | Off | SteadyState_C | SteadyState_C |
| EFG-006 | Transient_H | Transient_H | Off | Transient_C | SteadyState_C |
| EFG-002 | SteadyState_H | SteadyState_H | Off | Off | SteadyState_C |
| EFG-004 | Transient_H | Transient_H | SteadyState_H | SteadyState_C | SteadyState_C |
| TLP-004 | N/A | Transient_H | Off | Off | SteadyState_C |
| EFG-007 | SteadyState_H | SteadyState_H | Off | Off | SteadyState_C |
| TLP-001 | N/A | Off | Off | Off | Off |
| TLP-002 | N/A | Transient_H | Off | Off | Off |
| BNL-001 | Transient_H | Transient_H | Off | Off | Off |
| Ducted and Mixed | | | | | |
| CEE-002 | Transient_H | Transient_H | Off | SteadyState_C | Off |
| CEE-003 | Transient_Supp_H | Off | Transient_H | N/A | N/A |
| CEE-001 | Transient_Supp_H | Transient_H | Off | Off | Off |
| EFG-009 | Off | Off | Off | Off | Off |
| EFG-005 | SteadyState_H | SteadyState_H | Off | SteadyState_C | SteadyState_C |
| EFG-008 | Transient_H | Transient_H | Off | Off | Off |
| TLP-003 | Transient_H | SteadyState_H | Off | Off | SteadyState_C |
| EFG-003 | Transient_H | Transient_H | Off | Transient_C | Transient_C |
| Air-to-Water | | | | | |
| AWHP1 | Transient_Supp_H | SteadyState_H | Off | Off | Off |
| AWHP2 | Off | Off | Off | Off | Off |
| AWHP3 | Transient_H | Transient_H | Off | Off | Off |
| AWHP4 | Off | Off | Off | Off | Off |

# Heating Mode Performance Results

## 6.1 Coefficient of Performance

The average COP in each temperature bin was computed for each site with its associated uncertainty using the statistical error approach discussed in section 3.4 Performance Calculations. Larger error bars indicate a wider spread of COP and fewer data points collected in this temperature bin. The General Operating Results section may be referred to in discussing the results of this section. In this analysis, the COPs given in the text and the figures refer to the calculated COP using Eqn. (11) (which relies on Eqn. (2) and Eqn. (10)) for periods that were designated as in the 'SteadyState_H' mode. For comparative purposes, the rated COPs for the unit at its maximum and minimum output at 5 °F, 17 °F, and 47 °F are also included on the plots in purple and green, respectively.

The calculated average steady-state COP in each temperature bin for all ductless 1:1 sites is shown in Figure 27. A minimum COP of 1.32 at 5 °F occurred at EFG-002, while a maximum of 2.65 occurred at EFG-006. While the units were different in terms of manufacturer, they were of similar capacity and rated performance. However, the conditioned space at EFG-006 was nearly four times smaller in size than EFG-002. While this smaller conditioned space caused the unit to experience more transient heating, as shown in Figure 24, the heat output may have been closer to the minimum rated output due to the reduced heating demand. Further investigations in subsequent sections on output ranges and power consumption are necessary to form a definitive conclusion. In general, the COPs increased with increasing outdoor temperature to a maximum of 3.84 at 47 °F at EFG-001 and a minimum of 1.97 at EFG-004. Both units match the performance data for their COP at the maximum tested output and differ in size and capability. Consequentially, the resulting difference in performance is justifiable. In most cases, the calculated COP fell near or below the minimum rated COP values.

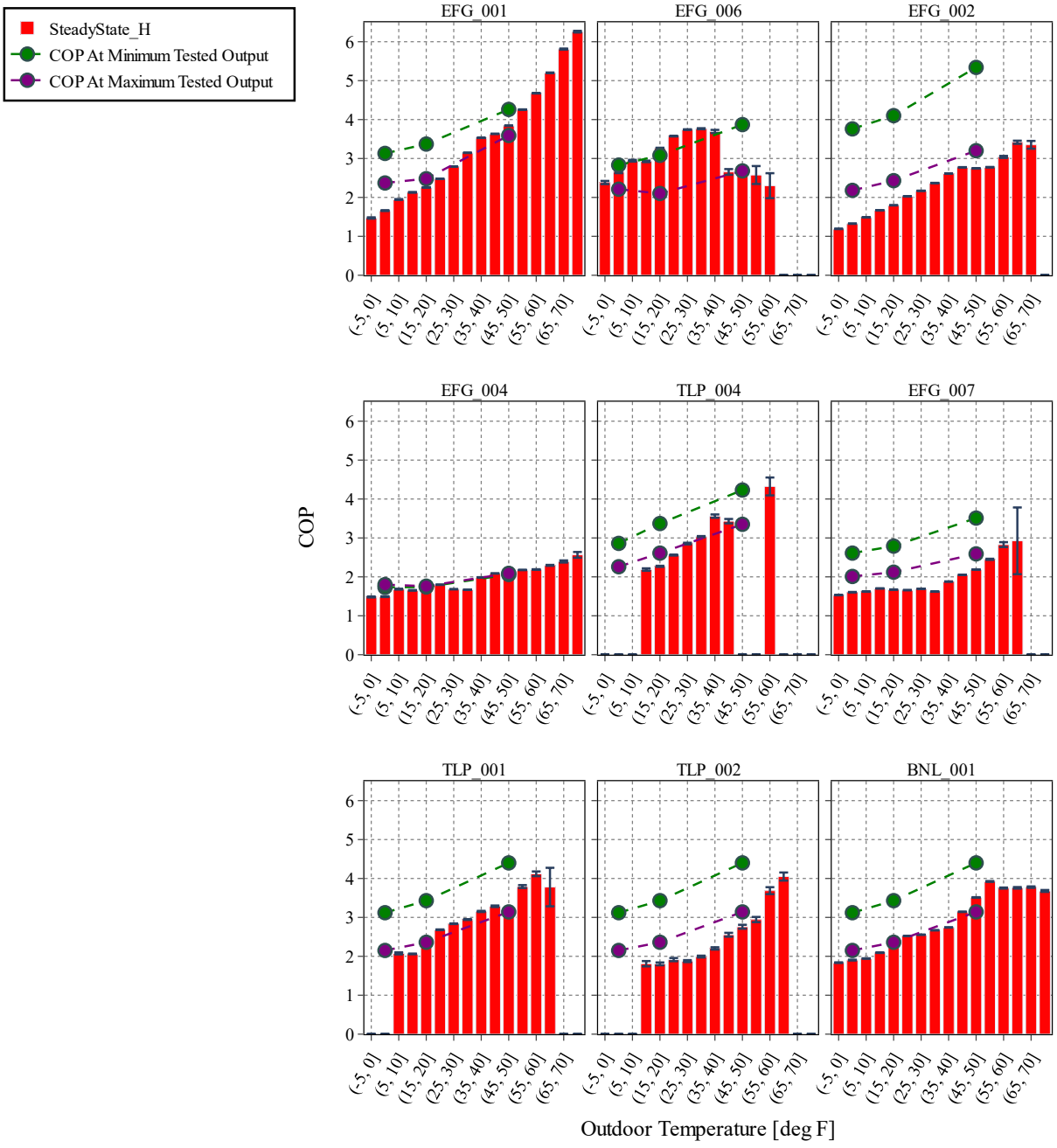


Figure 27: Steady-state heating COPs against available unit performance data for ductless 1:1 sites

Figure 28 shows the average steady-state COP in each temperature bin for all ducted, ductless 1:2, and mixed sites. The minimum COP at 5 °F was 1.31 at EFG-008, while a maximum of 3.46 occurred at CEE-002. CEE-002 is a centrally ducted site, while EFG-008 is a ductless 1:2, so the performance difference may be owed to that. The COP at CEE-002 is well above the rated COP at this temperature and may indicate undetected power sensor failures, as this site was prone to them

throughout the observation period. Once again, the COPs increased with increasing outdoor temperature to a maximum of 4.17 at 47 °F at EFG-005 and a minimum of 2.5 at CEE-002. The COP values assigned to EFG-008 were sourced directly from NEEP. It is plausible that the unit performs more efficiently (with a higher COP) at the minimum rated output compared to the maximum rated output under low-temperature conditions, possibly due to substantial icing effects from defrost.

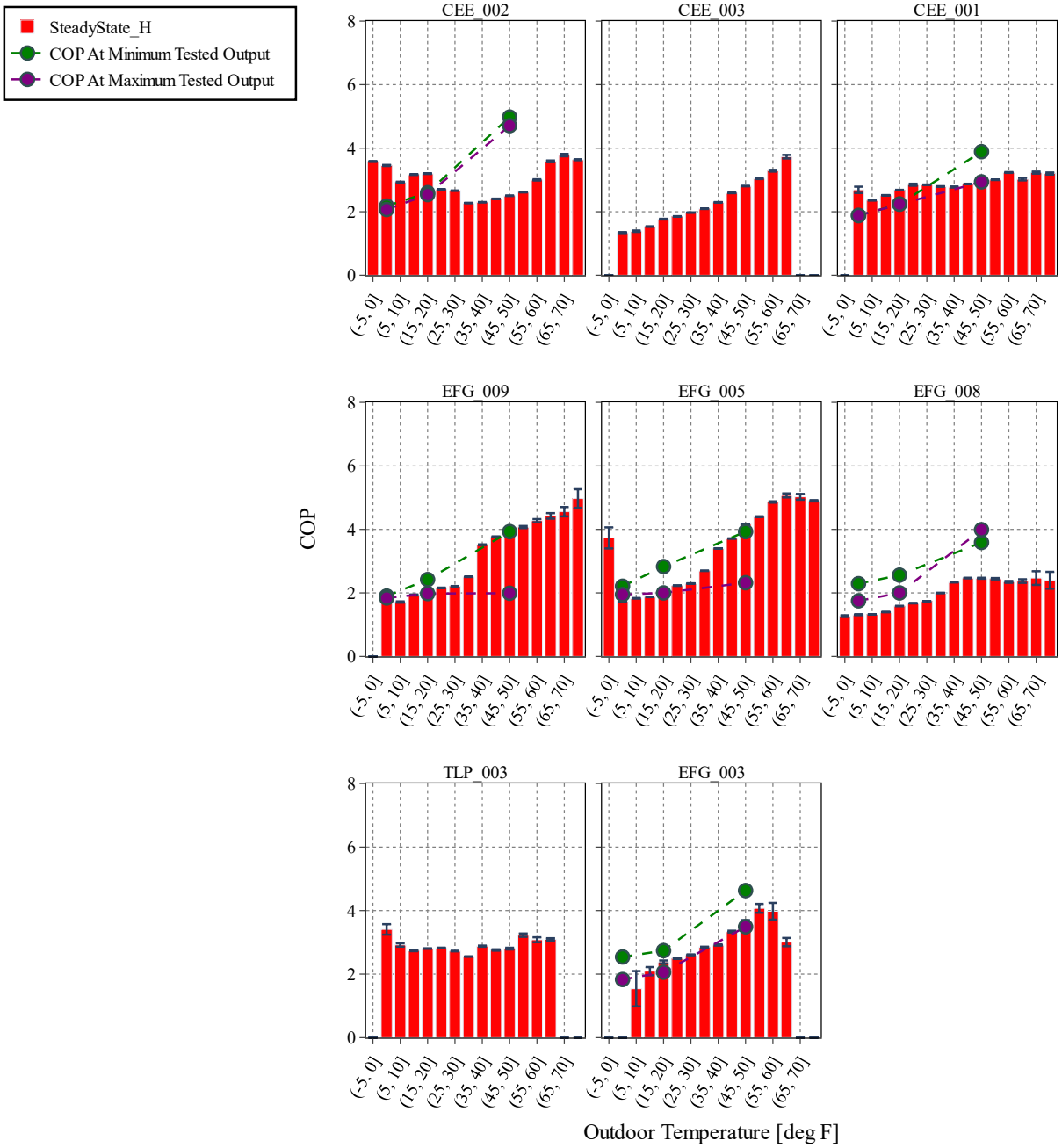

Figure 28: Steady-state heating COPs against available unit performance data mode for ducted, non-ducted 1:2, and mixed sites

Lastly, the average COP in each temperature bin for all air-to-water sites is displayed in Figure 29. No reported COPs were available for the air-to-water sites and, therefore, are not included in the figure for comparison. The air-to-water sites studied were all the same unit, and across all four sites, the average COP at 5 °F, 17 °F, and 47 °F were 1.56, 1.72, and 2.57, respectively. The minimum COP at 5 °F occurred at AWHP2, while the maximum occurred at AWHP3. The COPs increased with increasing outdoor temperature to a maximum of 2.98 at 47 °F at AWHP3 and a minimum of 2.03 at AWHP4.

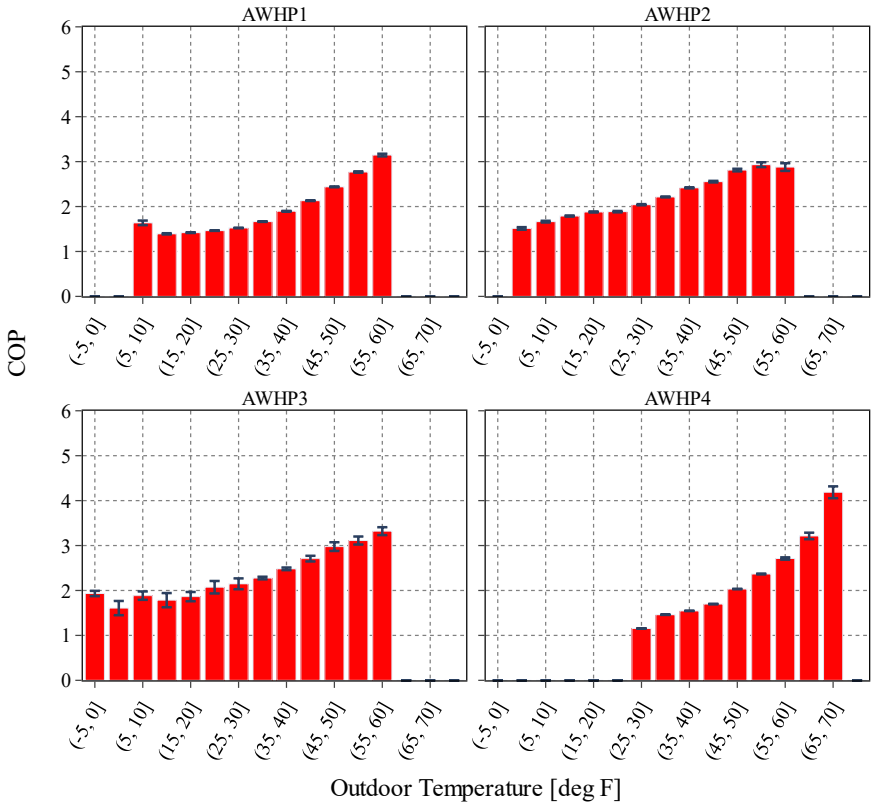


Figure 29: Steady-state heating COPs against available unit performance data for air-to-water sites

In summary, our findings indicate that heating COP generally increased with increasing temperature, as shown in Table 7. This trend is expected based on the thermodynamic limitations on performance imposed by the vapor-compression cycle; the peak COP should be approached as the outdoor temperature approaches the indoor setpoint temperature. For temperature bins where no steady-state heating data was collected, a value of 'N/A' is assigned. It should be noted that there may have been supplemental heat or transient heat operation at the low temperatures, but no

steady-state heat operation was captured. Only 11 of the 15 sites with available performance data matched closely with their rated values. The remaining four sites had COPs outside the expected range. In particular, EFG-007, EFG-002, EFG-008, and CEE-002 all had COPs below their rated values for some portion of the temperature ranges considered. A possible reason for this difference is debris buildup in the outlet of the heat pump if the filter is not regularly cleaned. This may reduce the heat transfer effectiveness to the return air and result in a lower overall output at the same level of power consumption, which is explored in subsequent subsections. Another potential cause may be errors in the initial airflow correlation development, the impact of which is discussed in section 8.4 Airflow Correlations.

Table 7: Summary of Steady-state COP at Various Operation Temperatures Across All Sites During Heating Mode.

| Site Name | Average Steady-state COP at Rated Outdoor Temperatures | | |
|---|---|---|---|
| | 5 °F | 17 °F | 47 °F |
| Ductless 1:1 | | | |
| EFG-001 | 1.66 | 2.26 | 3.84 |
| EFG-006 | 2.65 | 3.26 | 2.64 |
| EFG-002 | 1.32 | 1.80 | 2.75 |
| EFG-004 | 1.49 | 1.67 | 1.97 |
| TLP-004 | N/A | 2.27 | N/A |
| EFG-007 | 1.61 | 1.67 | 2.19 |
| TLP-001 | N/A | 2.44 | 3.19 |
| TLP-002 | N/A | 1.81 | 2.76 |
| BNL-001 | 1.90 | 2.40 | 3.51 |
| Miscellaneous (Ducted, Ductless 1:2, Mixed) | | | |
| CEE-002 | 3.46 | 3.20 | 2.50 |
| CEE-003 | 1.34 | 1.77 | 2.81 |
| CEE-001 | 2.69 | 2.68 | 2.97 |
| EFG-009 | 1.78 | 1.96 | 3.98 |
| EFG-005 | 1.73 | 2.09 | 4.17 |
| EFG-008 | 1.31 | 1.57 | 2.46 |
| TLP-003 | 3.41 | 2.80 | 2.80 |
| EFG-003 | N/A | 2.38 | 3.67 |
| Air-to-Water | | | |
| AWHP1 | N/A | 1.42 | 2.44 |
| AWHP2 | 1.51 | 1.88 | 2.81 |
| AWHP3 | 1.61 | 1.86 | 2.98 |
| AWHP4 | N/A | N/A | 2.03 |
| Summary | | | |
| Average (Ductless 1:1) | 1.77 | 2.18 | 2.86 |
| Average (Ducted) | 2.53 | 2.49 | 3.15 |
| Average (Air-to-Water) | 1.56 | 1.72 | 2.57 |
| Average (All) | 1.96 | 2.16 | 2.92 |

In addition to the average steady-state COP in each temperature bin, the impact of transient operation and defrost cycles on the overall COP was investigated. Scatterplots in Figure 30 were made to compare steady-state COP against an inclusive COP. The steady-state and inclusive COP values were calculated by averaging the total heat delivered and the total power consumed as the unit operated over a 24-hour period. The steady-state COP includes only the delivered heat and

power consumption when the unit at each site was in ‘SteadyState_H’ mode. The inclusive COP includes COPs calculated in all operating conditions, including: ‘Transient_H’, ‘SteadyState_H’, ‘Fan Only’, and ‘Defrost’.

In these plots, each red circle represents a pair of steady-state and inclusive COPs calculated over the same time period. A trend line fitted to these points is shown as a line of star markers of various colors, one for each plot. In comparison, the black line is a 1:1 trendline of the steady-state COP values. Extreme outliers were removed utilizing Cook’s Distance, which is a measure of the magnitude of the outlier as well as the influence on the line of best fit. The *expected* behavior is that the inclusive COP should fall below the black line, as defrost and transient operation are not as efficient operating modes as steady-state operation. This analysis was performed only for the ductless 1:1 sites, as the other sites had added complexity, such as the influence of supplemental heating, which changes the performance behavior of the device, as well as other effects, such as excessive solar gains for ducted sites, routed through the attic.

The correlations in Figure 30 show that the total time-integrated performance was generally much lower than steady-state performance, with the difference being as high as 100% in site TLP-002, with a steady-state COP approximately double the total COP. The magnitude of the difference between steady-state COP and inclusive COP increased at higher steady-state COPs for sites EFG-006, TLP-004, TLP-001, and TLP-002 while staying relatively constant for the other sites. For the correlations with a correlation coefficient above 0.8, we can confidently use the correlations to project the total time-integrated performance of the heat pump as a function of steady-state COP. For example, the correlation for site EFG-001 can be used to predict what the overall time-integrated COP would be if the steady-state COP is known. For a COP of 2, this results in a 7.65% decrease in performance from steady state to inclusive COP. Overall, this highlights the importance of ensuring units spend as much time as they can operating under steady-state conditions in order to achieve peak efficiency.

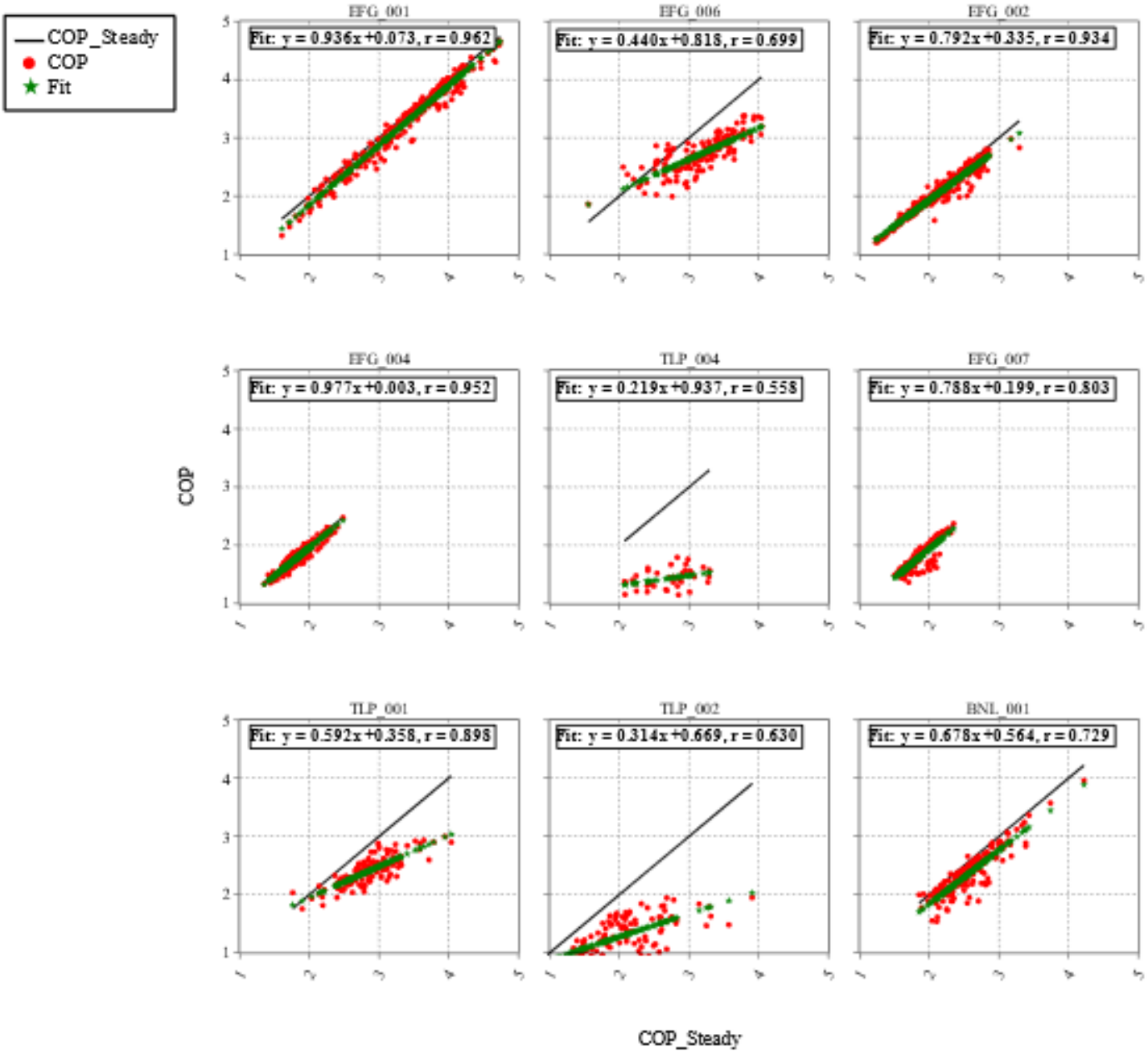


Figure 30: Time-integrated overall COP against the steady-state COP with line of best fit and correlation coefficient for ductless 1:1 sites

## 6.2 Capacity Modulation and Cycling

The delivered heat output is best displayed using a boxplot binned by outdoor temperature. For example, a wider spread indicates that at a particular temperature, the heat pump can modulate its output—allowing the unit to satisfy the current heating demand without over or under-supplying, potentially leading to power savings. Additionally, the number of compressor cycles per hour, binned by outdoor temperature, is indicative of the devices' ability to readily match heating load demands.

### 6.2.1 Output Capacity Ranges and Power Consumption

Figure 31 through Figure 33 show the range of output produced by the heat pump at different temperatures across each site. The figures are shown as box-and-whisker plots indicating median and quartile values for capacity for each temperature bin. The whiskers in these plots extend to the maximum and minimum of the data in each bin. The box represents the interquartile range from the 25$^{th}$ percentile (lower quartile) to the 75$^{th}$ percentile (higher quartile). A larger interquartile range (larger box) indicates significant variation in heat output (owed to the units' ability to modulate), which is preferable. The line within the box indicates the median value. A device that can supply a variety of different heat outputs at a given outdoor temperature is preferable to prevent excessive cycling. Given the same heating demand, a single output device that operates at a high output would turn on and off repeatedly to meet demand, while a variable output device can remain on in a low output mode and avoid the parasitic energy losses associated with having the unit turn on and off. For comparative purposes, the rated maximum and minimum output of the unit at 5 °F, 17 °F, and 47 °F are also included on the plots in purple and green, respectively.

Figure 31 shows the median steady-state output in each temperature bin for all ductless 1:1 sites. In all ductless sites, the median output decreased as outdoor temperature increased. Additionally, some units operated near the minimum rated output—and always below the maximum rated output.

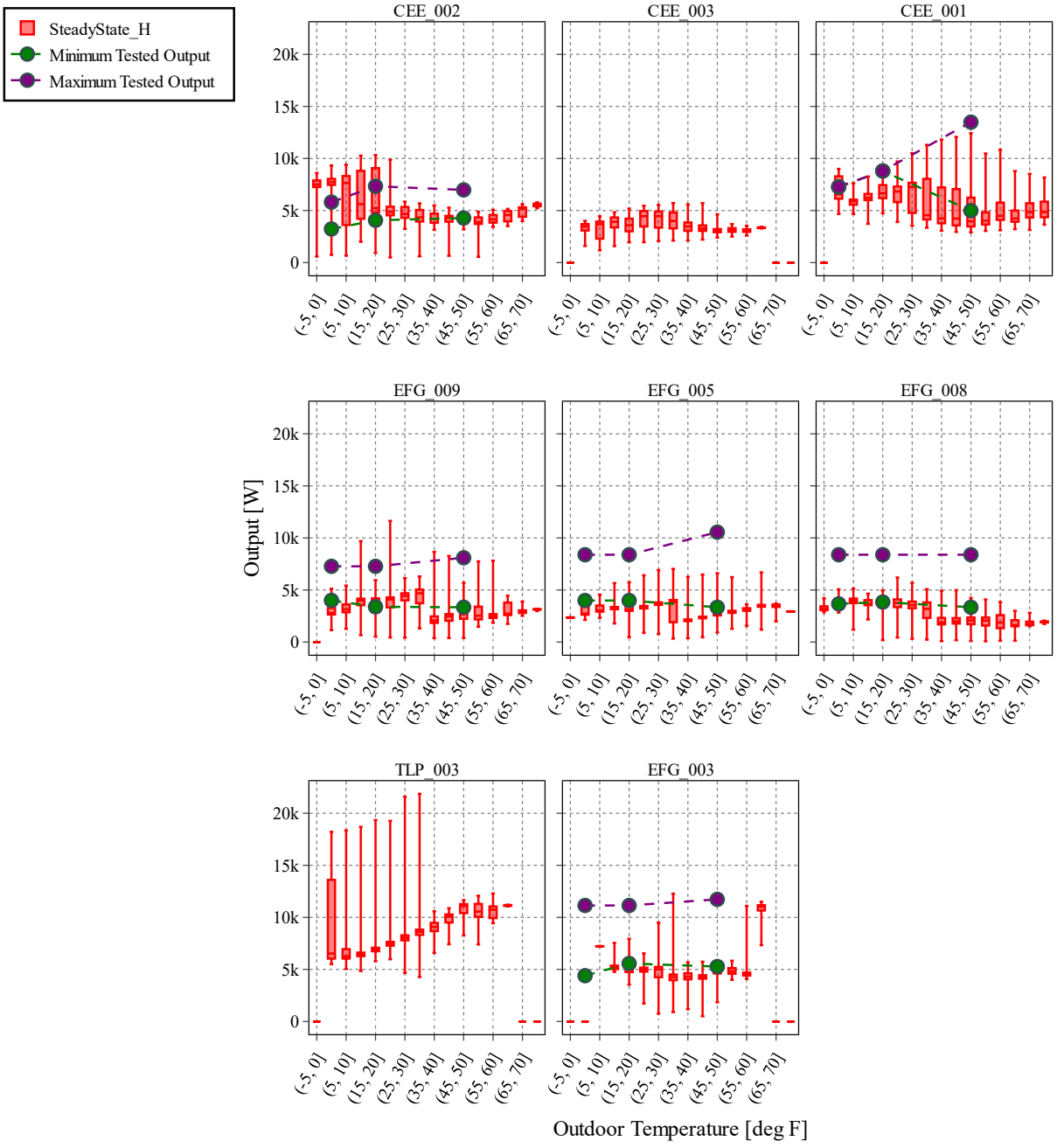


Figure 32 shows the median steady-state output in each temperature bin for all ducted, ductless 1:2, and mixed sites. Unlike the ductless systems, the output for these units did not change with increasing or decreasing outdoor temperature. More specifically, ducted sites CEE-001 and EFG-003 may have been oversized, as they stuck largely to their minimum outputs during the observation period. Unfortunately, ducted sites CEE-003 and TLP-003 had no literature values for comparative purposes. Figure 33 shows the output for all the air-to-water sites. Dissimilar from the previous sites, the air-to-water sites had an increasing trend in output with increasing outdoor temperatures.

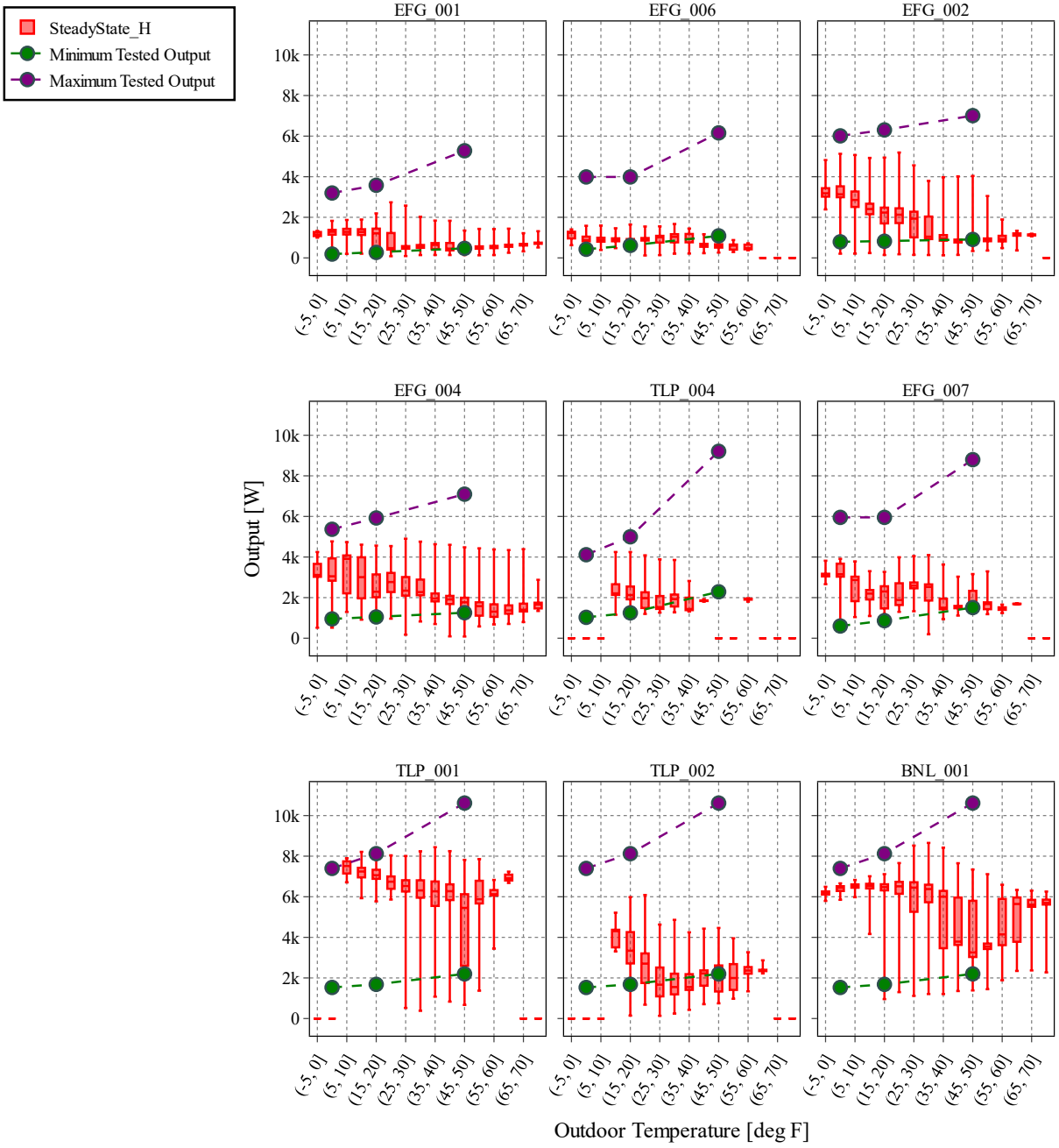


Figure 31: Heat output boxplot binned by outdoor temperature compared to available unit performance data for ductless 1:1 sites during steady-state heating

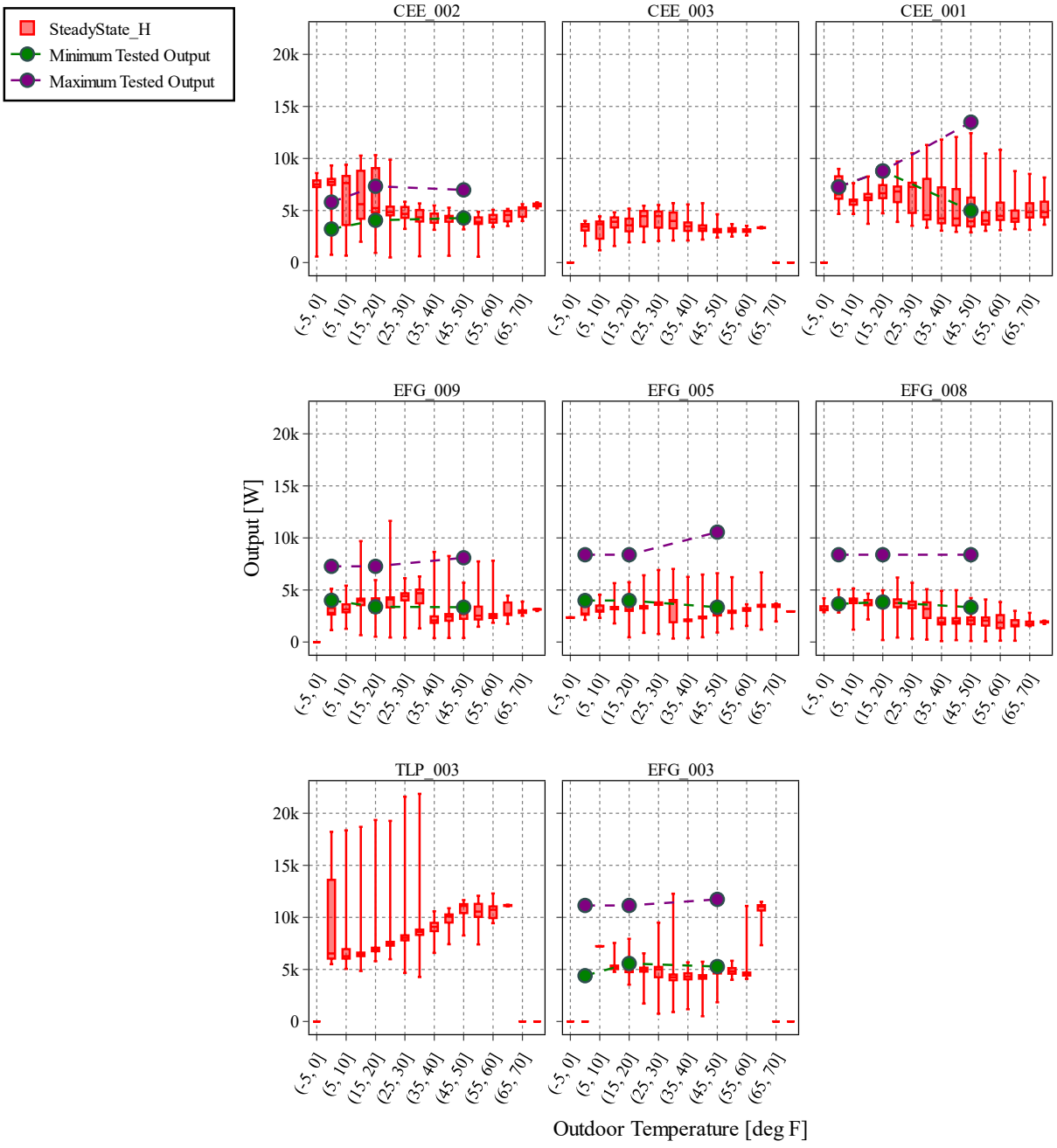


Figure 32: Heat output boxplot binned by outdoor temperature compared to available unit performance data for ducted, non-ducted 1:2, and mixed sites

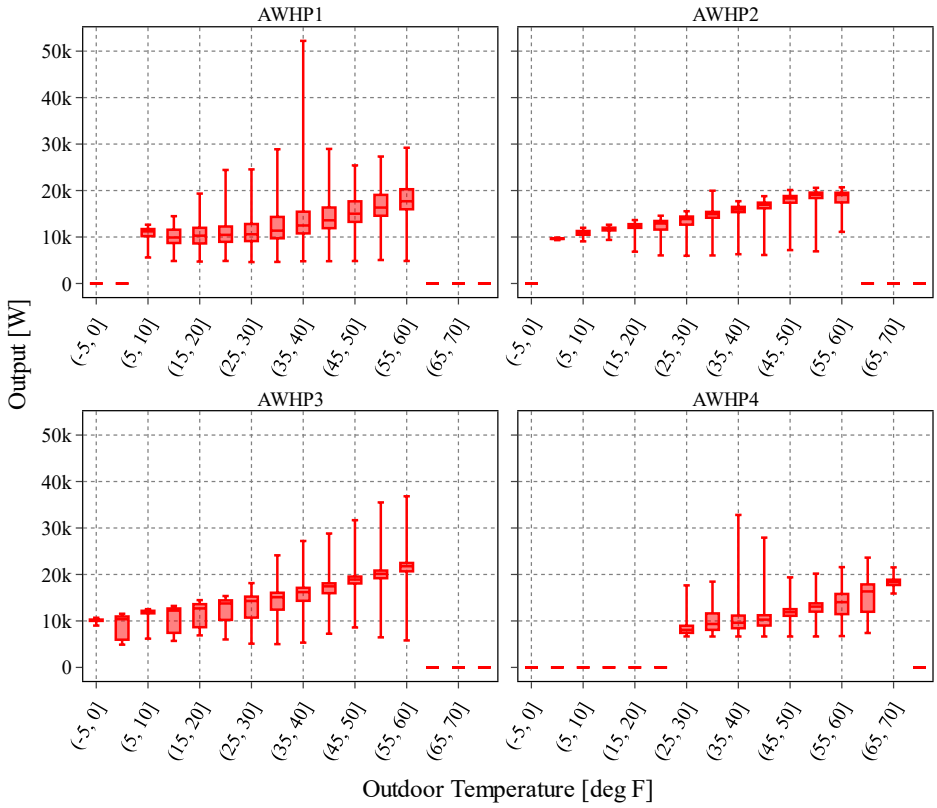


Figure 33: Heat output boxplot binned by outdoor temperature compared to available unit performance data for air-to-water sites during steady-state heating

Table 8 summarizes the median steady-state heating output at several outdoor temperatures of interest in the study. In summary, the median heat output decreased as the outdoor temperature increased for the ductless 1:1 sites, while the air-to-water sites showed an increasing trend, and the ducted sites had no clear trend with outdoor temperature.

Table 8: Summary of Steady-state Median Output at Various Operation Temperatures During Heating Mode.

| Site Name | Median Steady-state Output [W] | | | |
|---|---|---|---|---|
| | 5 °F | 17 °F | 47 °F | Entire Heating Season |
| Ductless 1:1 | | | | |
| EFG-001 | 1287 | 1208 | 436.3 | 539.7 |
| EFG-006 | 873.5 | 841.9 | 605 | 944.4 |
| EFG-002 | 3135 | 2234 | 832.2 | 1067 |
| EFG-004 | 3051 | 2290 | 1768 | 1954 |
| TLP-004 | N/A | 2126 | N/A | 1956 |
| EFG-007 | 3153 | 2301 | 1668 | 2036 |
| TLP-001 | N/A | 7062 | 5450 | 6464 |
| TLP-002 | N/A | 3342 | 1957 | 1881 |
| BNL-001 | 6442 | 6474 | 3257 | 6067 |
| Miscellaneous (Ducted, Ductless 1:2, and Mixed) | | | | |
| CEE-002 | 7740 | 5232 | 4172 | 4452 |
| CEE-003 | 3459 | 3581 | 3074 | 3443 |
| CEE-001 | 6552 | 6663 | 3975 | 5310 |
| EFG-009 | 2797 | 3728 | 2691 | 2804 |
| EFG-005 | 2710 | 3109 | 2634 | 2666 |
| EFG-008 | 3370 | 3725 | 2081 | 2618 |
| TLP-003 | 6535 | 6910 | 11101 | 7734 |
| EFG-003 | N/A | 5248 | 4727 | 4399 |
| Air-to-Water | | | | |
| AWHP1 | N/A | 10288 | 15019 | 12000 |
| AWHP2 | 9609.1 | 12412 | 18295 | 14679 |
| AWHP3 | 10373 | 12693 | 18909 | 17253 |
| AWHP4 | N/A | N/A | 11894 | 10550 |
| Summary | | | | |
| Average (Ductless 1:1) | 2990 | 3098 | 1997 | 2545 |
| Average (Ducted) | 5399 | 5124 | 4947 | 4667 |
| Average (Air-to-Water) | 9991.1 | 11798 | 16029 | 13621 |
| Average (All) | 4739 | 5073 | 5727 | 5277 |

While the output ranges are important in further determining the sizing and behavior of the units, they alone do not fully explain the difference in COP for some sites. Trends in the COPs discussed in the previous section can be further explained by comparing the heat output ranges with the power consumption. Figure 34, Figure 35, and Figure 36 show the power consumption for the ductless 1:1 sites, ducted and miscellaneous sites, and air-to-water sites, respectively. Recall from previous sections that four sites showed dissimilar COPs for a portion of their operating range from the available performance data. Site EFG-002 and CEE-002 underwent power consumption

that was uncharacteristically high when compared to their performance data for the regions where the COPs did not closely match, indicating that more power was consumed than what was typically observed during the COP rating process. However, the discrepancy for sites EFG-007 and EFG-008 is not explained by this and instead reduces the main culprit of disagreement to minute errors in the airflow correlation's development or supply temperature measurements, discussed in subsequent sections.

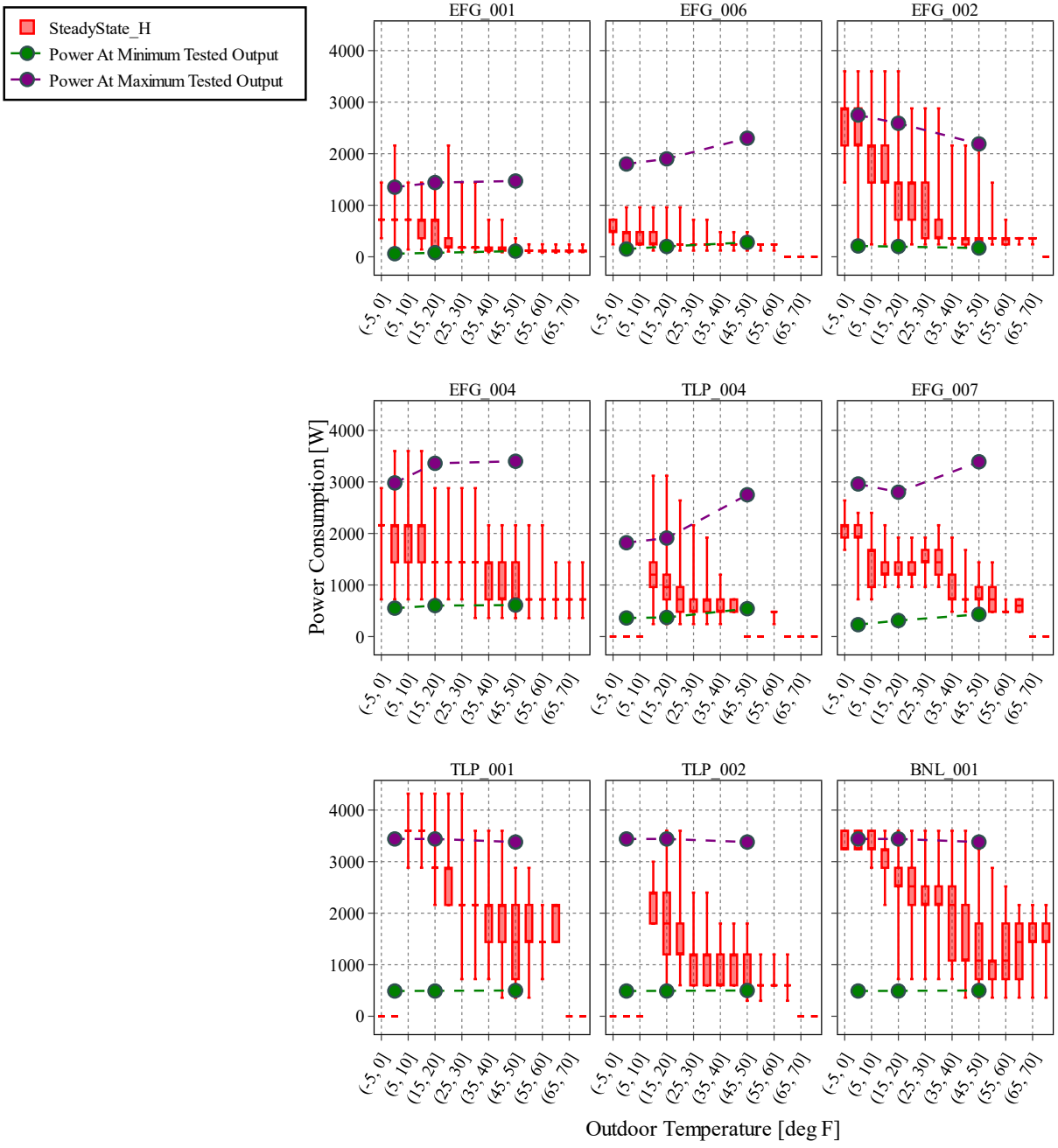


Figure 34: Power consumption boxplot binned by outdoor temperature for ductless 1:1 sites during steady-state heating

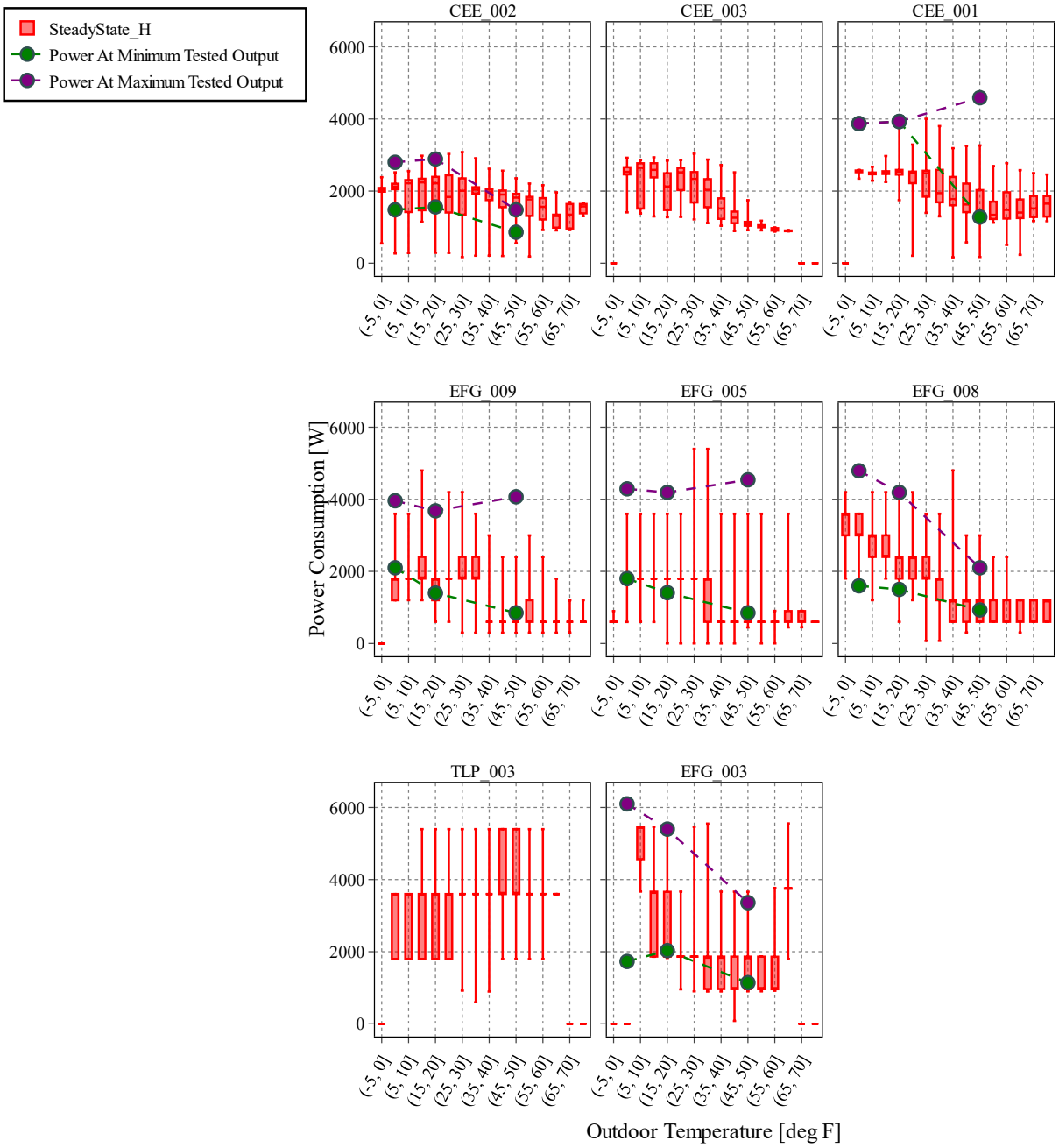


Figure 35: Power consumption boxplot binned by outdoor temperature for ducted, non-ducted 1:2, and mixed sites during steady-state heating

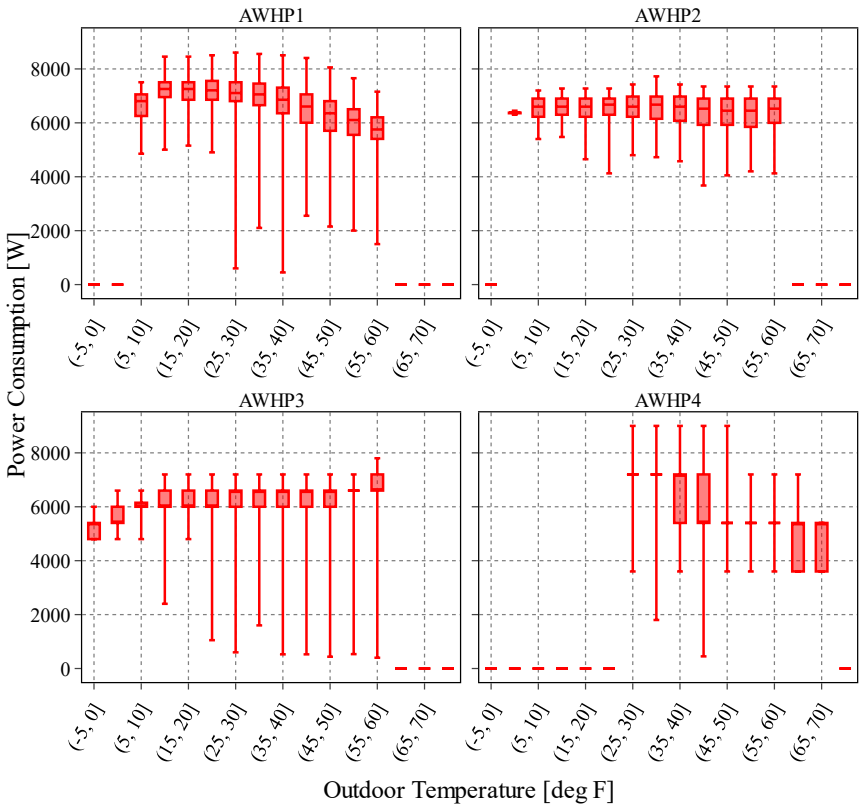


Figure 36: Power consumption boxplot binned by outdoor temperature for air-to-water sites during steady-state heating

### 6.2.2 Average Cycles Per Hour

In this study, one "cycle" is considered to be one transition from an off to an on state *and* the subsequent transition from an on to an off state *or* the transition from an on state to a defrost state *and* return to normal operation. A defrost cycle ends after the recovery to steady-state output has been reached.

Cycling of heat pump units between off and heating (including steady-state, transient, or supplemental heating modes) is common when the units are being used to heat. While cycling is common, a high cycling rate is indicative of a poorly designed system, an oversizing issue, or an issue with the equipment. Conversely, low cycling rates may indicate the heat pump is correctly sized and operating near its capacity, or the heat pump is undersized and struggling to meet heat demand—the latter could easily be refuted by comparing the supply temperature to other temperature sensors located within the conditioned space.

As the transition to steady-state conditions is not immediate, the heat pump requires a certain duration of operation to reach this higher-efficiency operating mode. Consequently, cycling rates

surpassing 5 cycles (on and off) per hour are unlikely to achieve a significant duration of steady operation. Cycling rates lower than this are more likely to include steady operation and are thus preferred. Lower cycling rates, such as 1 or 2, indicate that the unit either had to be consistently on to meet demand or was not utilized often at the corresponding outdoor temperature. Figure 37 shows the average cycles per hour during heating mode for the ductless 1:1 sites binned by the outdoor air temperature. Roughly half of the sites exhibited heightened cycling frequency with increasing outdoor temperature, while the remaining sites showed minimal alteration. Units that deviate from this pattern may do so due to the following reasons: 1) they may be over or undersized, as they either are on consistently at all temperatures or can meet the heating demand with a minimal number of cycles or, 2) they may be able to better modulate their output, and thus operate in a steady condition for a wider range of outdoor temperatures.

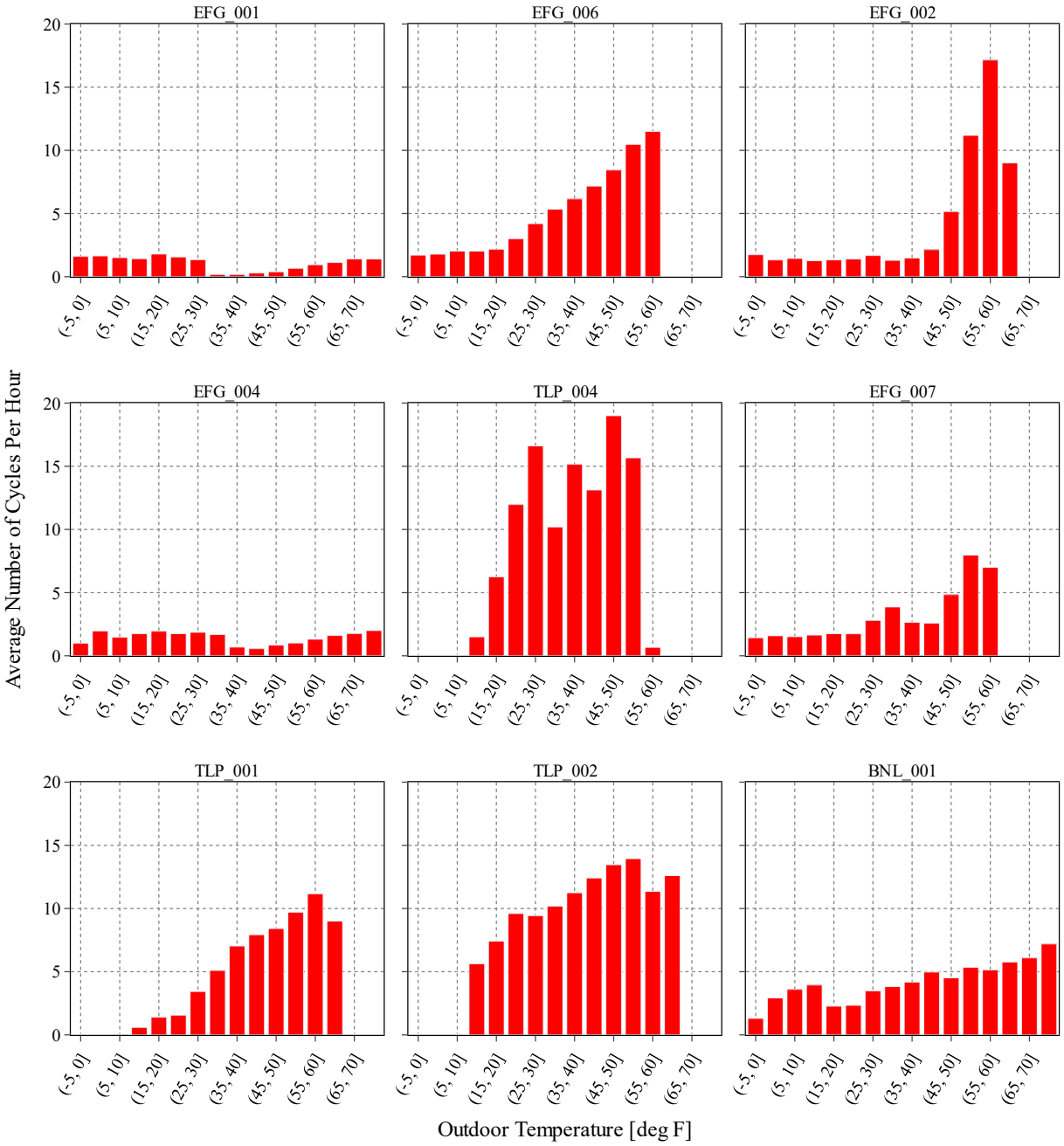


Figure 37: Average number of cycles per hour binned by outdoor temperature during heating mode for ductless 1:1 sites

Figure 38 shows the average cycles per hour binned by outdoor temperature for centrally ducted, ductless 1:2, and mixed sites. Generally, these sites had low average cycling rates—usually less than 5, except for sites CEE-001 and TLP-003. Additionally, there was a general trend of increasing cycling rate with outdoor temperature.

At the ductless 1:2 site, EFG-008, the cycling rate was low and somewhat constant between 5 and 35 °F but changed behavior to an increasing trend with increasing outdoor temperatures. This two-part trend could indicate that at low temperatures cycling behavior was due to outdoor coil defrost cycles. When observing the defrost trends in Figure 25 above or Figure 46 below, the trend correlates well with the frequency of defrost periods—particularly, the time spent in defrost slightly decreases from -5 to 10 °F and then increases from 10 to 40 °F.

Four of the five centrally ducted sites showed a similar two-part trend, the exception being EFG-003, which showed an increasing trend in cycling rate with outdoor temperature. Notably, CEE-001 and TLP-003 showed abnormally high cycling rates, but the two-part trend was apparent. For site CEE-001, the compressor frequency sensor suffered repeated unusual failures that were documented during the testing phase. As a result, the compressor current was utilized as a backup measurement. A higher-than-expected average number of cycles in the following temperature bins was reported (15,20]: 16, (20, 25]: 23, (25, 30]: 24, (30, 35]: 16, (60, 65]: 17, (65, 70]: 25). Due to the repeated failure of this sensor, it was difficult to establish a clear and defined threshold for the compressor current when the unit was operating as expected to act as a true stand-in replacement in our algorithm. The hourly heating cycle frequency at CEE-001 showed two peaks in its cycle frequency—one at the (25, 30] °F range and one at the (65, 70] °F range. This result suggests that although the sensor failures impacted the magnitude of the detected heating cycle frequency, the overall trend seems reliable, as a similar trend was detected at other sites.

At the mixed site, EFG-009, the cycling rate was low across the entire outdoor temperature range. This site also showed a slight two-part trend, with an increase in time spent in defrost as seen in Figure 25 above or Figure 46 below, attributing to more cycling observed during temperatures lower than 35 °F.

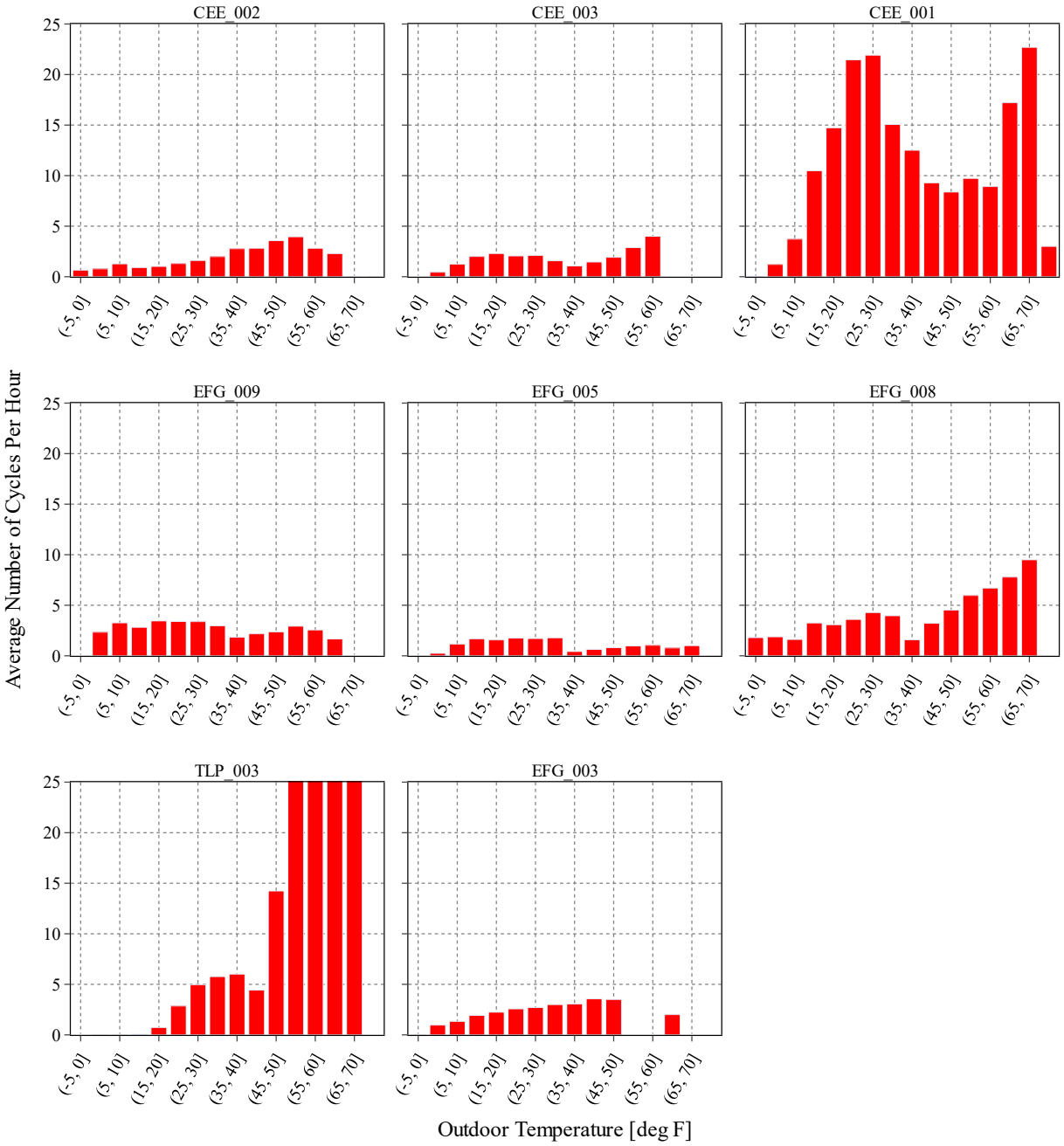


Figure 38: Average number of cycles per hour binned by outdoor temperature during heating mode for ducted, non-ducted 1:2, and mixed sites

Across the four air-to-water sites, three of the four had cycling rate data collected over a wide enough range to make conclusions, the exception being AWHP4. At the remaining sites, the cycling rate increased with increasing temperature and had a mean cycling rate of less than 5 at each temperature range, as shown in Figure 39.

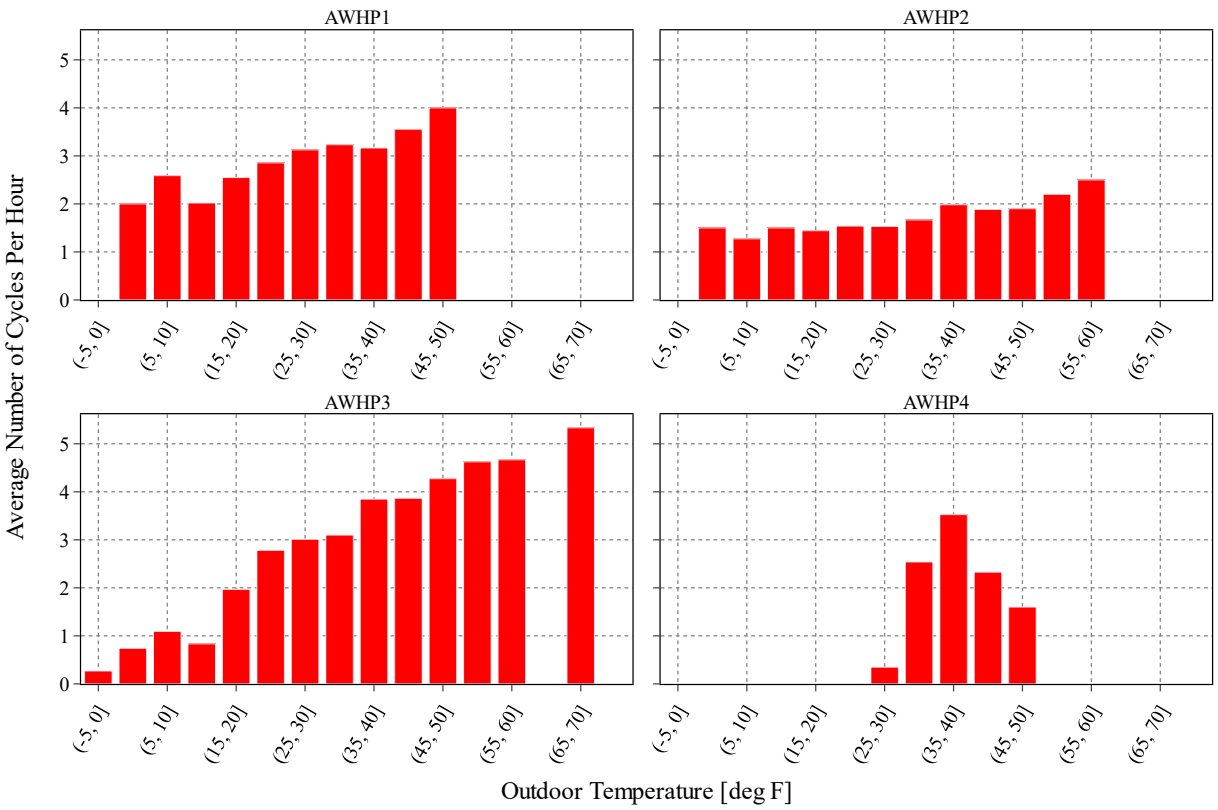


Figure 39: Average number of cycles per hour binned by outdoor temperature during heating mode for air-to-water sites

In summary, an overall increasing trend in cycling for most sites was observed with increasing outdoor temperature. The 1:1 ductless units had the highest cycling counts; however, some sites did cycle less than 5 times. Additionally, some sites had correlations in their cycle counts with their fraction of time spent in defrost. This trend may indicate continuous operation with periodic interruption by defrost cycles. Lastly, units with high runtime fractions showed the lowest cycling rates as the equipment was operating and heating for a large fraction of the time. Units that showed low runtime fractions during more mild temperature bins had larger cycling rates due to spending much of their time in an 'Off' mode.

## 6.3 Defrost

Characterizing defrost mode operation is critical in understanding the behavior of heat pumps when utilized over a wide range of outdoor temperatures. The duration of the measured defrost periods for each site is depicted in Table 9. Sites typically experienced defrost modes from just under one minute to under 15 minutes in length, with the ducted and air-to-water sites typically having longer defrost periods than ductless 1:1 sites.

Table 9: Summary of defrost period durations across all sites.

| Site Name | Length of Defrost Periods [min] | |
|---|---|---|
| | 10th Percentile | 90th Percentile |
| Ductless 1:1 | | |
| EFG-001 | 0.83 | 10.92 |
| EFG-006 | 0.75 | 2.00 |
| EFG-002 | 0.83 | 6.25 |
| EFG-004 | 1.42 | 4.50 |
| TLP-004 | 0.67 | 1.92 |
| EFG-007 | 1.67 | 3.83 |
| TLP-001 | 1.00 | 1.85 |
| TLP-002 | 1.00 | 3.51 |
| BNL-001 | 0.75 | 5.58 |
| Miscellaneous (Ducted, Ductless 1:2, Mixed) | | |
| CEE-002 | 1.58 | 6.83 |
| CEE-003 | 1.25 | 4.56 |
| CEE-001 | 0.67 | 6.25 |
| EFG-009 | 0.67 | 5.42 |
| EFG-005 | 1.42 | 5.00 |
| EFG-008 | 0.75 | 5.33 |
| TLP-003 | 1.87 | 9.68 |
| EFG-003 | 0.67 | 1.72 |
| Air-to-Water | | |
| AWHP1 | 7.00 | 8.30 |
| AWHP2 | 9.00 | 9.00 |
| AWHP3 | 7.00 | 13.60 |
| AWHP4 | 0.58 | 3.02 |
| Summary | | |
| Average (Ductless 1:1) | 0.99 | 4.48 |
| Average (Ducted) | 1.24 | 5.67 |
| Average (Air-to-Water) | 5.90 | 8.48 |
| Average (All) | 1.97 | 5.67 |

The outdoor behavior of these devices during defrost mode is the same across all sites; the heat pump operates in the reverse direction to heat the outer coil and melt any frost accumulation. The indoor side behavior is somewhat different, with ductless 1:1 sites showing a decreased indoor fan current, as in Figure 40. This means that during defrost mode, the indoor fan is turned off to prevent the distribution of cooler air throughout the home. This is counter-productive to the goal of heating the home, and minimizing the length and occurrence of these periods is critical. This is especially so if the unit is already operating 100% of the time and struggling to meet demand or if the periods consume an excessive amount of power. The ducted sites in Figure 41 with supplemental heating, namely CEE-001 and CEE-003, show different behavior. This is due to the fact that the air handler is still utilized when the supplemental heating is engaged; thus, the indoor current remains high. The remaining sites show similar behavior to the ductless 1:1 sites. The ability of these devices to switch to supplemental heating during defrost periods may be critical to their deployment in subzero temperatures when heating demand is high. Whereas for ductless 1:1 sites, the lack of this integration makes the characterization of defrost mode all the more important. The air-to-water sites are not included in this discussion as they do not utilize an air handler unit for heating the home and, therefore, do not have an indoor current measurement associated with them.

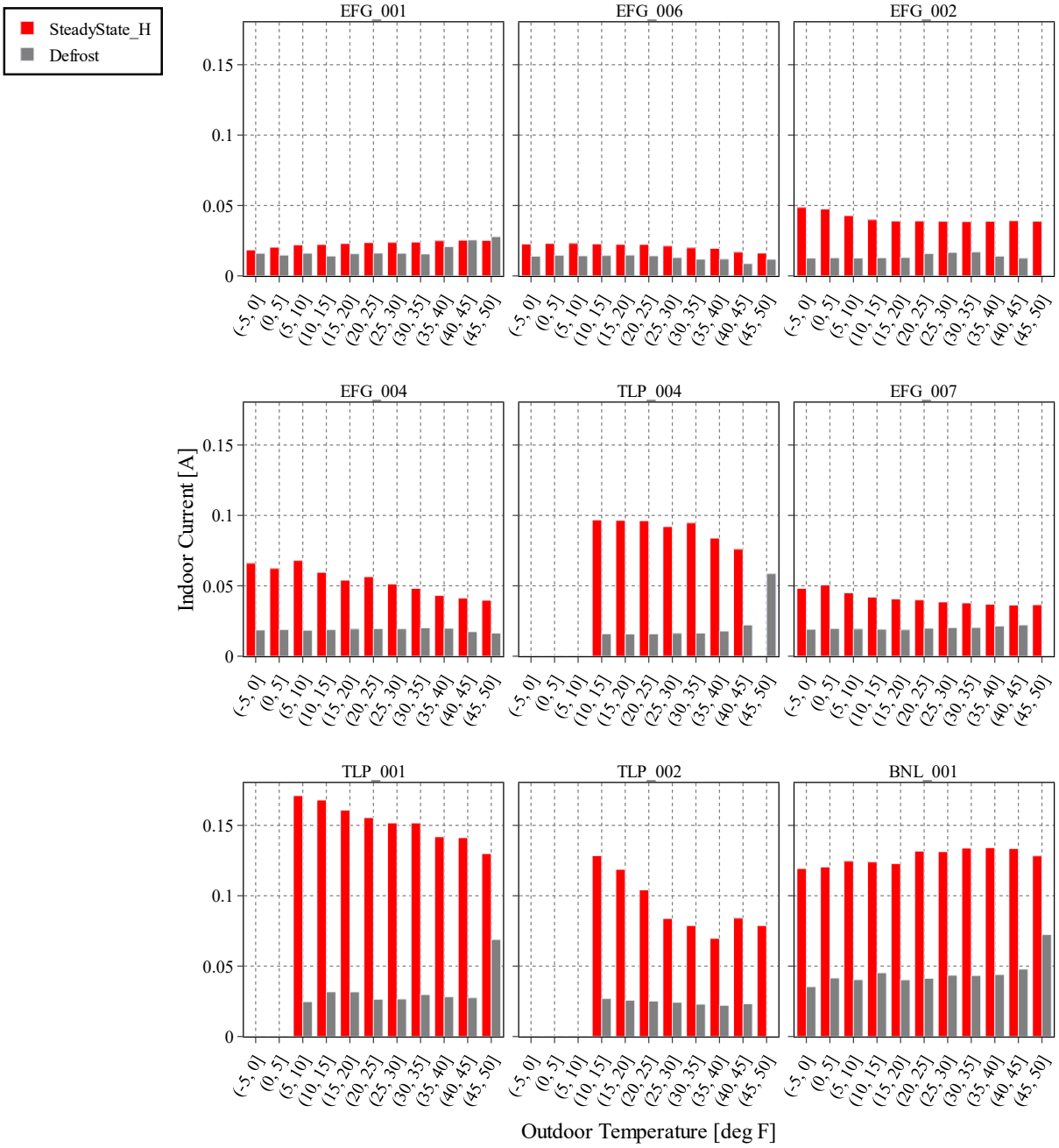


Figure 40: Indoor current for steady-state heating and defrost modes binned by outdoor temperature for ductless 1:1 sites

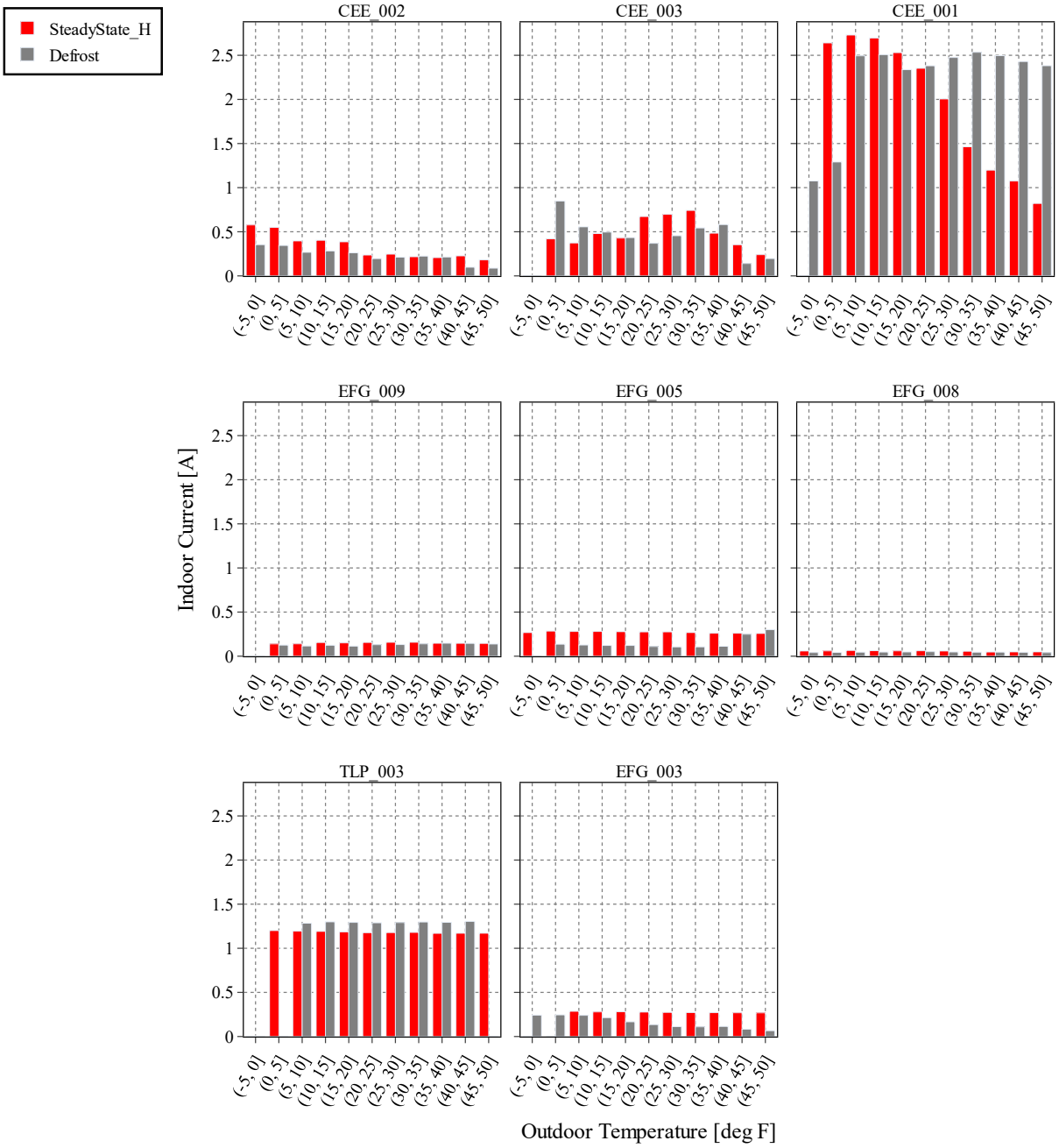


Figure 41: Indoor current for steady-state heating and defrost modes binned by outdoor temperature for ducted, non-ducted 1:2, and mixed sites.

Power consumption during defrost is important in determining the energy losses associated with the mode, as this energy would have otherwise gone to heating the home. Figure 42, Figure 43, and Figure 44 show the power consumption during steady-state heating, transient heating, and defrost mode for the ductless 1:1 sites, miscellaneous sites, and air-to-water sites, respectively. All

sites have a defrost power consumption on the same order of magnitude as steady-state or transient heating, with 12 of 21 sites having power consumption approximately the same as steady-state heating. TLP-003 suffered from power sensor failures, particularly during periods of rapid change. As the error is extraordinarily large, we cannot make a definitive statement regarding transient heating power consumption. However, our algorithm was able to correct and identify steady-state heating power requirements, which were larger than those of defrost mode.

With the exception of EFG-006, the remaining sites have lower defrost power consumption than during the heating modes. A potential cause for this relates to the fact that EFG-006 is a very small site; from previous plots, it is noted that the heat pump runs at its minimum output to meet the heating demand. With oversizing in mind, the outdoor coil still encounters the same temperature conditions as other units of similar size (such as EFG-002) and, therefore, may require a similar amount of energy to defrost the outer coil. For the remaining sites, defrost energy consumption was lower than the heating modes. For the air-to-water sites in particular, this may be due to the specific heat of the refrigerant relative to the working fluid. For air-to-air sites, the refrigerant and air have specific heats that are close to one another. Air-to-water sites, however, use two working fluids that differ greatly in their specific heats, with water's specific heat being nearly four times higher. This means that less energy is required to bring the refrigerant up to temperature to defrost the coil than it is to heat the water to distribute throughout the home.

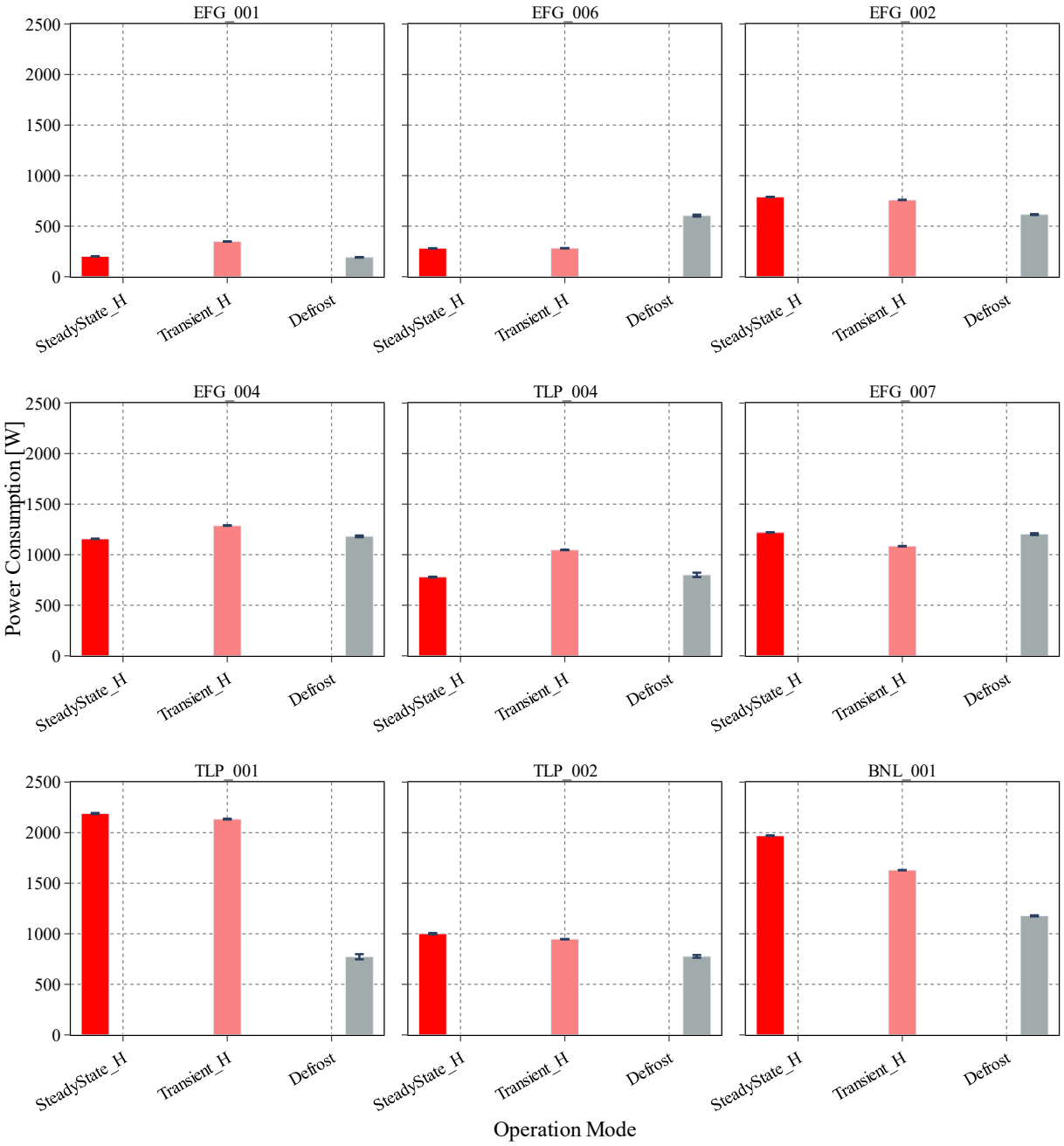


Figure 42: Average power consumption in steady-state heating, transient heating, and defrost mode for ductless 1:1 sites

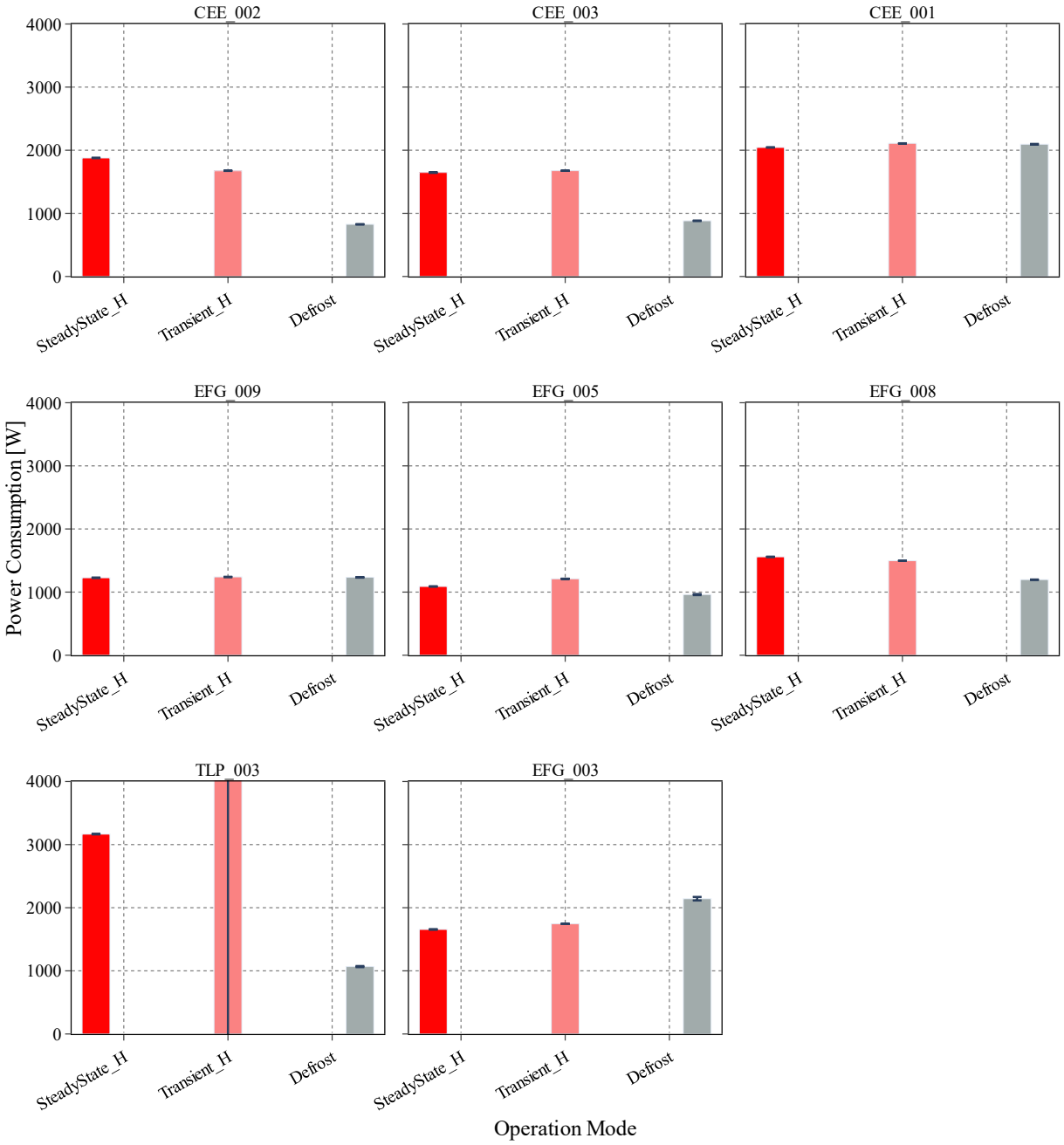


Figure 43: Average power consumption in steady-state heating, transient heating, and defrost mode for ducted, non-ducted 1:2, and mixed sites

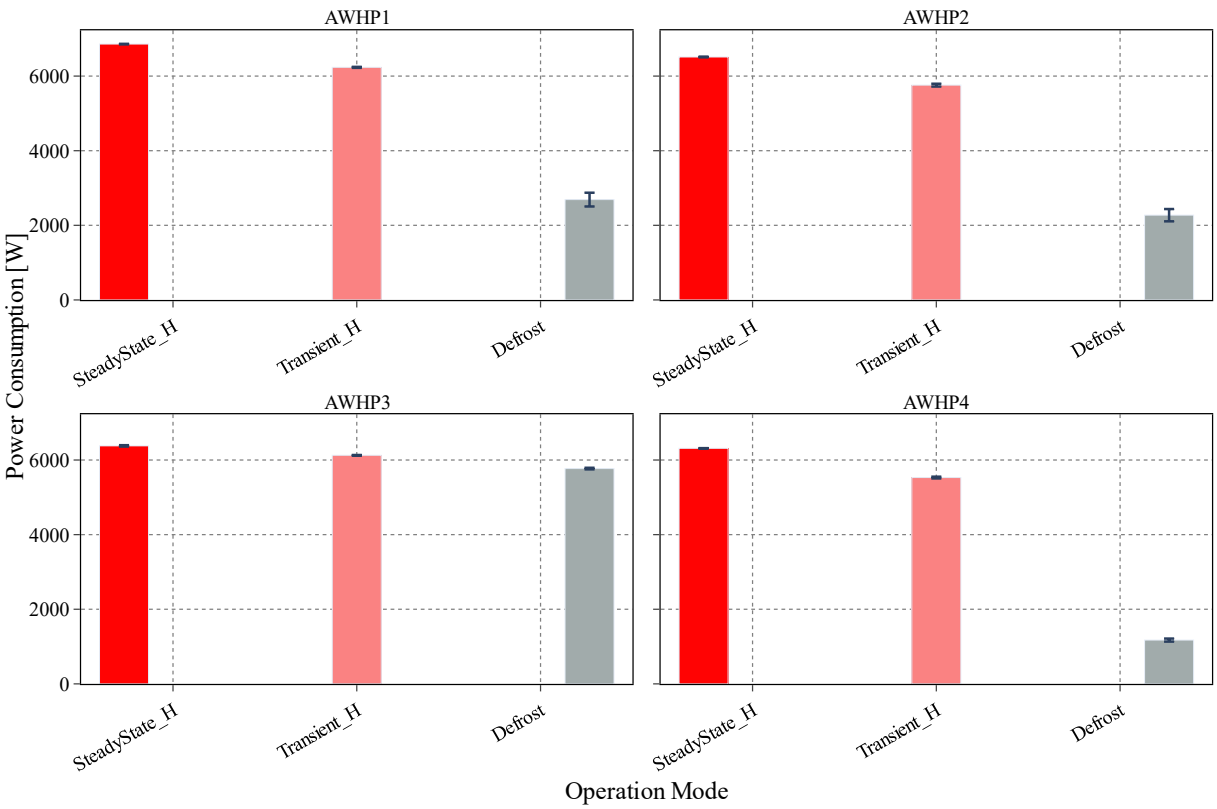


Figure 44: Average power consumption in steady-state heating, transient heating, and defrost mode for air-to-water sites

While knowing the defrost mode's typical durations, power consumption, and behavior relative to the indoor unit is important, understanding the prevalence of defrost mode with regard to outdoor temperature is necessary. Figure 45, Figure 46, and Figure 47 show the previous runtime fraction plots for the ductless 1:1, miscellaneous, and air-to-water sites with *only* defrost mode displayed. Most sites saw a peak defrost fraction between 10 and 30 °F and decreased as outdoor temperature moved away from this range. The manufacturer's proprietary control scheme determines the necessary defrost period during colder outdoor temperatures, and the degree of variation in this occurrence is observed in the data below.

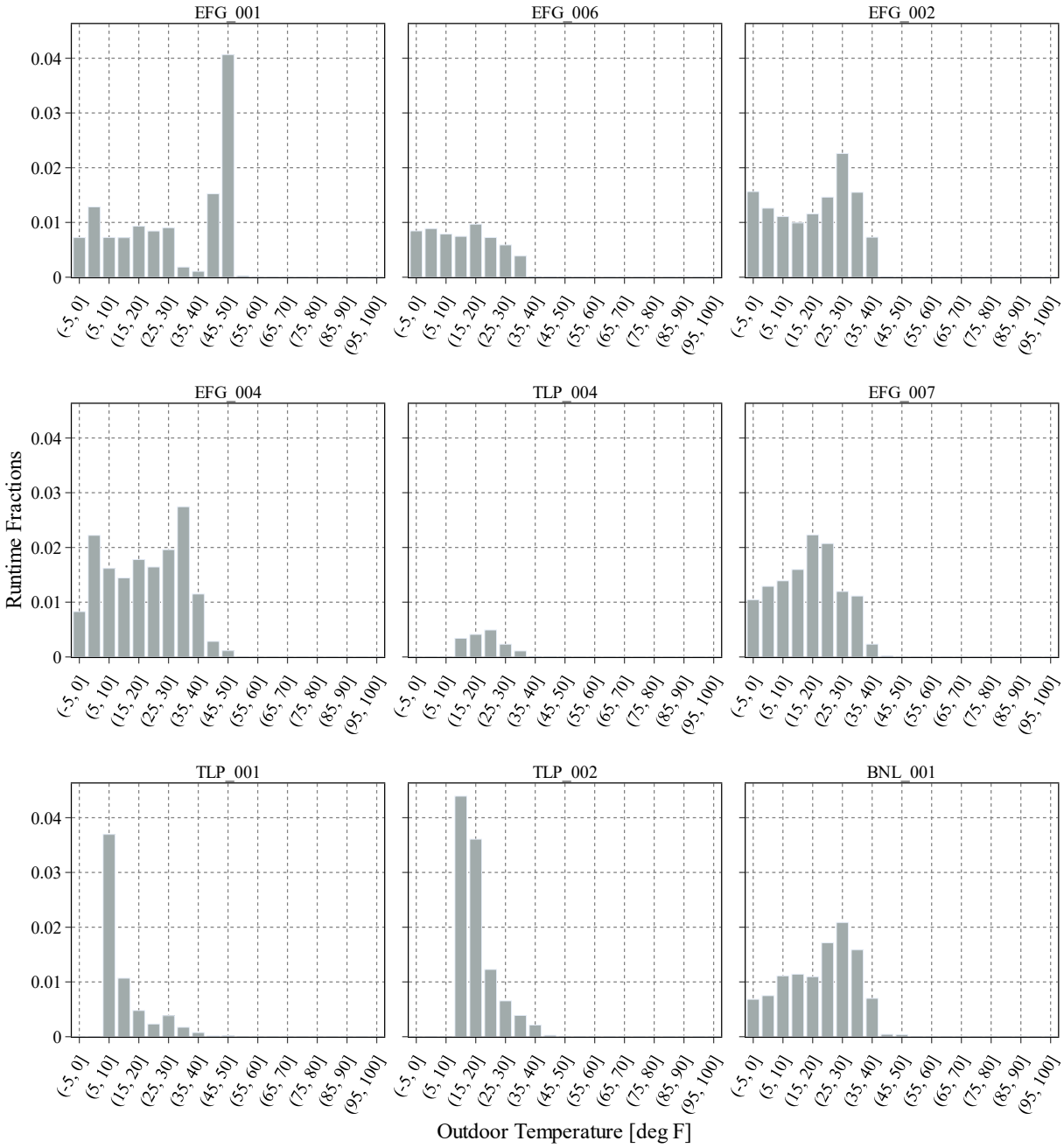


Figure 45: Defrost runtime fraction binned by outdoor temperature for ductless 1:1 sites

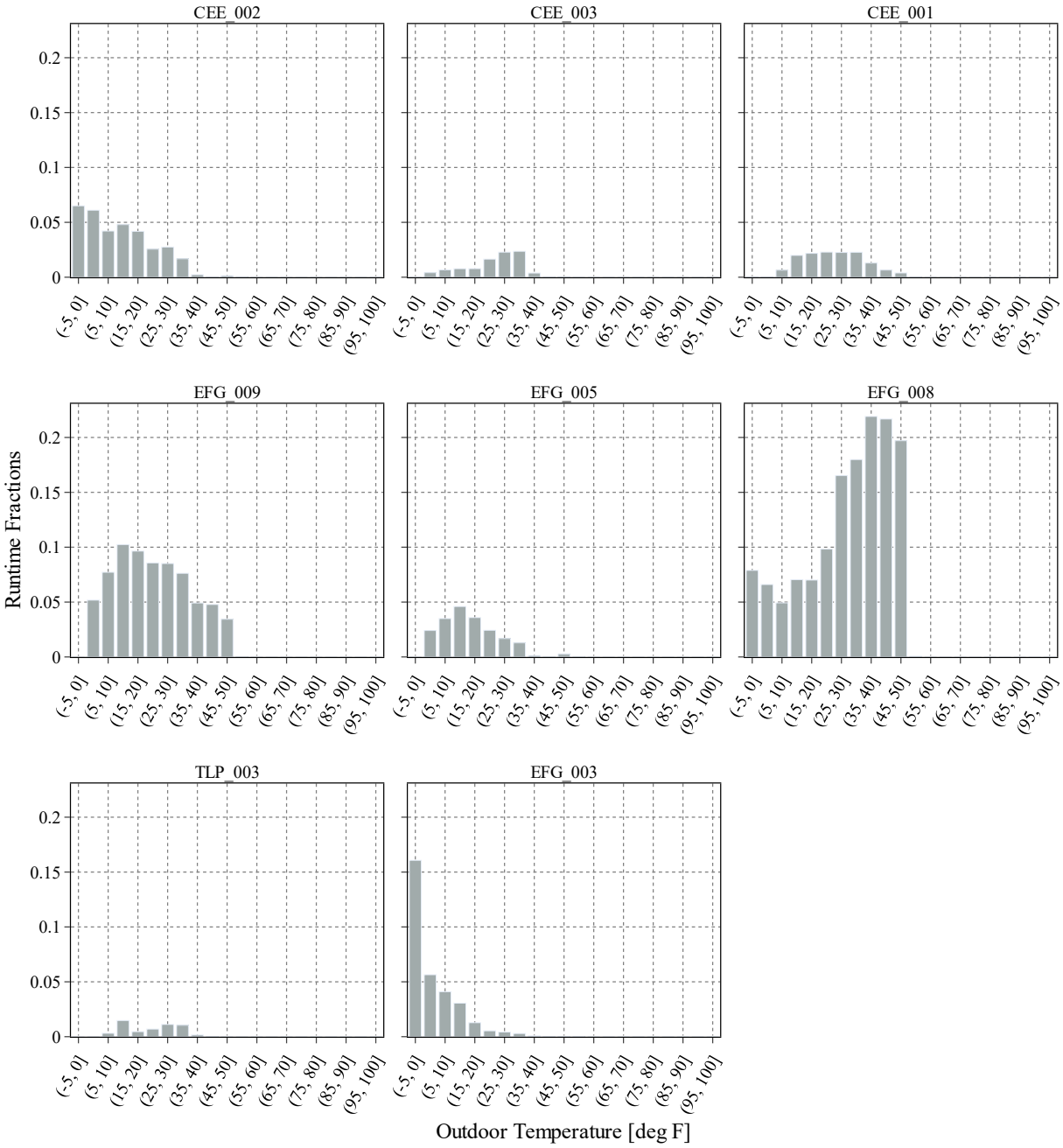


Figure 46: Defrost runtime fraction binned by outdoor temperature for ducted, non-ducted 1:2, and mixed sites

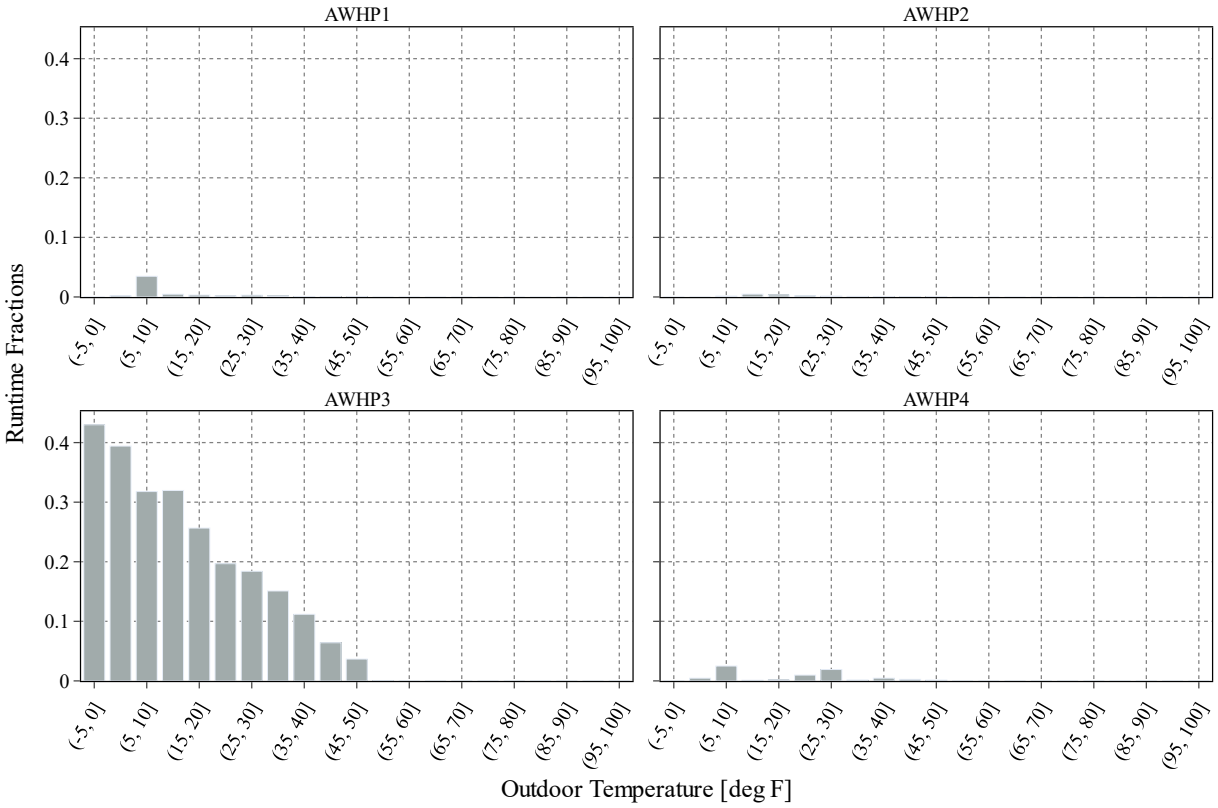


Figure 47: Defrost runtime fraction binned by outdoor temperature for air-to-water sites

Overall, the defrost mode's power consumption is significant, and the mode prevents certain heat pump configurations from heating the home for an extended period of time. Defrost periods typically last several minutes and occur at a maximum of just under 5% of the total operating time in any one temperature bin for the ductless 1:1 sites. This, combined with the previous subsections, illustrates the impact defrost mode has on performance compared to steady-state heating periods. Furthermore, this does not consider the actions immediately post-defrost, wherein a transient heating recovery period must occur to return to serving the baseline heating demand, as in Figure 48.

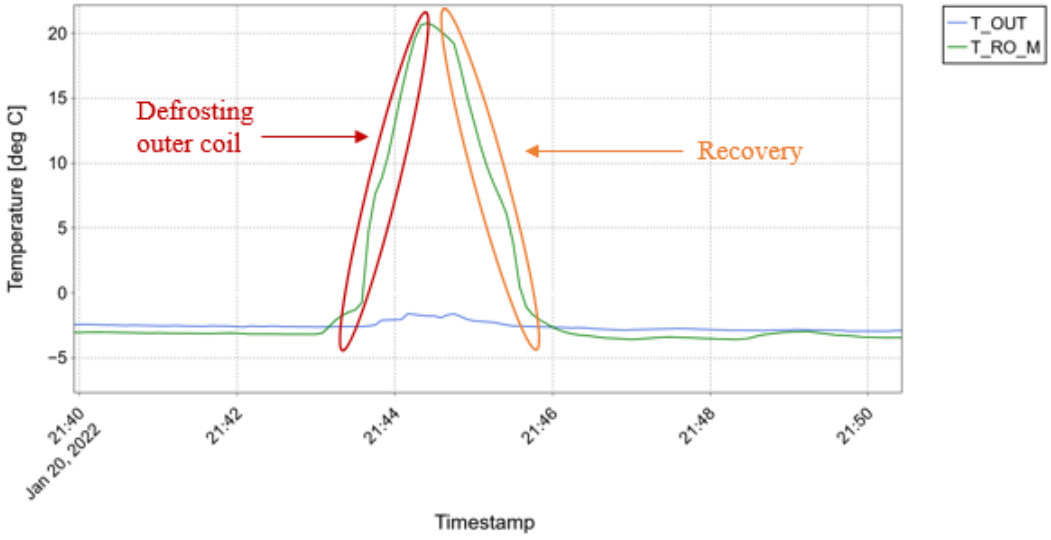


Figure 48: Time series of a typical defrost period showcasing additional transient heating.

Observing the defrost runtime fractions shown above in Figure 45 to Figure 47, as well as the number of cycles in each temperature bin in Figure 37 to Figure 39, may help answer the question raised earlier in the General Operating Results section—whether the large percentage of transient heating at low temperatures was a result of oversizing or defrost events. Looking at the temperature bins below freezing, the cycling rates were low (< 5 cycles per hour) but had increased defrost cycles. This indicates that the increase in transient heating may be due to defrosting events and is less likely due to oversizing. However, when observing milder temperatures > 35 °F, the fraction spent in defrost generally decreases, and the number of cycles increases, indicating the units are short cycling more frequently due to poor modulation or oversizing at that particular temperature.

## 6.4 Supply Temperature

The supply temperature in heating mode as a function of outdoor temperature for each site is shown in Figure 49 to Figure 51. Within the plots for each site are box-and-whisker diagrams, which show the median (central dark line), interquartile range (box with lower (Q1) and upper (Q3) bounds), and minimum and maximum (whisker lower and upper bounds). There is one box-and-whisker diagram for each temperature bin where the installation operated in steady-state heating mode. All sites operated in a steady-state heating mode at 47 °F, while only 15 of 21 sites had logged steady-state hours at temperatures of 5 °F and 17 °F. Sites TLP-004, TLP-001, TLP-002, EFG-003, AWHP1, and AWHP4 did not log any hours at 5 °F. The AWHP4 site also had no logged hours at 17 °F.

Across all ductless 1:1 sites, the median heating supply temperatures at 5 °F, 17 °F, and 47 °F were 116 °F, 111 °F, and 101 °F, respectively. The overall average median heating supply temperature, across all temperatures, was 105 °F. The lowest median heating supply temperature at 5 °F occurred at EFG-006 with a value of 88.0 °F. EFG-006 had the smallest area to condition, and it is possible the heating supply temperature remained low at this site because the heat demand was

satisfied without requiring the heat pump to modulate to a higher output mode, and thus the supply temperature seldom rose to its theoretical maximum for the unit. The highest median heating supply temperature at 5 °F occurred at EFG-007 with a value of 126 °F. Generally, all 1:1 non-ducted sites had a relatively steady supply temperature range with little trend of increasing or decreasing outdoor temperature.

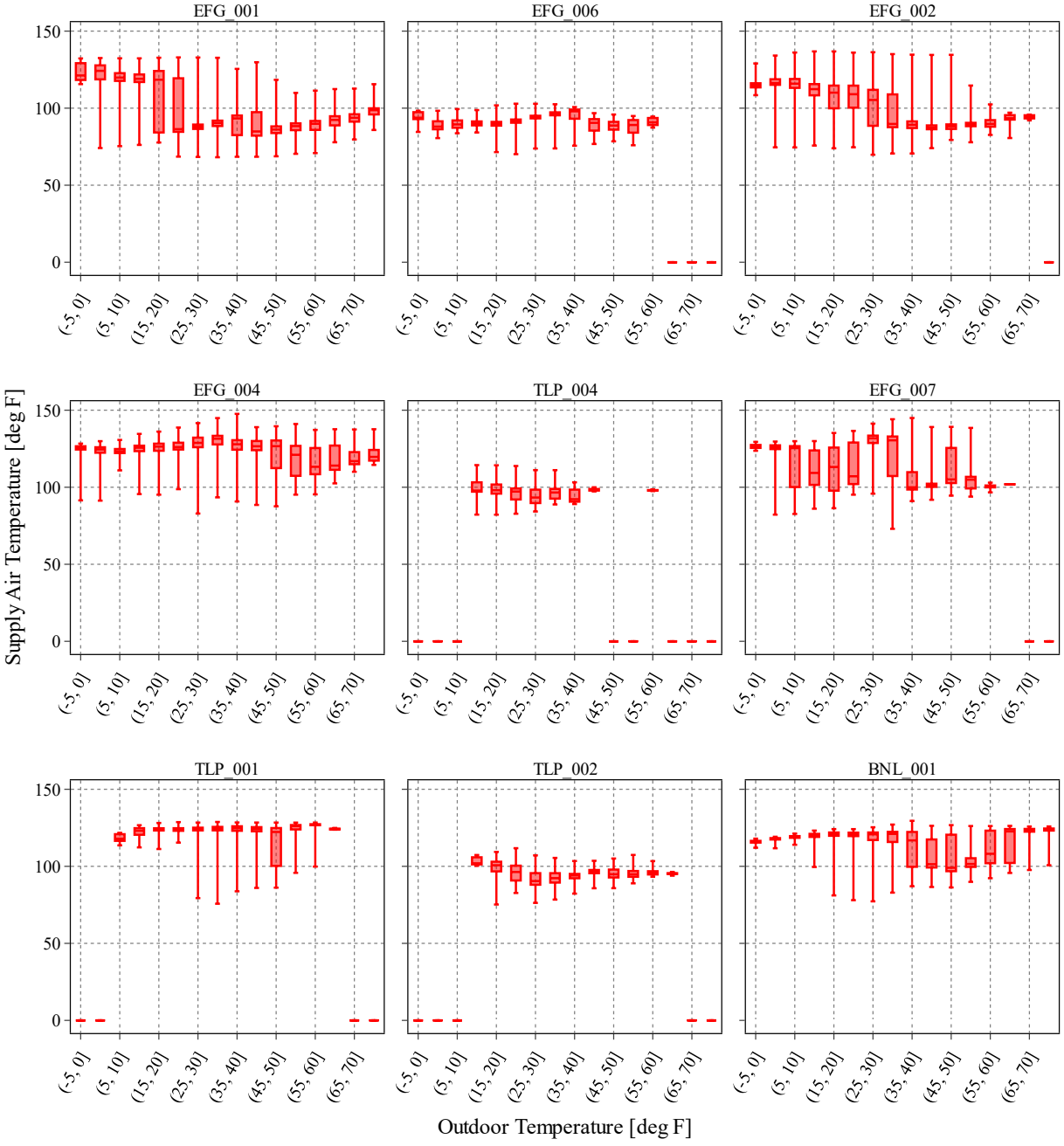


Figure 49: Heating supply temperature binned by outdoor temperature for ductless 1:1 sites

The ductless 1:2 (EFG-008) site median heating supply temperatures 5 °F, 17°F, and 47 °F were 120 °F, 125 °F, and 113 °F, respectively. The overall average median heating supply temperature at this site was 117 °F. The supply temperature at this installation increased from -5 to 35 °F and dropped to a low value for this site, about 110 °F, and then increased at a much slower rate across the remainder of the temperature range.

Across all centrally ducted sites, the median heating supply temperatures at 5 °F, 17 °F, and 47 °F were 97.1 °F, 97.4 °F, and 100 °F, respectively, with an overall average value of 96.4 °F. Of the five centrally ducted sites with heating mode data, two sites showed relatively constant supply temperatures, while three sites had increasing trends. CEE-001 and TLP-003 were the only ducted sites to show a slight decrease in the median supply temperature with decreasing outdoor temperature. Overall, the centrally ducted sites had lower median heating supply temperatures than the ductless 1:1 sites.

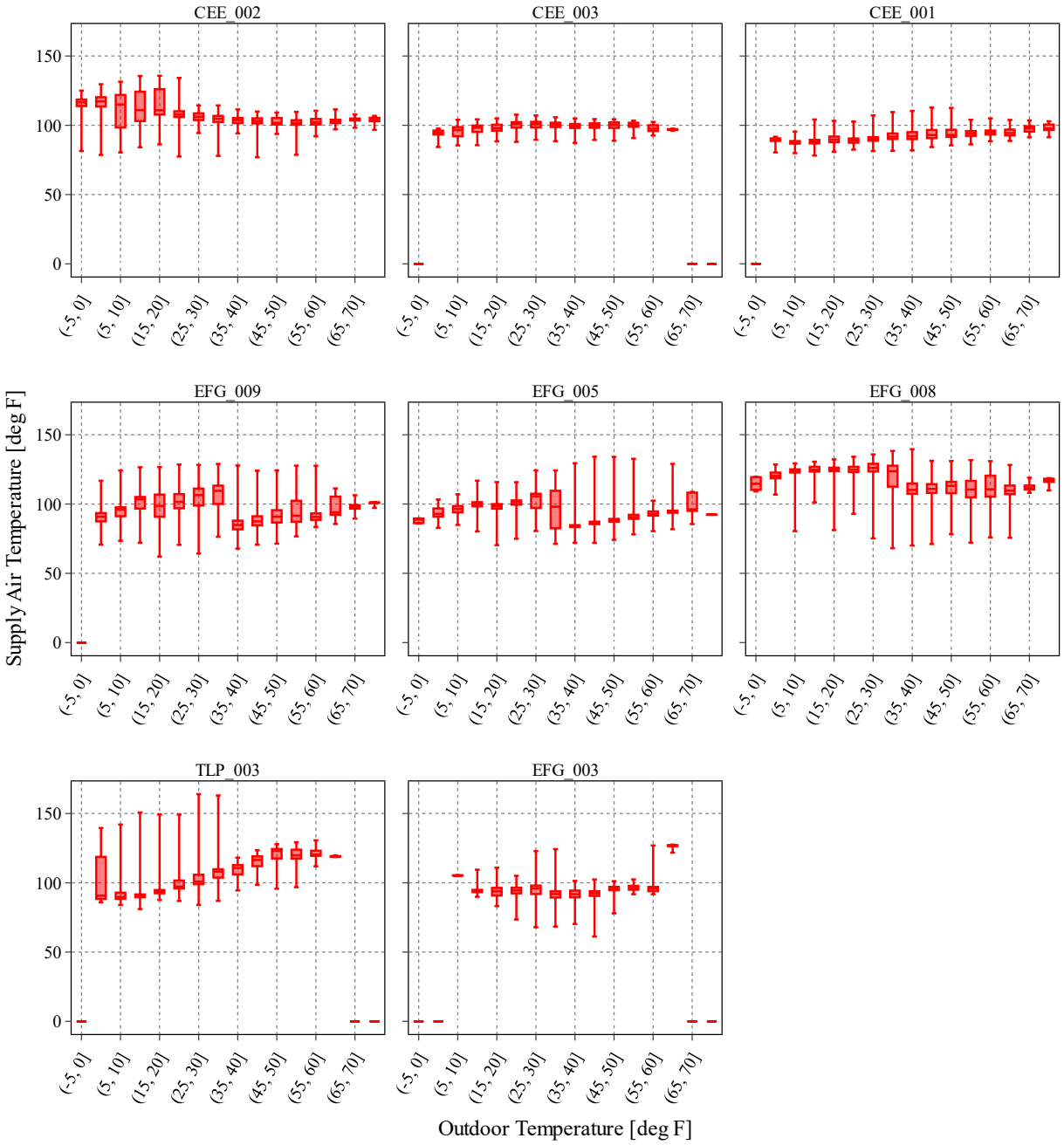


Figure 50: Heating supply temperature binned by outdoor temperature for ducted, non-ducted 1:2, and mixed sites

Across all four air-to-water sites the median heating supply temperatures at 5 °F, 17 °F, and 47 °F were 115 °F, 125 °F, and 120 °F, respectively, with an overall average value of 124 °F. Two of the four air-to-water sites, AWHP1 and AWHP4, exhibited a decreasing water supply temperature as outdoor temperature increased, while the remaining sites had a direct relationship with outdoor temperature. The air-to-water sites had a higher overall average heating supply temperature than

the ductless sites. However, the range in supply water temperatures was generally smaller than the range in supply temperatures of the other installation types.

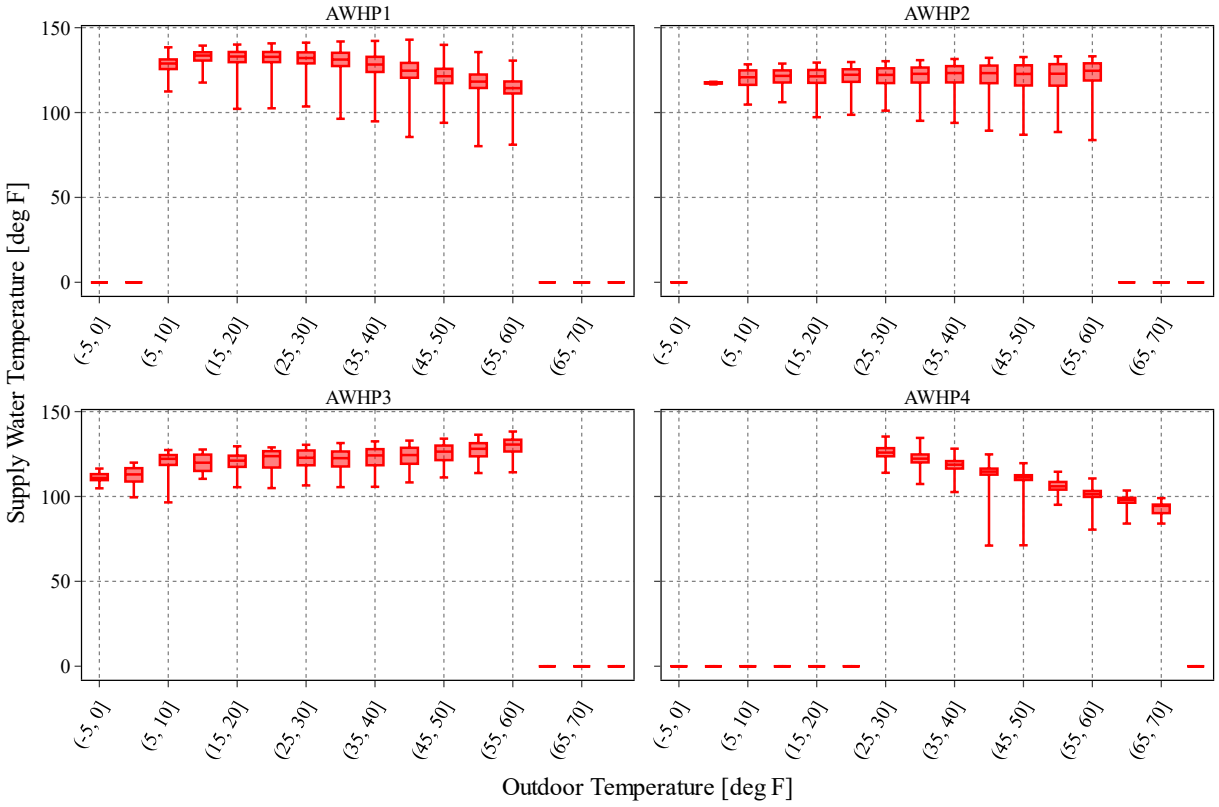


Figure 51: Heating supply temperature binned by outdoor temperature for air-to-water sites

The main findings from our analysis of heating supply temperatures are that the median temperatures can range between 90 and 130 °F and that at most 1:1 non-ducted sites, supply temperature decreases with increasing outdoor temperature. At the same time, a less noticeable trend is observed for ducted or mixed sites, as seen in Table 10. Furthermore, our analysis revealed that ductless sites had higher supply air temperatures than centrally ducted sites, while the air-to-water sites had the highest supply temperatures. However, these temperatures remain considerably below the range of traditional gas or electric boilers.

Traditional baseboard radiators are incompatible with air-to-water heat pumps due to their reliance on high supply temperatures of 170 – 180 °F. The lower supply temperatures of air-to-water heat pumps might not provide sufficient heat output for traditional baseboard radiators to function optimally. When the supply water temperature is significantly lower than what the baseboard radiators are designed for, they might not be able to produce the desired level of warmth within

the living spaces, leading to subpar heating performance. Alternative heating distribution systems, such as underfloor radiant heating or specialized low-temperature baseboard radiators, are often recommended to accommodate air-to-water heat pumps. These systems are designed to efficiently transfer heat from the lower supply water temperatures associated with heat pumps, ensuring effective and comfortable heating while maximizing the heat pump's efficiency.

The air-to-water heat pump sites all utilized lower-temperature heat delivery devices. Improving the envelope in residential buildings to reduce design day heat demand would enhance the ability to use air-to-water heat pumps, possibly even with existing, common baseboards. The low output associated with common baseboard radiators at low temperatures is recognized as a concern with high-efficiency condensing boilers. Manufacturers are starting to introduce products that perform better at low water temperatures. The development of retrofit forced-air concepts has also begun to enhance the performance of existing baseboard radiators.

Table 10: Summary of Steady-state Supply Temperature at Various Operation Temperatures During Heating Mode.

| Site Name | Median Supply Temperature [°F] | | | |
|---|---|---|---|---|
| | 5 °F | 17 °F | 47 °F | Entire Heating Season |
| Ductless 1:1 | | | | |
| EFG-001 | 124 | 118 | 86.1 | 89.1 |
| EFG-006 | 88 | 89.7 | 88.7 | 93.5 |
| EFG-002 | 116 | 110 | 88.2 | 90.7 |
| EFG-004 | 124 | 126 | 127 | 127 |
| TLP-004 | N/A | 98.1 | N/A | 97.2 |
| EFG-007 | 126.1 | 113 | 105 | 108 |
| TLP-001 | N/A | 124 | 122 | 124 |
| TLP-002 | N/A | 101 | 94.8 | 94.1 |
| BNL-001 | 118 | 121 | 99.1 | 120 |
| Miscellaneous (Ducted, Ductless 1:2, Mixed) | | | | |
| CEE-002 | 117 | 111 | 102 | 105 |
| CEE-003 | 95 | 97.9 | 100 | 100 |
| CEE-001 | 90 | 89.7 | 93.1 | 91.6 |
| EFG-009 | 90.9 | 98.7 | 90.9 | 93.1 |
| EFG-005 | 92.9 | 98.5 | 88.3 | 89.1 |
| EFG-008 | 120 | 125 | 113 | 117 |
| TLP-003 | 90.7 | 93.5 | 123 | 99.7 |
| EFG-003 | N/A | 93.8 | 95.8 | 92.7 |
| Air-to-Water | | | | |
| AWHP1 | N/A | 133 | 121 | 130 |
| AWHP2 | 117 | 121 | 123 | 123 |
| AWHP3 | 113 | 121 | 126 | 125 |
| AWHP4 | N/A | N/A | 111 | 116 |
| Summary | | | | |
| Average (Ductless 1:1) | 116 | 111 | 101 | 105 |
| Average (Ducted) | 97.1 | 97.4 | 100 | 96.4 |
| Average (Air-to-Water) | 115 | 125 | 120 | 124 |
| Average (All) | 108 | 109 | 105 | 106 |

# Cooling Mode Performance Results

## 7.1 Coefficient of Performance

Similarly, as in heating mode, the cooling mode steady-state ('SteadyState_C') COP was computed for each site and its associated uncertainty using the statistical error approach, as discussed in Section 3.3. In the following figures (Figure 52 and Figure 53), larger error bars indicate a wider spread of COP and fewer data points collected in this temperature bin. Overall, the results show that cooling COPs matched or exceeded the appliance ratings at the minimum and maximum tested outputs at the design temperatures of 82°F and 95°F, shown in green and purple, respectively, in the plots. Site CEE-003 was decommissioned before the cooling season began and thus had no cooling data. Other sites, such as TLP-002, did not experience the full range of temperatures considered in the study.

Across all the ductless 1:1 sites, a minimum COP of 3.97 at 95 °F occurred at TLP-001, while a maximum of 6.14 occurred at BNL-001. As shown in Figure 52 below, TLP-004 depicts the highest COP but presents a value sufficiently far from its specifications. This could be due to issues with the airflow correlation or irregularly low measured power consumption. As a result, TLP-004 is not included in any cross-site averages. The observed minimum value at TLP-001 could be attributed to the limited number of recorded hours in the 'SteadyState_C' mode, which might be a consequence of overall low utilization. In general, the COPs decreased or stayed constant with increasing outdoor temperature among ductless 1:1 installations. All nine of the ductless 1:1 sites in the study met or exceeded the appliance ratings at 82 °F at 95 °F, and eight of nine met expectations.

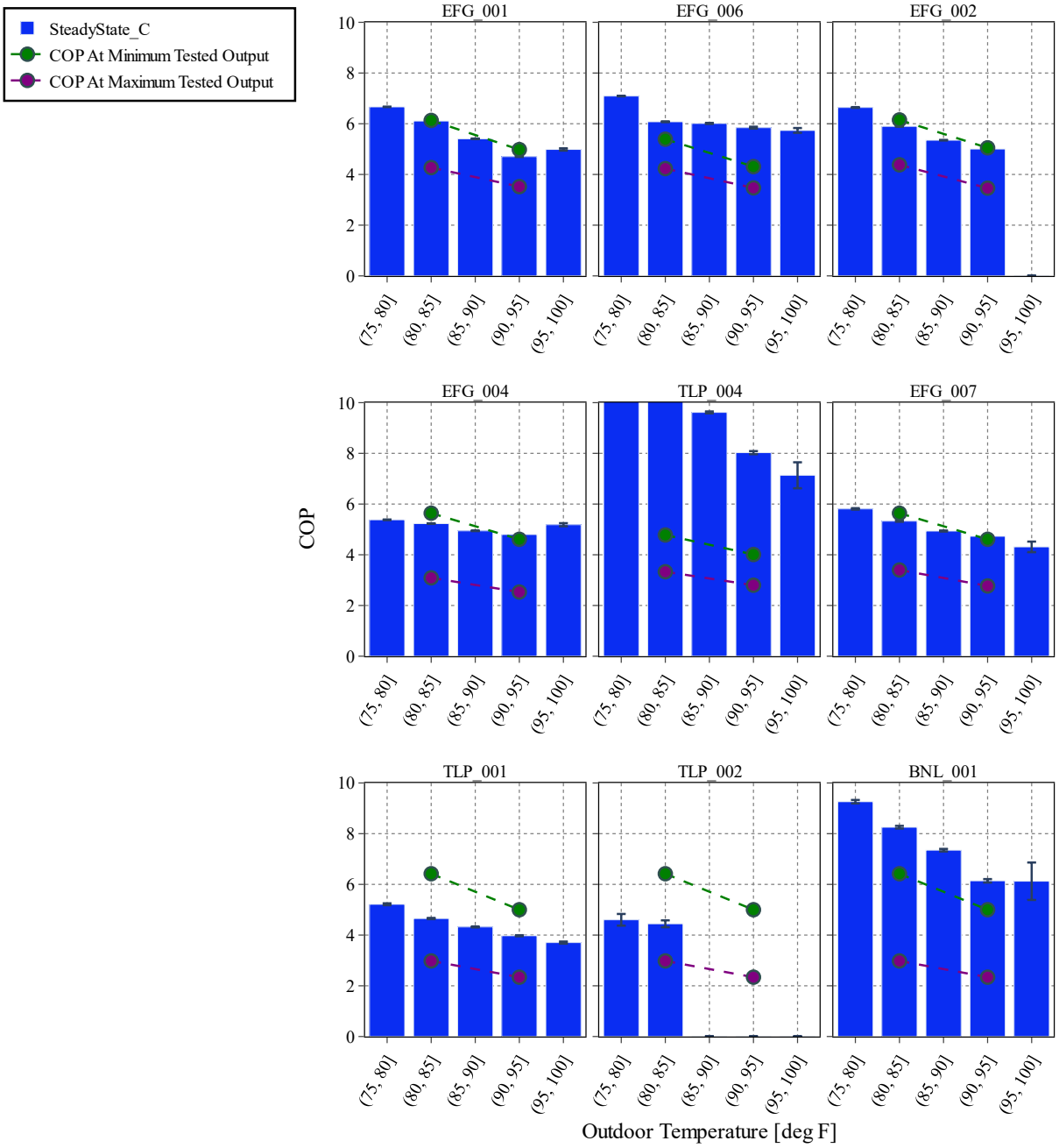


Figure 52: Steady-state cooling COPs against available unit performance data for ductless 1:1 sites

At the ductless 1:2 site (EFG-008), the average COP at 82 °F and 95 °F was 4.87 and 4.66, respectively. At this site, COP remained relatively constant with respect to temperature and had average values within the expected range. Across the centrally ducted sites, the lowest COPs occurred at CEE-002 and EFG-005 with values of 3.32 and 3.20, respectively. Notably, these sites underperformed with respect to design expectations. The maximum COP in this group of 4.55 was

found at EFG-003, which exceeded design expectations. Generally, COP decreased slightly with increasing temperature at the centrally ducted sites. At the mixed site (EFG-009), the average COP at 82 °F and 95 °F was 5.00, and 4.42, respectively. At this site, COP decreased with ambient temperatures and, similar to the ductless 1:2 unit, had average COP values within the expected range.

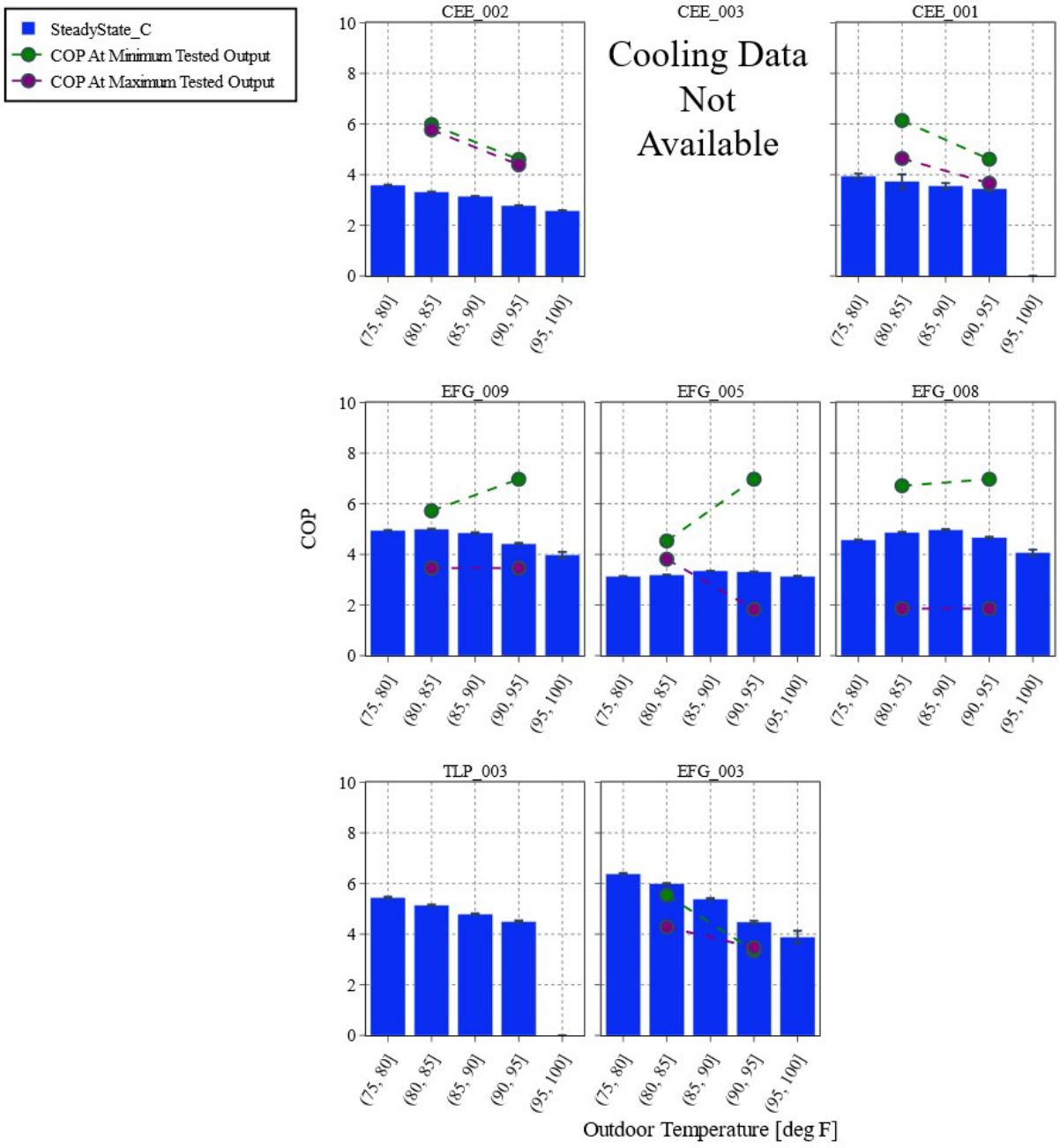


Figure 53: Steady-state cooling COPs against available unit performance data for mixed sites

Table 11 shows that as the outdoor temperature increases, the COP decreases for all sites except EFG-005 and EFG-008. However, the decreasing trend is much more significant for the ductless 1:1 sites than the centrally ducted or mixed sites COP. As expected, the COP for cooling was greater than heating due to a decrease in lift (smaller temperature differential). Additionally, COPs for the ductless 1:1 sites were considerably larger than the same at the centrally ducted sites.

Table 11: Summary of Steady-state COP at Various Operation Temperatures During Cooling Mode.

| Site Name | Average Steady-state COP | |
|---|---|---|
| | 82 °F | 95 °F |
| Ductless 1:1 | | |
| EFG-001 | 6.11 | 4.70 |
| EFG-006 | 6.08 | 5.84 |
| EFG-002 | 5.90 | 5.00 |
| EFG-004 | 5.23 | 4.80 |
| TLP-004 | 10.5 | 8.03 |
| EFG-007 | 5.33 | 4.73 |
| TLP-001 | 4.65 | 3.97 |
| TLP-002 | 4.45 | N/A |
| BNL-001 | 8.25 | 6.14 |
| Miscellaneous (Ducted, Ductless 1:2, Mixed) | | |
| CEE-002 | 3.32 | 2.78 |
| CEE-001 | 3.73 | 3.45 |
| EFG-009 | 5.00 | 4.42 |
| EFG-005 | 3.20 | 3.31 |
| EFG-008 | 4.87 | 4.66 |
| TLP-003 | 5.14 | 4.50 |
| EFG-003 | 5.99 | 4.48 |
| Summary | | |
| Average (Ductless 1:1) | 5.75 | 5.03 |
| Average (Ducted) | 4.28 | 3.70 |
| Average (All) | 5.15 | 4.48 |

## 7.2 Capacity Modulation and Cycling

### 7.2.1 Output Capacity Ranges and Power Consumption

The steady-state cooling output (referred to as the cooling capacity and labeled as 'SteadyState_C') at different outdoor temperatures at each site is shown in Figure 54 and Figure 55. Within the plots for each site are box-and-whisker diagrams, which show the median (central dark line) first and third quartiles (box lower and upper bounds) and minimum and maximum (whisker lower and upper bounds) for each 5-degree temperature bin. The majority of sites had logged 'SteadyState_C' hours at the appliance design temperatures of 82 and 95 °F; the exceptions were TLP-002 and CEE-003, as mentioned previously. A trend of increasing median cooling output with increasing temperature was expected, as more cooling capacity was required to meet the setpoint temperature or demand load with higher outdoor temperatures. Additionally, a larger interquartile range represented by a wider box indicates units operated at various cooling outputs within a given temperature bin due to their variable compressor speeds or indoor fan speeds.

Some of the units show thin boxes near the minimum tested output, with even outliers falling short of the maximum tested output. This may provide an indication that the units were sized close to the rated cooling output. If the units were oversized for cooling, the measured outputs would have fallen below the minimum tested outputs (or cycled more often, as investigated in subsequent subsections). If the units were significantly undersized for a cooling load, they would have fallen closer to the maximum tested output. A specific indicator of possible oversizing would be a thin box very close to the minimum output design rating with a stagnant median compared across multiple increasing temperature bins; this trend would indicate that the appliance is operating at its minimum across multiple outdoor temperature bins and could likely be scaled down.

For the ductless 1:1 sites, no general trend can be concluded, as seen in Figure 54. The lowest median output at 95 °F occurred at EFG-001, while the highest occurred at BNL-001. However, the cooling output is within the expected range for the installation in both instances. Seven of the nine ductless 1:1 sites had median cooling outputs between the meeting or exceeding appliance design ratings at 82 °F, while all sites met or exceeded appliance ratings at 95 °F. With the exception of TLP-001 and TLP-002, the median cooling output was closer to the minimum tested output than the maximum. The interquartile range in cooling output was relatively small, except at TLP-001.

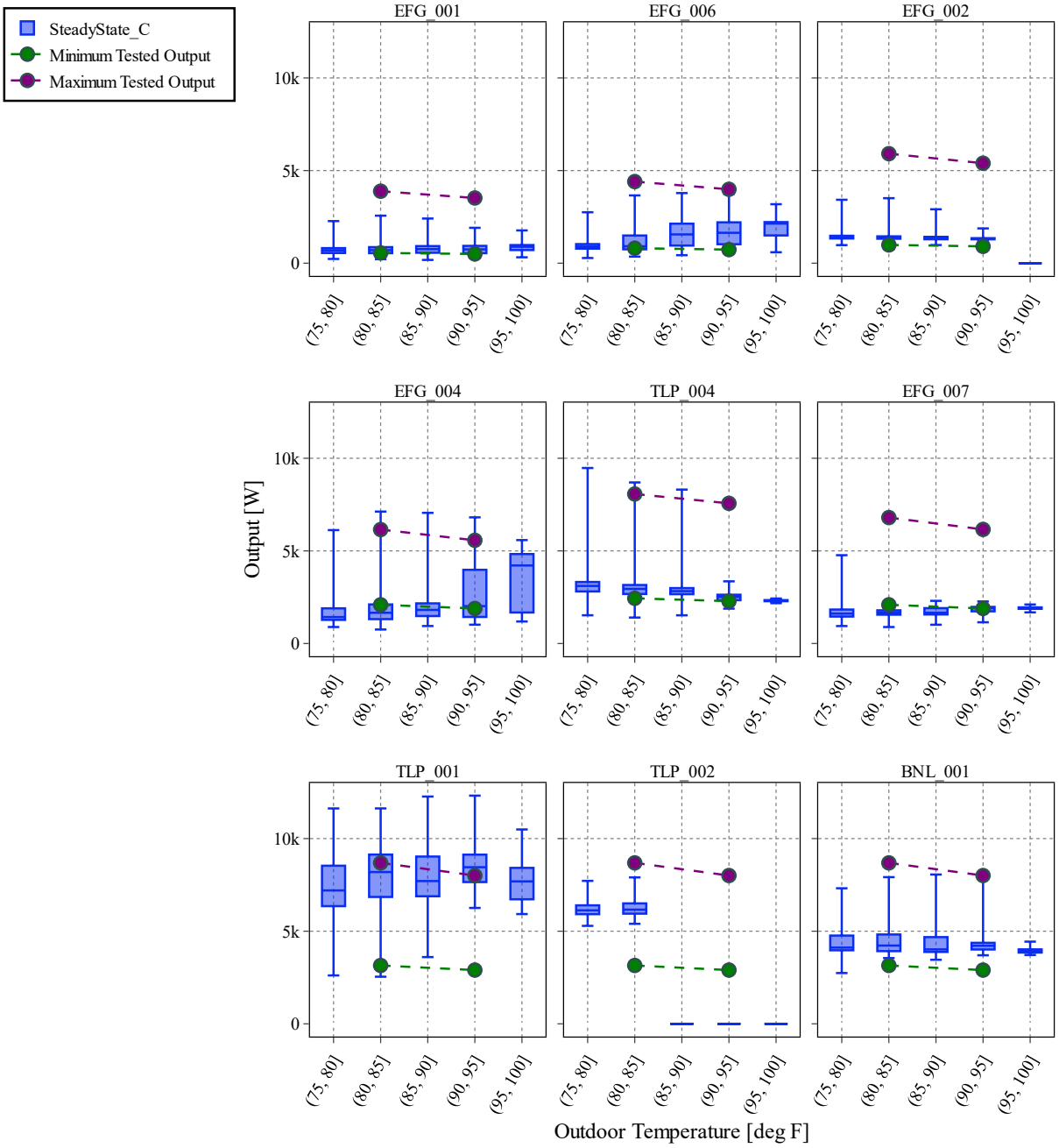


Figure 54: Heat removal boxplot binned by outdoor temperature compared to available unit performance data for ductless 1:1 sites during steady-state cooling

At the ductless 1:2 (EFG-008) site, the median cooling output at 82 and 95 °F were 2,958 and 2,650 W, both of which were below the minimum appliance design rating. The median cooling output at this site increased slightly with increasing temperature, and the interquartile range was relatively small.

The centrally ducted sites shown in Figure 55, more often than with the ductless 1:1 sites, fell below the minimum tested output—indicating they may have been oversized for cooling loads. Analyzing the trends in median cooling output by temperature bins showed that two installations had increasing trends (EFG-005 and EFG-003), one installation had a decreasing trend (CEE-001), and two sites had little to no change in median output with temperature (CEE-002 and TLP-003). The lowest median cooling output at 95 °F occurred at EFG-005 with a value of 2,114 W. The highest median output of 10,269 W occurred at TLP-003 at 82 °F. Notably, out of the centrally ducted sites, only EFG-003 had a median cooling output between the minimum and maximum appliance design ratings. At the mixed site (EFG-009) investigated in this study, the median cooling output at 82 and 95 °F specifically were 3,095 and 3,263 W, both of which were below the minimum appliance design rating. The median cooling output remained constant with the temperature at this site, and the interquartile range was relatively small and stable across all cooling season temperature bins.

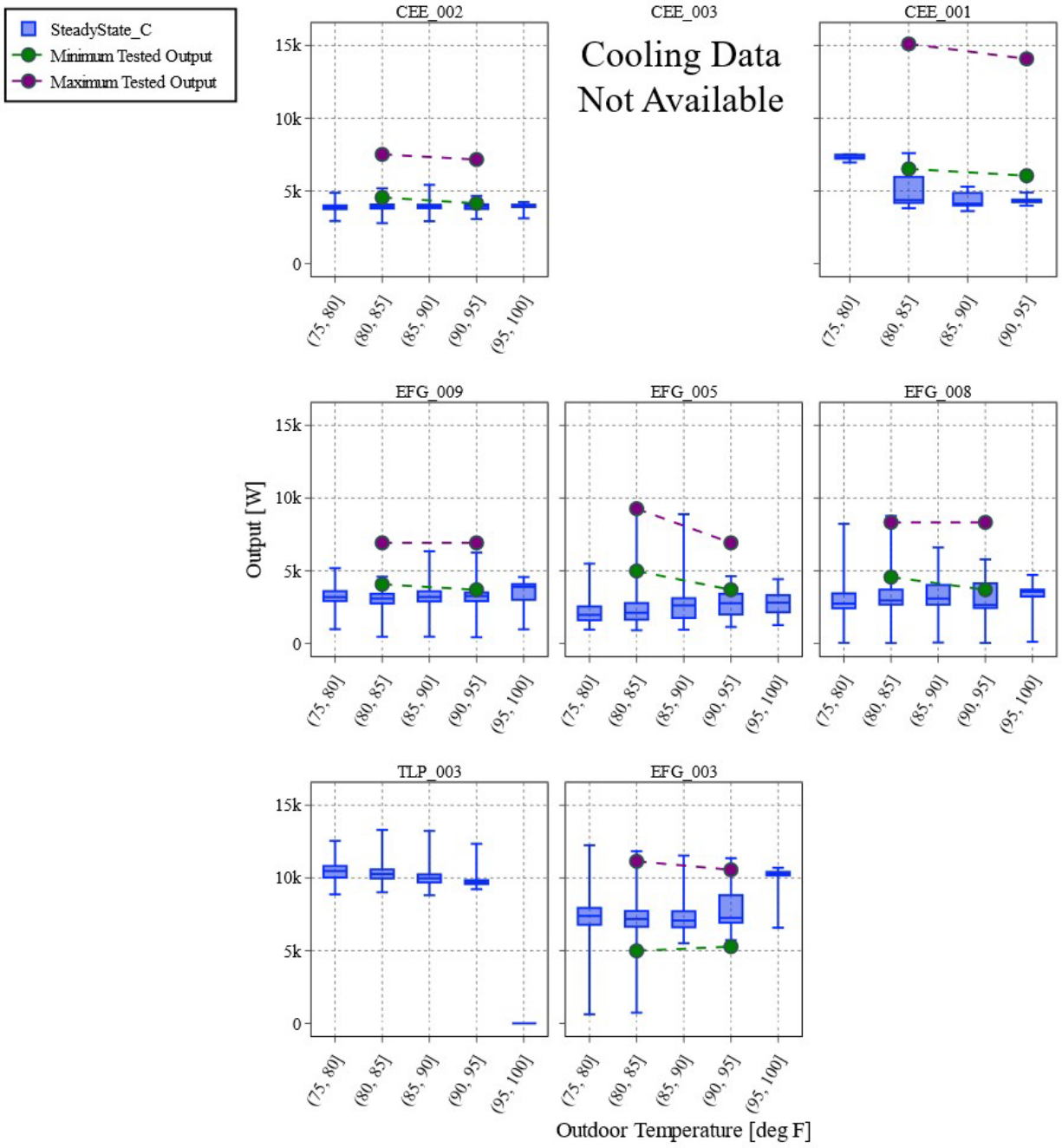


Figure 55: Heat removal boxplot binned by outdoor temperature compared to available unit performance data for ducted and mixed sites during steady-state cooling

In summary, our cooling output analysis indicated that most ductless 1:1 sites operated with median cooling outputs within design expectations, while the ductless 1:2, centrally ducted, and mixed sites had outputs below the minimum tested value. Trends in median cooling output can increase, decrease, or remain relatively constant with respect to increasing outdoor temperatures, as shown in Table 12.

Table 12: Summary of Steady-state Median Output at Various Operation Temperatures During Cooling Mode.

| Site Name | Median Steady-state Output [W] | | |
|---|---|---|---|
| | 82 °F | 95 °F | Entire Cooling Season |
| Ductless 1:1 | | | |
| EFG-001 | 702.2 | 745.2 | 707.4 |
| EFG-006 | 912.3 | 1641 | 976.4 |
| EFG-002 | 1377 | 1317 | 1376 |
| EFG-004 | 1659 | 2018 | 1609 |
| TLP-004 | 2948 | 2513 | 2920 |
| EFG-007 | 1665 | 1903 | 1687 |
| TLP-001 | 8193 | 8453 | 7912 |
| TLP-002 | 6163 | N/A | 6150 |
| BNL-001 | 4224 | 4214 | 4106 |
| Miscellaneous (Ducted, Ductless 1:2, Mixed) | | | |
| CEE-002 | 3917 | 3927 | 3901 |
| CEE-001 | 4366 | 4296 | 4264 |
| EFG-009 | 3095 | 3263 | 3172 |
| EFG-005 | 2114 | 2770 | 2189 |
| EFG-008 | 2958 | 2650 | 2896 |
| TLP-003 | 10269 | 9696 | 10053 |
| EFG-003 | 7177 | 7255 | 7235 |
| Summary | | | |
| Average (Ductless 1:1) | 3112 | 2899 | 3065 |
| Average (Ducted) | 5579 | 5589 | 5528 |
| Average (All) | 3919 | 3868 | 3882 |

Cooling output and heat pump energy consumption are the key data for calculating the COP in cooling mode. In Figure 56 and Figure 57, the power consumption for all steady-state cooling periods ('SteadyState_C') by outdoor temperature bin is plotted. Similar to the figures above, the plots are shown as box-and-whisker diagrams.

Across the ductless 1:1 sites, Figure 56 shows nearly identical trends for power consumption as for output—indicating the power consumption was within design specifications at the design temperatures of 82 and 95 °F for nearly all sites. The TLP-004 site showed a lower-than-expected power consumption at both design temperatures, while the TLP-002 site data showed power consumption in the expected range at 82 °F, but no cooling data was collected at 95 °F. Power consumption at seven of nine ductless 1:1 sites was relatively constant with respect to temperature, with median values close to the minimum tested output at each site. The TLP-001 and TLP-002 sites were closer to the middle of the expected range.

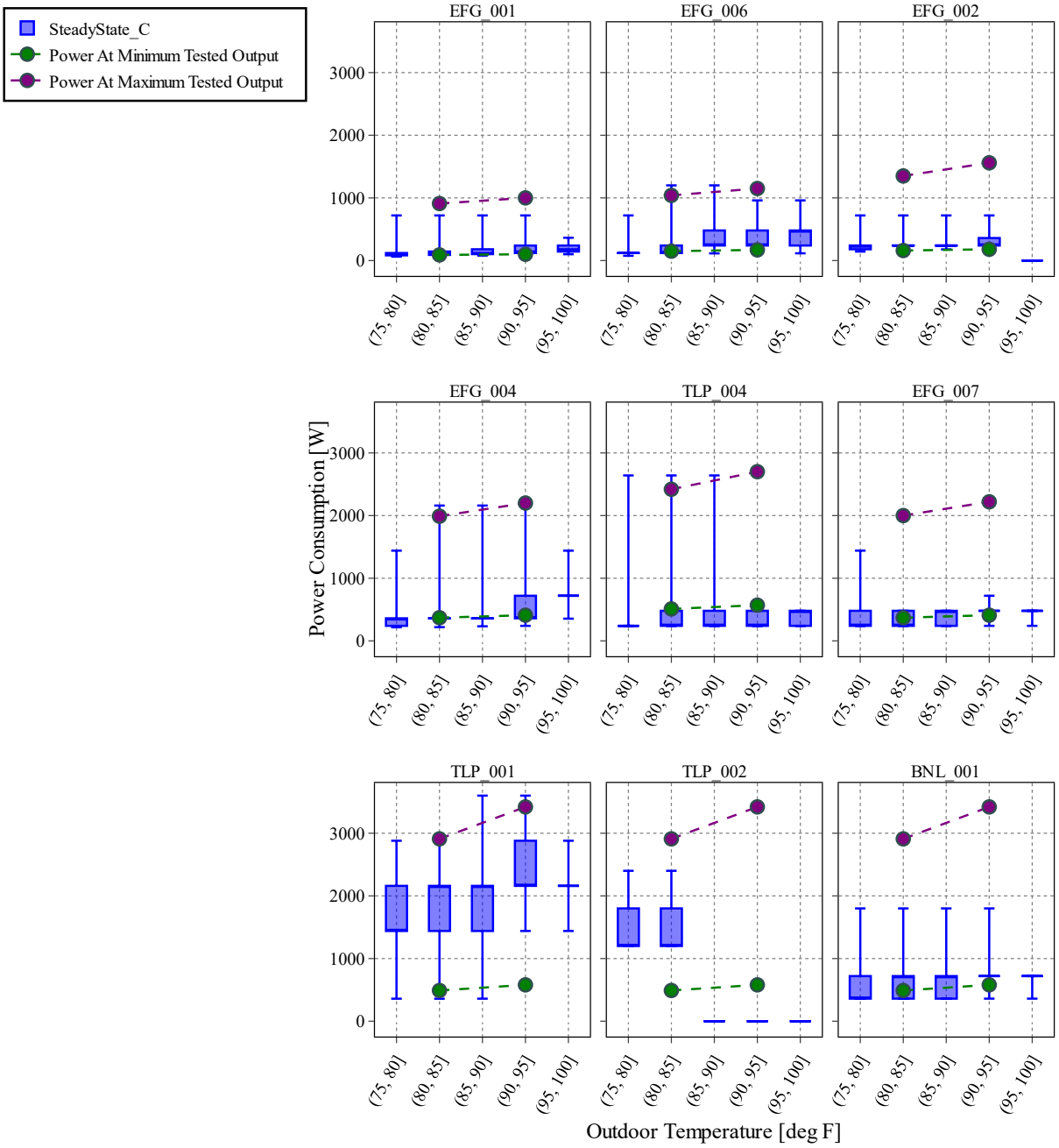


Figure 56: Power consumption boxplot binned by outdoor temperature for ductless 1:1 sites during steady-state cooling

Similar trends were found at the ductless 1:2, centrally ducted, and mixed installation sites. At these sites, power consumption was within design specifications at the design temperatures for five of the seven total. Power consumptions at the ductless 1:2, centrally ducted, and mixed sites were relatively constant with respect to temperature.

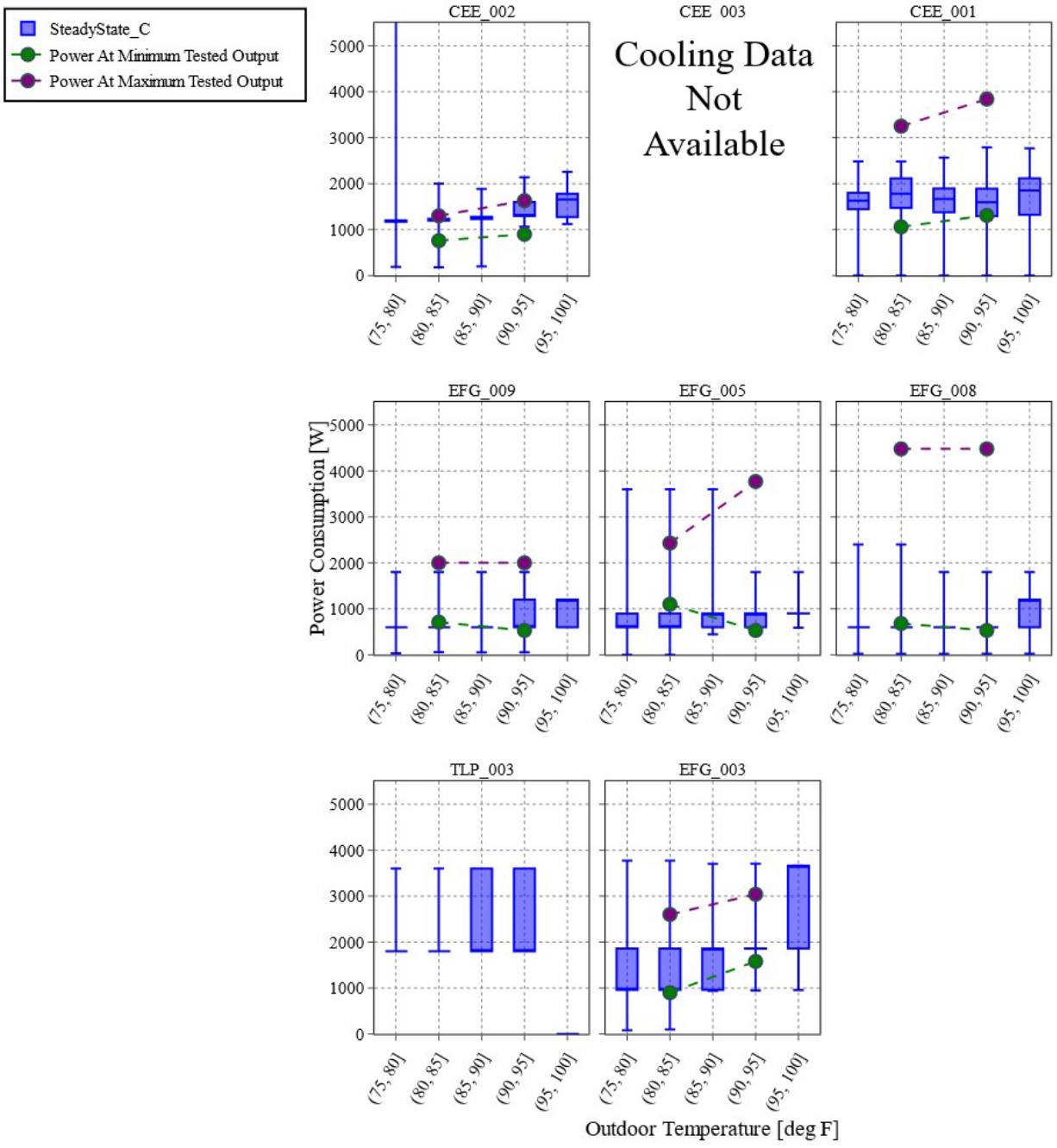


Figure 57: Power consumption boxplot binned by outdoor temperature for ducted and mixed sites during steady-state cooling

### 7.2.2 Average Cycles Per Hour

An analysis of the cycling behavior of the heat pump installation at each site in this study is presented below in Figure 58 and Figure 59. Each individual plot depicts the hourly cooling mode cycling rate, binned by temperature range, each heat pump site experienced. Each bar represents the average hourly cooling mode cycling rate within a specific outdoor temperature range. For context, a low hourly cooling mode cycling rate indicates the heat pump was running nearly continuously, while a high hourly cooling mode cycling rate indicates the heat pump rapidly turned on and off. Thus, a high hourly cooling mode cycling rate is expected at low outdoor temperatures, and a low hourly cooling mode cycling rate is expected at high outdoor temperatures. A constant low hourly cooling mode cycling rate across all temperatures could indicate that the appliance is properly sized. Conversely, excessively high cycling rates could indicate oversizing. Hourly cooling mode cycling rate was measured at all sites with logged 'SteadyState_C' hours.

Across the ductless 1:1 sites, the average cycles per hour were low, typically less than five. Five sites had cycling rates of less than one, indicating near-constant operation. Five out of the nine ductless 1:1 sites showed the expected decreasing trend in hourly cooling mode cycling rate with temperature; as in the other four sites, the cycling rate was relatively constant. Notably, the BNL-001 site had a high cycling rate greater than 10.

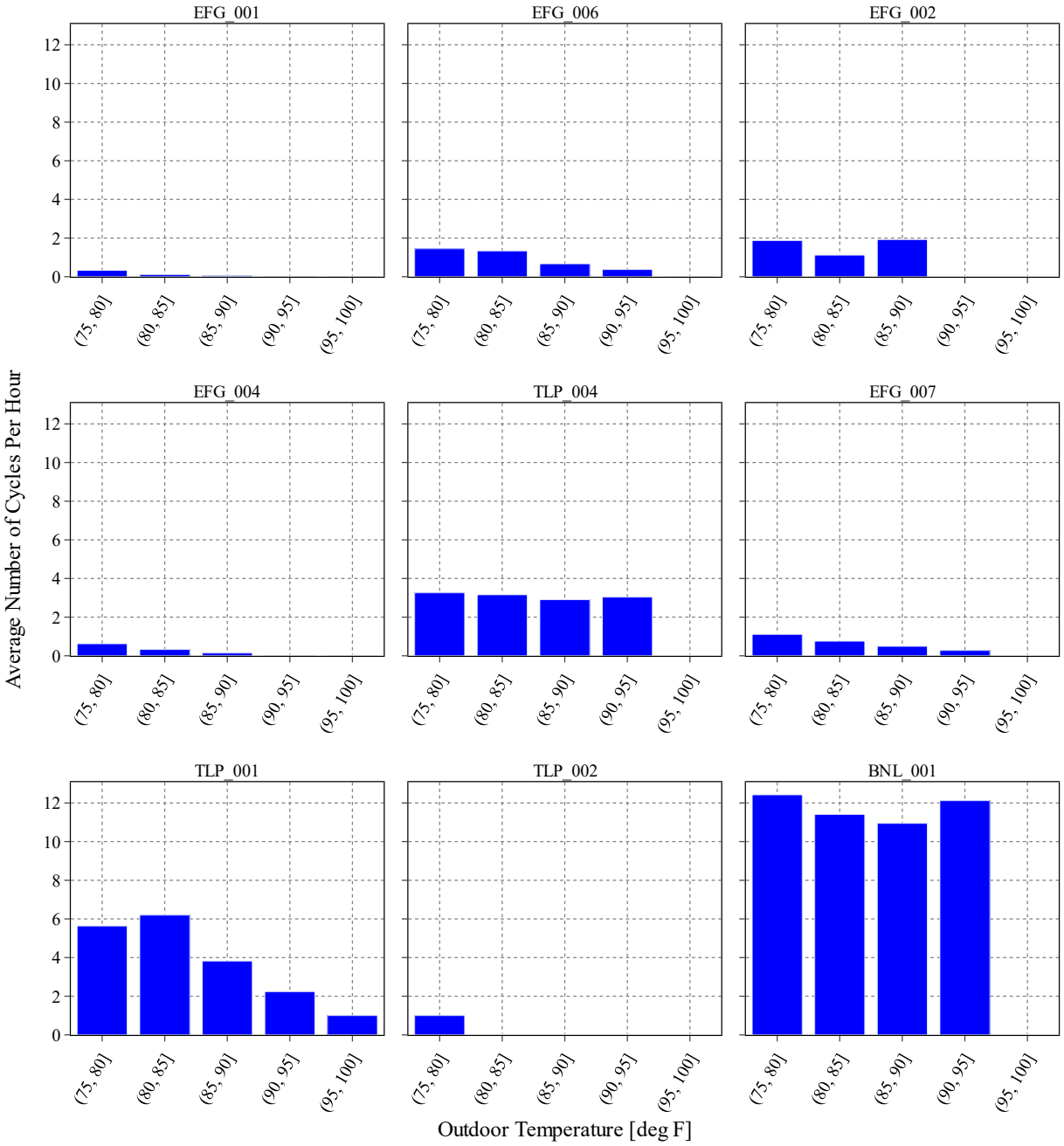


Figure 58: Average number of cycles per hour binned by outdoor temperature during cooling mode for ductless 1:1 sites

At the ductless 1:2 site, EFG-008, the average cycling rate was less than one, indicating that the heat pump at this site ran nearly continuously. Further, the cycling rate changed little with temperature. At the five centrally ducted sites with cooling data, the results are bimodal, with the TLP-001, EFG-003, and CEE-003 sites all having cycling rates generally greater than or equal to

five, and CEE-002 and EFG-005 both having cycling rates less than 1. Cycling rates were relatively constant with respect to temperature, except for site CEE-001, which shows a local maximum in the (85, 90] temperature bin for unknown reasons. At the mixed site, EFG-009, the hourly cycling rates at 82 and 95 °F were each approximately one, and the cycling rate did not trend with temperature. It follows that the heat pump at this site ran nearly continuously across the cooling season temperature range.

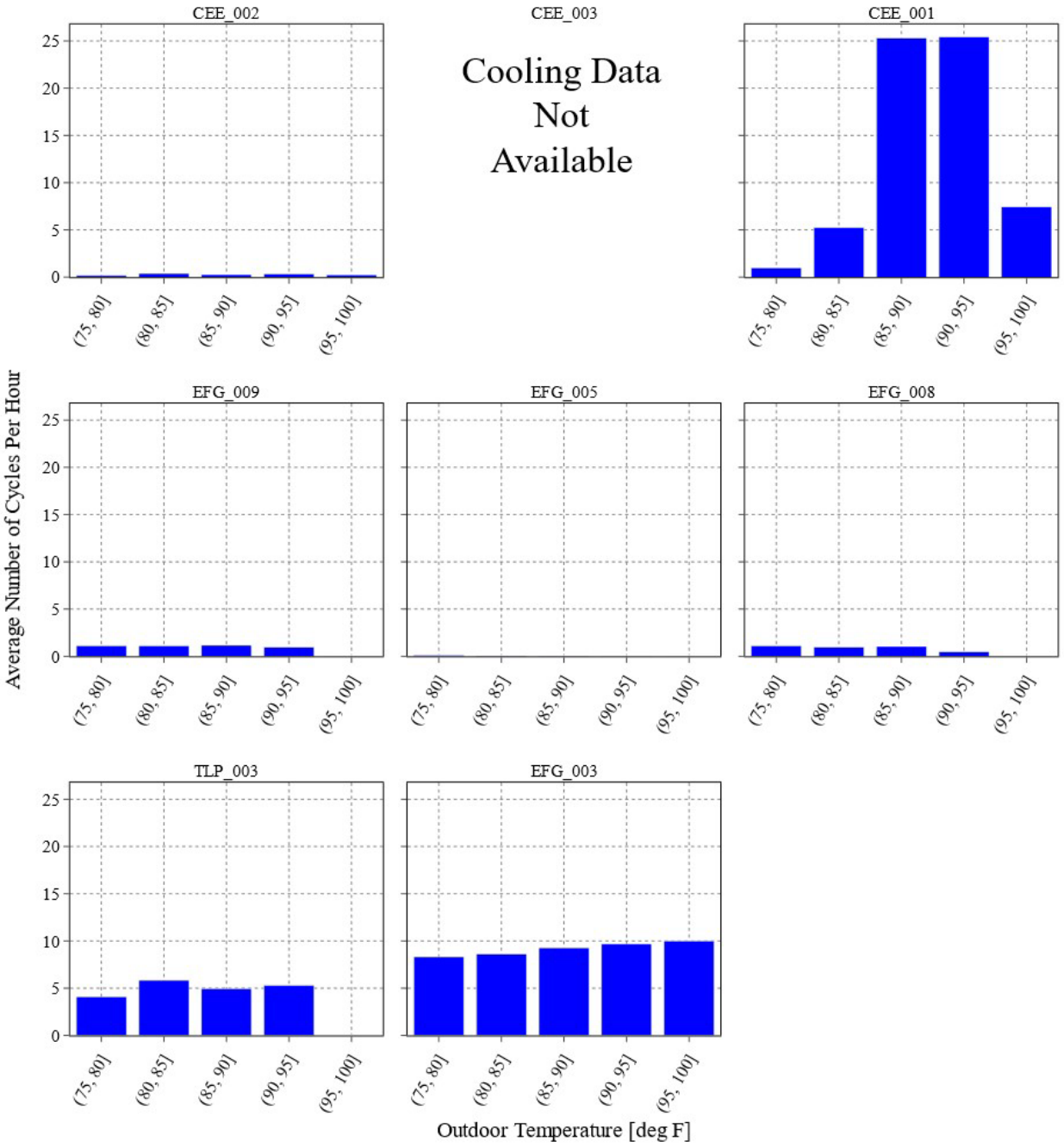


Figure 59: Average number of cycles per hour binned by outdoor temperature during cooling mode for ducted and mixed sites

In summary, the hourly average cooling mode cycling rate data showed that there is quite a large range in cycling rate between appliance installations, but for most installations in our study, the cycling rate at a specific site did not vary much with temperature. A small majority of the ductless 1:1 installations showed a trend of decreasing cycling rate with temperature, but the ductless 1:2,

centrally-ducted, and mixed sites had relatively constant cycling rates throughout the cooling season temperature range.

## 7.3 Supply Temperature

The supply temperature data as a function of ambient temperature for each site is shown in Figure 60 and Figure 61. Each site-specific plot contains box-and-whisker diagrams with the same designations for median, first and third quartile, and maximum and minimum values, as used in previous sections. The outdoor temperature range bins are the same as those used in previous sections. In a heat pump system, the supply temperature, the indoor air temperature, and the air delivery rate determine the heating or cooling load applied to the living space. Supply temperature is a limiting factor in this equation when cooling as it must be below the desired room temperature, as a portion of the heat removed manifests as latent heat, which serves to condense any water vapor in the return air. As a result, the lower limit may be limited to the dew point temperature at the return temperature and relative humidity. It follows that the supply temperature in cooling mode is typically a fixed value for a given heat pump installation. Thus, relatively constant values are expected for cooling supply temperatures at all sites.

Across all ductless 1:1 sites, the average median cooling supply temperatures at 82 and 95 °F were 52.6 and 53.6°F, respectively, as seen in Figure 60. The average median cooling supply temperature across the entire temperature range for this appliance category was 52.7 °F. All ductless 1:1 site median cooling supply temperatures were maintained in a range of 1 to 4 °F around a central value between 40 and 60 °F. The interquartile range was also small, on the order of 1 to 4 °F.

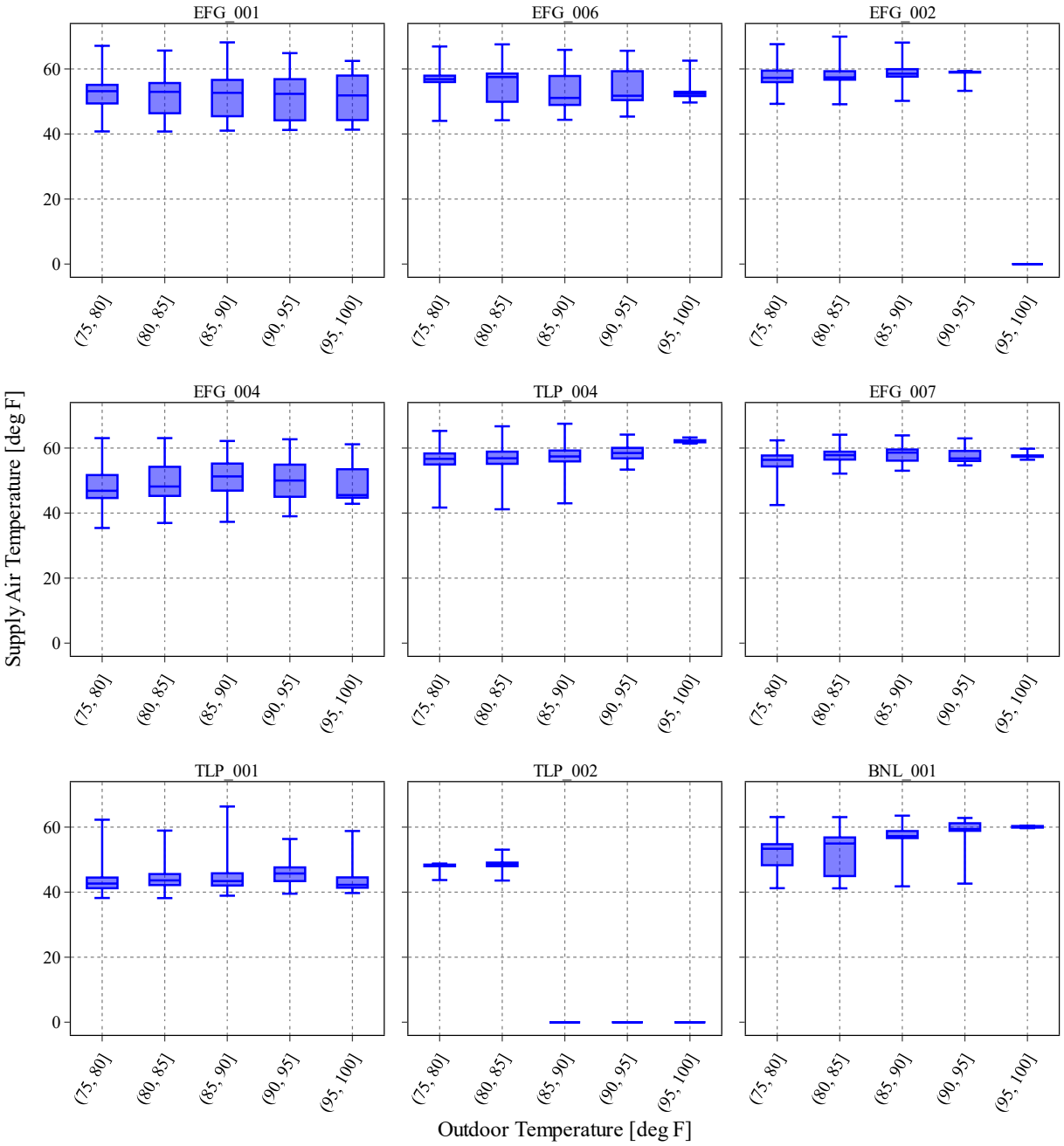


Figure 60: Cooling supply temperature binned by outdoor temperature for ductless 1:1 sites during steady-state cooling.

At the ductless 1:2 site, the average median cooling supply temperatures at 82 and 95 °F were 41.7 and 43.1 °F, respectively, as shown in Figure 61. The overall average median cooling supply temperature at this site was 42.5 °F. This site had the lowest median supply temperature across the study. Across all centrally ducted sites, the average median cooling supply temperatures at 82 and

95 °F were 49.5 and 50.2°F, respectively. The average median cooling supply temperature across the entire temperature range for this appliance category was 49.6 °F. The results for the centrally ducted sites were similar to those for the ductless 1:1 sites. At the mixed site, the average median cooling supply temperatures at 82 and 95 °F were 53.4 and 54.5 °F, respectively. The overall average median cooling supply temperature at this site was 52.8 °F.

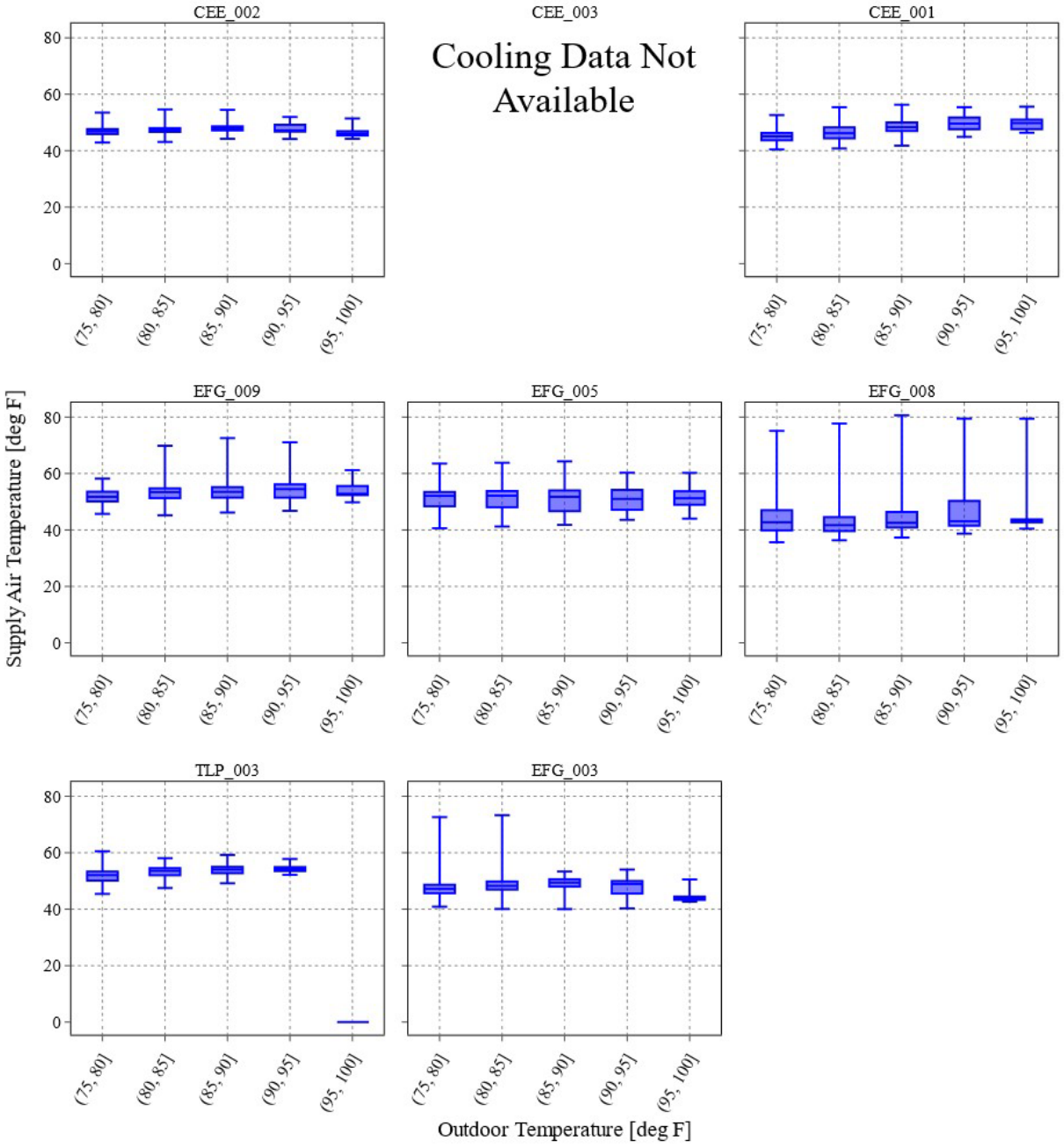


Figure 61: Cooling supply temperature binned by outdoor temperature for ducted and mixed sites during steady-state cooling.

Table 13 summarizes the major results from our study of cooling supply temperatures. It shows that the median supply temperature at each site was relatively constant with respect to temperature. At all sites the median supply temperatures were maintained in a range of 1 to 4 °F around a central value between 40 and 60 °F. Additionally, the interquartile range in any given temperature was small, on the order of a few degrees.

Table 13: Summary of Steady-state Median Supply Temperature at Various Operation Temperatures During Cooling Mode.

| Site Name | Median Supply Temperature [°F] | | |
|---|---|---|---|
| | 82 °F | 95 °F | Entire Cooling Season |
| Ductless 1:1 | | | |
| EFG-001 | 53.0 | 52.3 | 53.0 |
| EFG-006 | 57.5 | 51.8 | 56.8 |
| EFG-002 | 57.4 | 59.0 | 57.7 |
| EFG-004 | 48.2 | 50.0 | 48.4 |
| TLP-004 | 56.8 | 58.5 | 57.1 |
| EFG-007 | 57.8 | 56.8 | 57.6 |
| TLP-001 | 43.6 | 45.7 | 43.5 |
| TLP-002 | 48.6 | N/A | 48.4 |
| BNL-001 | 55.0 | 59.4 | 55.9 |
| Miscellaneous (Ducted, Ductless 1:2, Mixed) | | | |
| CEE-002 | 47.3 | 47.2 | 47.3 |
| CEE-001 | 46.2 | 49.6 | 46.8 |
| EFG-009 | 53.4 | 54.5 | 52.8 |
| EFG-005 | 52.1 | 51.0 | 52.0 |
| EFG-008 | 41.7 | 43.1 | 42.5 |
| TLP-003 | 53.6 | 54.2 | 53.7 |
| EFG-003 | 48.3 | 48.9 | 48.1 |
| Summary | | | |
| Average (Ductless 1:1) | 52.6 | 53.6 | 52.7 |
| Average (Ducted) | 49.5 | 50.2 | 49.6 |
| Average (All) | 50.9 | 51.7 | 51.0 |

# Discussion

## 8.1 Equipment Issues and Underutilized Systems

Throughout the study, multiple incidents occurred related to sensor, equipment, or communication failures or unusual usage patterns that may have affected the data. Those incidents are reported below. One common issue across many sites was the Campbell HygroView sensor (T_RHS_SUP, RH_SUP), which was a challenge to install on systems with articulated supply vanes. The sensor element was located in the supply flow for only certain damper positions, and when the unit shut down, the sensor protruded from the unit substantially. In addition, the HygroView sensor read considerably lower than the thermistors during heating cycles and higher than the thermistors during defrost operation, as shown in Figure 62. A decision was made early in the study to relocate the indoor fan current sensor to the outside data logger, to free up a channel on the interior logger and install an additional supply thermistor, bringing the total to three (3) supply thermistors for all other deployments (EFG-001 and EFG-002 were the only sites with two thermistors).

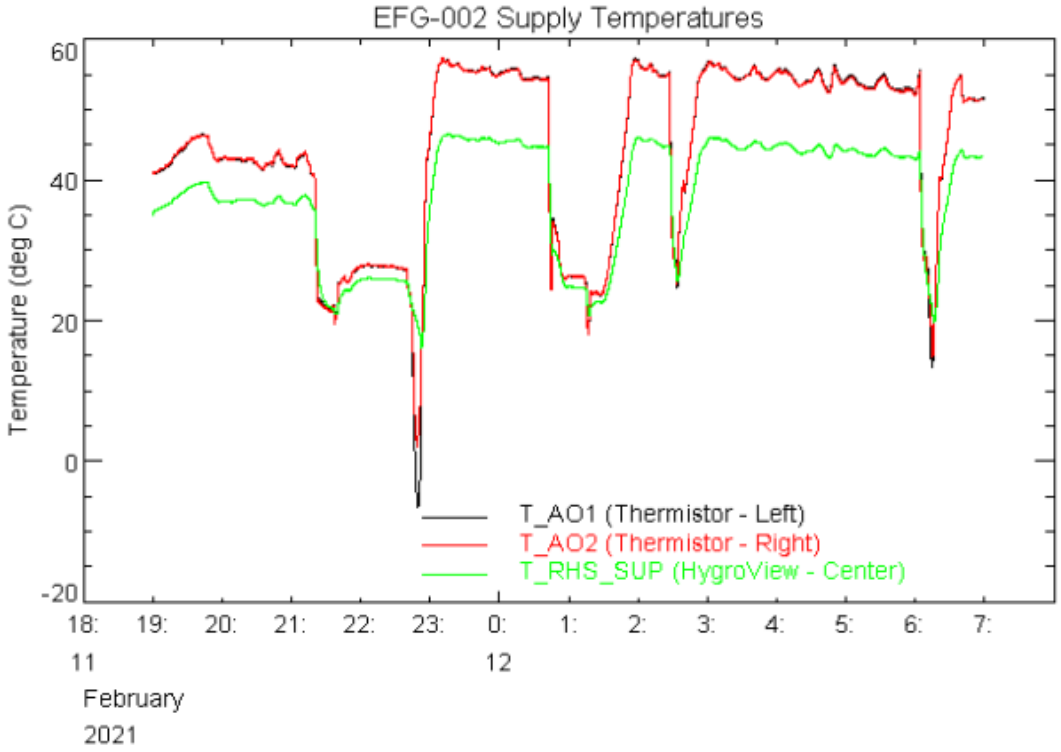


Figure 62: Difference in temperature measurements

Site **EFG-001** had a liquid line thermistor installed incorrectly in February 2021 and moved to the correct position on October 28th, 2021 for the upcoming heating season. The location change is seen in Figure 63 and Figure 64.

Figure 63: Original liquid line thermistor that was installed incorrectly in February 2021

Figure 64: Liquid line thermistor moved to correct position on October 28th, 2021

Site **EFG-002** on Feb 21st, 2022, the household cat knocked the RH sensor off the supply of the ductless unit for a second time. Unfortunately, the homeowner was unaware of how long it had been that way, but the issue was fixed once they noticed. The homeowner also indicated they had cleaned their filters in late February of 2022, which may have changed the static resistance compared with the original, shifting the airflow-current correlation.

Site **EFG-004**'s thermistor had an incorrect reading on the return temperature inlet, and therefore, it was recommended to use the measurement from the RH sensor inlet (T_RHS_IN ~ T_AI)

Site **EFG-008** had issues with data collection from poor cell modems. The team resolved the problem in May 2021 with a Campbell firmware update to dramatically increase cellular usage and bandwidth.

Site **TLP-001** had an unusually low usage of the heat pump. Contact with the homeowner did not indicate why they did not use the heat pump more often, but rather they had gone back to using the legacy natural gas-fired furnace "to save money". Additionally, there were maintenance issues related to the heat pump's thermostat.

Site **TLP-002** had issues with condensate at the indoor head and the outdoor logger flooding. Condensate issues at the indoor head began in June 2021. This stopped the homeowner from operating the indoor head until this was fixed in mid-September. The fix required many visits from the contractor, who only responded after repeated service requests from the homeowner and TLP.

Because of the condensate issues, the unit was rarely run in the cooling season, and window units were used for cooling in its place.

The outdoor logger then flooded in early September 2021, which resulted in the radio and CR1000x to stop operating, as seen in Figure 65. The homeowner was out of the country in October 2021, pushing logger replacement until November 2021, as shown in Figure 66. Complete airflow testing (heating and cooling) was then redone and completed during the November 24th, 2021 visit.

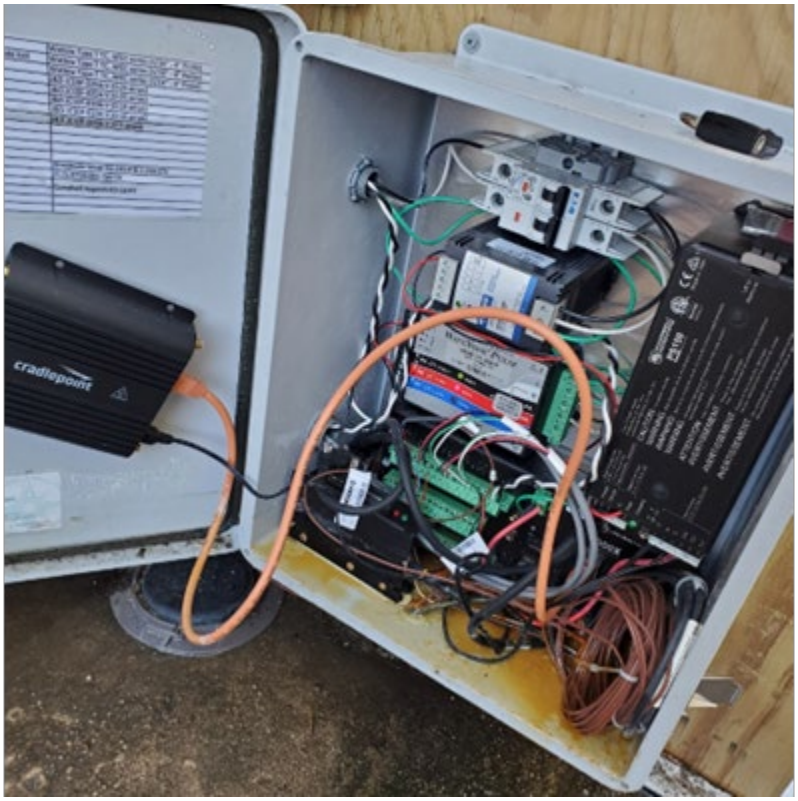

Figure 65: TLP-002 logger flood issue, September - November 2021

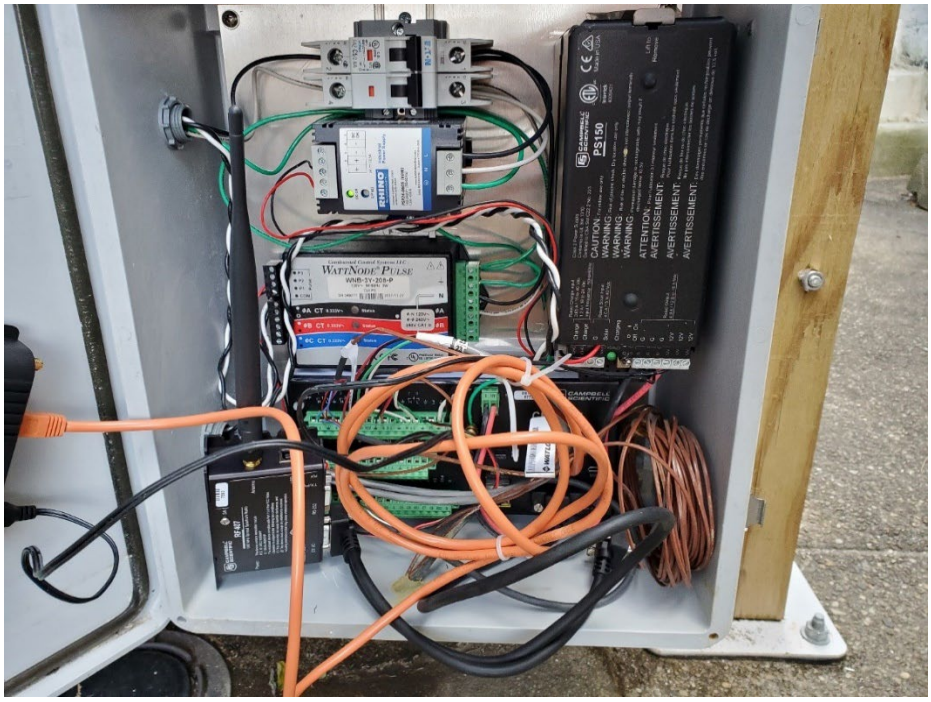

Figure 66: TLP-002 replacement logger, November 24, 2021

Later, on April 19th, 2022, communications were again lost. When contacting the homeowner, they indicated there had been about 2 feet of flooding from the recent storm, which was high enough to submerge the outdoor panel. This, unfortunately, killed the main logger and stopped data collection at the site. It was proposed to end monitoring at this location given that the area is prone to flooding and that the unit had control issues. The owner also indicated that the indoor head was not heating properly and was trying to get a contractor to service it. They were not aware of the timing of this issue and could not describe specifics regarding what was wrong with the heat output.

Site **TLP-003** had a continuous issue of artificial temperature from electrical interference and later a communication issue in May of 2022. The homeowner checked power to the outdoor section on June 25th, 2022, and indicated an issue with the ASHP causing the breaker to flip off each time they attempted to power the unit from the main electrical panel. Additionally, they said that they had accepted an offer on their home and were prepping for home inspections. Given this, the equipment was removed on June 26th, 2022, so it would not get caught up in the home sale and the unit's repair. During the equipment removal, team members found a leak in the refrigerant line at the braze point for the AHU in the attic, which most likely led to the compressor failing.

Site **CEE-001** encountered repeated failures of the compressor frequency sensor. As noted in Figure 67, the compressor frequency signal was absent, partially present, or operating as expected during periods with obvious delivered capacity. No obvious modes of failure were present, as the site was checked for loose wiring or damages. Since the compressor frequency signal was not detected when the heat pump was off or in a fan-only mode, it was kept as a measurement and supplemented by the compressor current measurement. Additionally, the RH sensor went offline briefly in June 2021 and was fixed on July 1, 2021.

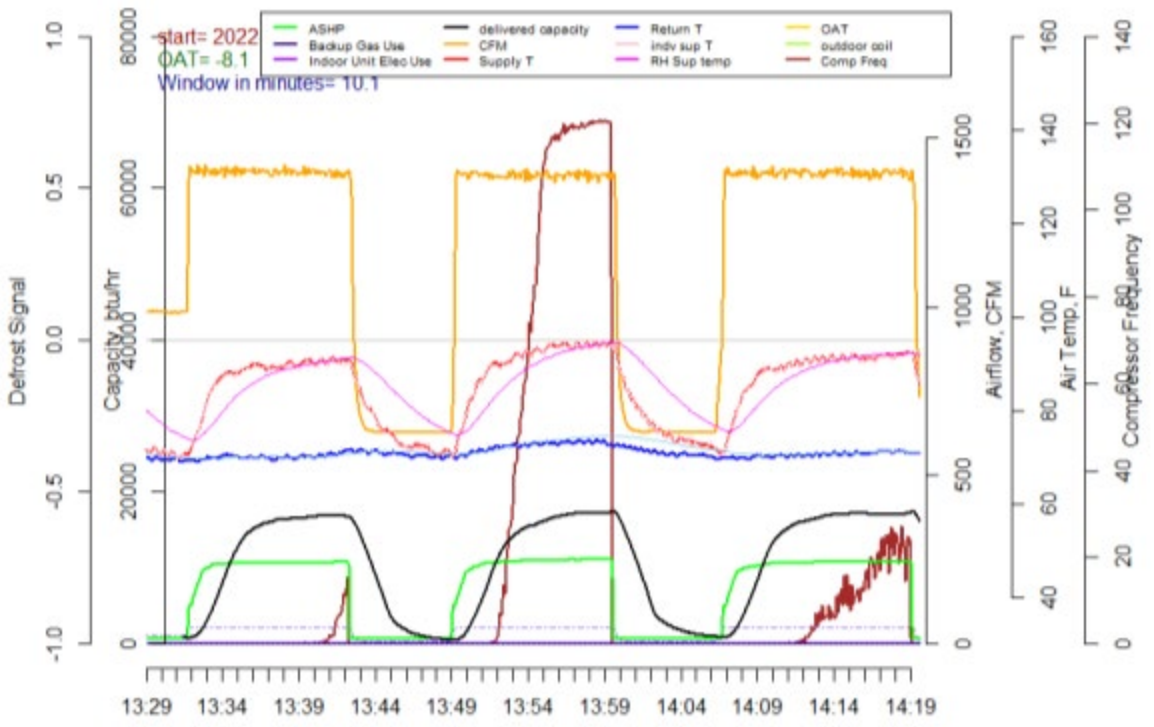


Figure 67: CEE-001 inconsistent compressor frequency(red) measurement that does not correlate with delivered capacity (black).

The heat pump at site **CEE-003** was monitored through April 2021. The team discovered that the equipment had gone offline and contacted the homeowner on April 21st, 2021, to troubleshoot. The homeowner then confirmed that they had moved out of their home and discontinued internet services, disrupting our data retrieval. The team was unable to confirm the date on which the homeowner moved out but could infer from the data that it was likely sometime at the beginning of April. The team requested that the homeowner inform us when their home was officially on the market for sale, but we were unable to connect after several attempts.

The team did attempt to remain in contact with the homeowner in hopes of keeping the site in the field study until its official conclusion date by introducing the project to new homeowners once the home was sold; however, we were unable to maintain contact with the existing homeowner causing us to pull the site from field monitoring.

The team monitored public housing listing sites such as Zillow to confirm when the home was put on the market for sale. We saw that the home was officially on the market on June 30th, 2021, and reached out to the homeowner to schedule a time to retrieve instrumentation loggers. Instrumentation was removed on July 15th, 2021. No photos were taken during the instrumentation removal.

The **BNL-001** site had a new wall-mounted thermostat installed in July 2020. The previous thermostat was the OEM remote located near the unit. The new wall-mounted thermostat was OEM but relocated to the kitchen, further away from the unit, to investigate the impact of demand

and cycling. Later in the study, in May of 2021, BNL-001 had an issue with reception and remote data collection, so a new logger and computer were installed to help download the data remotely.

In early Q3 of FY21 (April – June), site **AWHP-004** had a cell modem failure. This was replaced in late June, and some back data was collected. As a heating-only site, this missing data is likely inconsequential but included here for transparency.

## 8.2 Relative Humidity Sensor Measurements and Impact on COP

In general, it was noted that there were several incidents across the sites where the supply air temperature measurement did not agree with the temperature recorded by the relative humidity sensor at the outlet of the unit with temperature differences greater than 5 °C. This implied that the relative humidity sensor had been dislodged from its installation location to a region outside the outlet airflow stream. A reliable measurement for relative humidity could thus not be determined. For such cases where this has occurred, an assumption that the outlet air was fully saturated (100% relative humidity) at the supply temperature was used. This impacts the calculated COP and capacity of cooling mode calculations, which rely on the relative humidity measurements. Since a lower supply air relative humidity implies more water has been condensed out of the return air, calculations for these instances may underestimate the actual cooling load. Thus, the calculated cooling COPs represent the lower bound of what may be achievable for the unit when the relative humidity measurement was unavailable.

## 8.3 Performance Maps

With the data collected, empirical performance maps of the ccASHPs can be developed. This would include, for example, COP as a function of outside and delivered air temperature and flow and compressor speed. This approach should lead to nearly the same performance maps for identical units based on data from different sites. From these performance maps, model equations for the performance of the ccASHPs will be developed that can be used in building energy modeling programs such as EnergyPlus and TRNSYS.

## 8.4 Airflow Correlations and Flow Measurement

Properly constructing the airflow correlation curves as a function of indoor current is essential for properly calculating the unit's COP. Even minor errors in the data collection process during the construction of the curve can offset the results greatly. For instance, Figure 68 shows the airflow correlations evaluated at different indoor currents in steps of 0.01 A at sites BNL-001, TLP-001, and TLP-002. These sites have the same indoor and outdoor units yet have drastically different airflow curves.

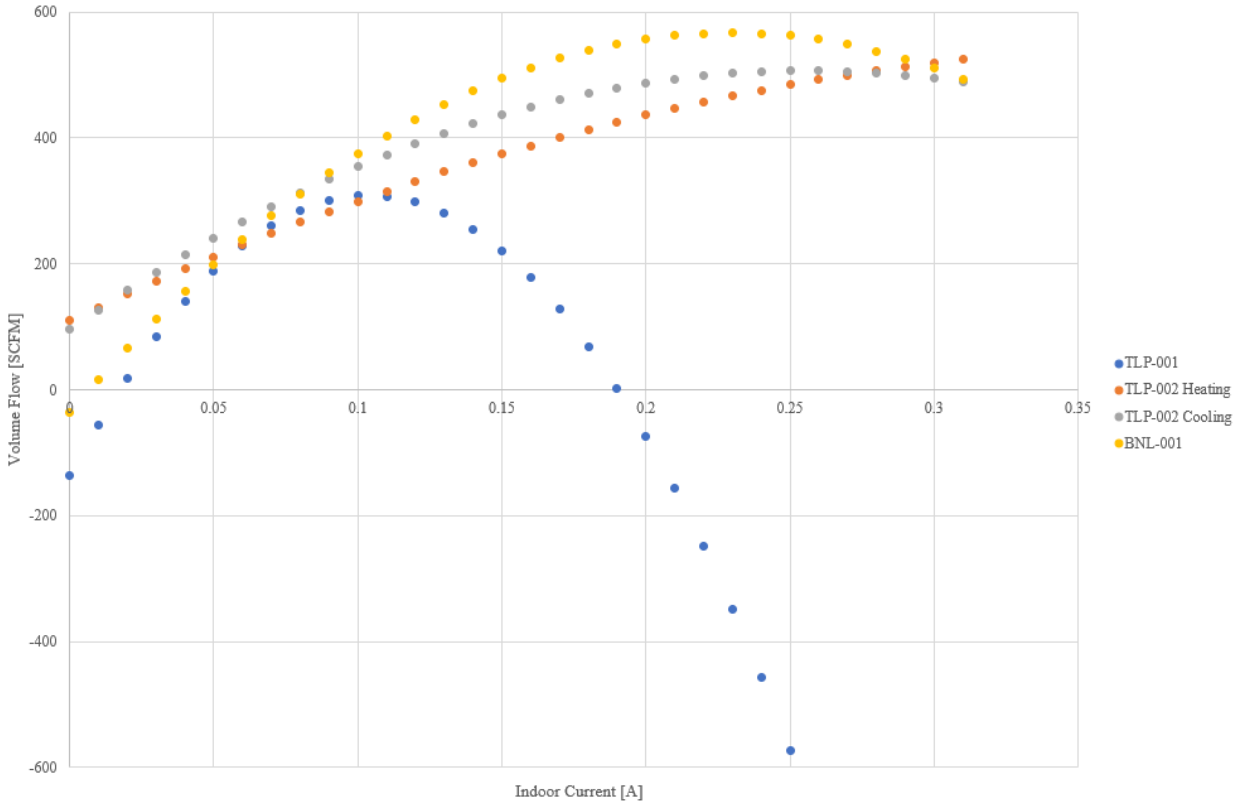


Figure 68: Airflow correlations for identical indoor and outdoor units at sites TLP-001, TLP-002, and BNL-001.

Small differences in the curves are expected, given the different geometries of the conditioned space at the outlet of the unit. However, TLP-001's original flow curve was only valid over a small portion of the dataset; the airflow eventually went negative as higher currents were encountered. To remedy this, the BNL-001 airflow curve was utilized instead. This issue was only detected once reported COPs of less than 1 began to be computed (which has since been corrected). This showcases the need for careful calibration of the airflow curve, as well as the potential need for a redundant measurement for airflow. One such option includes low-cost Microelectromechanical system (MEMS) micro-anemometers, which would fit on either the air supply or return on the unit without obstructing the flow path. The resulting sensor could then be used to calculate average velocity and combined with the geometric information about the heat pump's outlet area, an estimate for the volume flow rate. This would act as a backup measurement to ensure the calculated airflows from the correlation continue to be accurate over the observation period.

## 8.5 Temperature Tolerances and Low Output Modes

Defining specific allowable tolerances has been widely utilized throughout our algorithm in order to determine the device's operation mode, as well as to correct for any errors between sensors. Over the course of the study, proper placement and tight tolerances for the temperature sensors have been indicated to be incredibly important. Almost all the devices studied have operation modes that drop to low output configurations. These configurations typically have a small temperature difference between the supply and return air, usually only 5 °C. Since multiple supply

sensors are required to accurately depict the supply temperature, errors in the temperature measurement are more critical during this period. Originally, BNL had employed a 2 ℃ acceptable difference between these sensors. At the expected high output modes, this results in an insignificant error. At low outputs, the error can be as high as 20%, assuming two temperature sensors are off by this amount. This alone is enough to cause artificially low COPs during periods of low output.

## Summary and Conclusions

The goal of this project was to address the lack of in-field performance data for air-source heat pumps in cold climates—specifically climate Zones 5 – 7. This goal was accomplished by achieving the following key objectives:

- Development of a target range of heat pump types and locations
- Detailed plans for measurement points needed and suitable sensor systems
- Planning for data transfer, management, and quality control checks
- Preparation of detailed protocols for site surveys, instrumentation, and airflow calibration
- In-lab preliminary tests of the measurement protocols
- Establishing IRB protocols for protecting the privacy of participants
- Execution of the planned tests with continuous data review.

This project included data from 21 total sites, including 9 ductless 1:1 installations, 5 centrally-ducted installations, 1 ductless 1:2 installation, one mixed (ductless and centrally-ducted) installation, and 4 air-to-water installations. The results of this study are intended to be used by researchers and manufacturers to inform research and development of energy-efficient heat pump equipment, develop guidelines for optimizing primary energy savings in cold climates, and enable accelerated adoption of air-source heat pumps by designers, installers, state and regional energy efficiency organizations, and building owners.

Overall, the field study unveiled several important notes on the performance of heat pumps during real-world conditions. Defrosting of the outer coil was shown to be a major component of operation in heat pumps in extremely cold climates, as a significant portion of operating time is devoted to removing frost from the outdoor coils. Not only is the heating load not achieved during this time, but power consumption is the same magnitude as when operating in heating mode. More research is needed to determine how to reduce the time heat pumps must operate in defrost mode at colder outdoor temperatures. This may be through optimizing defrost cycle logic, incorporating coatings onto the exterior coils to reduce the possibility of frost accumulation, or incorporating additional resistive heating elements local to the coil. Additionally, the heat pumps showed a decrease in operating hours at milder outdoor temperatures but cycled frequently when they did operate in this temperature range. Further optimization of controls and design sizing criteria may be useful to reduce cycling frequency under mild conditions.

Supply temperature may also need to be considered when implementing heat pumps into existing building infrastructure, as incompatibilities may exist, particularly between air-to-water heat pump output and hydronic distribution systems. Hydronic distribution systems (baseboard radiators) require supply temperatures of 180 to 200 °F, significantly higher than the 130 °F provided by the air-to-water heat pumps. This means that unless existing distribution systems are replaced, air-to-water heat pumps may not be able to be substituted as the sole source of heat in existing buildings. The use of low-temperature baseboards, radiant floors, or high surface emitters are some examples used for low-temperature distribution systems. One article discusses two different options to integrate heat pumps into existing buildings, including 1) lowering the building's design heating load through better insulation, new windows, and reducing air leakage, and 2) adding additional heat emitters to the hydronic distribution system [3].

This study also served as a means of identifying measurement protocols for improving future studies. Future studies should incorporate continuous data checks and several layers of redundancy, as practical, by incorporating backup sensors for fundamental measurements. During long-term field studies, sensors will undoubtedly fail, and homeowner availability is critical in tending to these events. Lastly, the study underscored the need for long-term data collection periods, as they are essential to tease out a variety of different climate and user thermostat set-point conditions.

One site, TLP-002, had several sensors fail, and subcontractors could not enter the home and replace them due to the homeowner being out of the country for several months. Backup measurements not only alleviate this but also provide additional metrics to validate the collected data. With such backup measurements, there can be near zero downtime in data collection between repairs, unlike the often week-long gaps encountered in this current study.

Another site, CEE-001, had its compressor frequency sensor fail and was only able to have its data salvaged due to the presence of a backup measurement for the compressor current. These instances highlight this need for redundancy, but additional measurements of other parameters may also be useful.

For example, ducted sites in particular may benefit from additional refrigerant measurement points such that a refrigerant-side heat balance can be performed. This will help to establish an upper bound on heat output and help with error detection methods, as well as help allow other sites to detect cases where this is combined supplementary heating or solar gain for some sites. Air-to-water heat pump sites were noted to have a much smaller temperature difference between supply and return than their air-to-air counterparts. As a result, they may benefit from utilizing higher-accuracy thermocouples for their measurement.

Four major knowledge areas were designated over the course of the project as indicated by Section 1.3 Approach Overview: 1) Heat Pump Capacity and Efficiency, 2) Capacity Modulation and Installation Sizing, 3) Defrost Mode Energy Usage, and 4) Supply Air Temperature Variation. In addition to answering these key questions, other beneficial results were discovered throughout the project, such as cooling mode trends and field study lessons learned, and are explained within this report. The key questions within each knowledge area were as follows:

### Heat Pump Installed Capacity and COP

- Our findings indicate that steady-state heating COP generally increased with increasing temperature as shown in Table 8. However, only 11 out of the 15 sites that had available performance data matched closely with their rated values. Comparing installation types, centrally ducted sites had the highest COPs at the lowest design temperature and the lowest performance hit with respect to temperature.

- Inclusive heating COP, calculated using transient, steady-state, fan-only, and defrost mode output and consumption measurements, was also calculated and analyzed for the ductless 1:1 sites. Our findings indicate that inclusive COP is less than steady-state COP, as expected, but the extent of the difference is highly site-dependent. This result highlights a key improvement pathway: minimizing non-steady-state operations in order to increase heat pump performance efficiency. Avoiding oversizing and increasing product modulation range are important factors in achieving this.

### Variable-Capacity Modulation and Heat Pump Sizing

- Across the majority of sites, cycling rates (<5 cycles per hour) were observed during sub-freezing temperatures, signifying nearly continuous operation at lower temperatures, intermittently disrupted by defrost intervals. However, cycling rates increased as outdoor temperatures rose above freezing, suggesting intermittent operation during milder conditions. This behavior indicates that some units cannot meet the heat demand on the coldest days. Still, it is important to note that this is by design; installations are typically scaled to meet the average winter temperature. However, there may be room for optimization of the oversizing factor used in cold-climate installations to mitigate the defrost cycle's impact on heating COP or to provide guidance on incorporating backup heating systems to decrease demand on the heat pump on the coldest days. These solutions could enhance the heat pump's performance, minimize cycling events during milder temperatures, and achieve an overall optimized heating strategy.

### Defrost Mode Energy

- At some sites, heating mode cycling rates correspond directly with defrost runtime fraction at temperatures below 32 °F, indicating defrost periods impact steady-state operation, and changes in cycling rate can be used to detect defrost periods. This demonstrates that defrost not only consumes energy but also impacts COP negatively, as it impedes continuous operation. This likely affects user comfort as well.

- An analysis of the defrost runtime fraction showed that defrost mode typically makes up a small fraction of total operational time, less than 4 % for ductless 1:1 and air-to-water sites and less than 10 % for ducted sites, with some caveats. Reducing defrost mode frequency and duration is thus a good pathway for increasing heat pump performance in cold climates.

- Additional analysis showed that the average defrost cycle duration is between 30 seconds and 15 minutes. Therefore, the defrost cycle time can make up a considerable

portion of operation when cycling rates are high. Additionally, as each defrost cycle is followed by a period of transient operation, reducing the frequency of defrost cycles would also have the added benefit of reducing the transient heating mode runtime fraction, further improving performance.

- An investigation of the defrost power consumption indicated the consumption is of the same order of magnitude as steady-state or transient heating, with 12 of 21 sites having power consumption approximately the same as steady-state heating. Therefore, decreasing the defrost mode power requirements could also increase device performance.

## Supply Air Temperature

- Through our examination of heating supply temperatures, we observed that the median supply temperatures were in the range of 90 to 130 °F. Moreover, for most 1:1 non-ducted sites, a decrease in supply temperature was evident as outdoor temperatures increased. This trend was less distinct for ducted and air-to-water sites. Notably, we did not identify a pronounced correlation between outdoor air temperature and supply temperature.

- Ductless sites also had higher supply air temperatures than centrally ducted sites, and air-to-water sites had the highest supply temperatures. However, these temperatures are lower than traditional boilers. Baseboard radiators aren't suitable for air-to-water heat pumps due to lower supply temperatures, impacting their effectiveness. Alternative systems like underfloor heating or low-temperature baseboard radiators are recommended to use air-to-water heat pumps efficiently.

-

## Other Details

- Heat pumps are capable of heating and cooling, but a heat pump installation may be sized to meet the cooling demand instead of heating and require an auxiliary heating source. Some sites in this study utilized their heat pumps predominately for cooling despite being in a “cold climate”.

- The most common setting across all air-to-air sites at design temperatures below 47 °F was either transient or steady-state heating. At 47 °F, the most common setting was off; above 47 °F, the most common setting was ‘Off’ or steady-state cooling.

- Many trends presented themselves, which suggest an installation is oversized. However, this determination is not definitive without performing an energy audit. In future studies, this additional step is highly recommended.

- Future studies should accurately collect and log temperature set-point data to help determine trends. Additionally, user feedback more frequently may be important to understand how heat pumps meet user expectations.

- Our analysis of cooling mode COP showed that performance in cooling mode was higher than in heating mode. The temperature difference between the evaporator and compressor is simply lower in cooling.
- The measured cooling mode COP at each of the nine ductless 1:1 sites in the study exceeded the appliance ratings at 82 °F. Cooling mode COPs decreased or stayed constant with increasing outdoor temperature among ductless 1:1 installations. In contrast, only one of the four centrally ducted sites met or exceeded design expectations at this temperature, and the same trend was apparent, but to a lesser extent.
- The cycling rate data for cooling mode operation showed large site-to-site variations, where some sites showed cycling rates greater than 5 and others less than 1. These results suggest that some sites may better utilize variable speed compressor technology. An analysis of fan speed versus compressor frequency-based output control may be warranted.
- Understanding the reason for cycling may shed additional insights into performance. For instance, cycling may be due to stratification issues and how the controls determine a satisfied temperature or demand.
- Future studies should include additional room temperatures to understand better stratification issues and homeowners' "level of comfort".

# References


[1] US Department of Housing and Urban Development, "Heating Degree Days Database Area Selection," [Online]. Available: https://www.huduser.gov/portal/resources/UtilityModel/hdd.html.

[2] ICC, "2020 ANSI/RESNET/ACCA/ICC 310 Standard for Grading the Installation of HVAC Systems-Design Temperature Limits by State and County, and US Territory," ICC, 2020. [Online]. Available: https://codes.iccsafe.org/content/ICC3102020P1/appendix-a-normative-design-temperature-limits-by-state-and-county-and-u-s-territory.

[3] Frontier Energy Inc. and Owahgena Consulting Inc., "Field Monitoring of Air-to-Water Heat Pumps Retrofitted into Homes," New York State Energy Research and Development Authority, Albany, 2020.

[4] New York State Energy Research and Development Authority, "New Efficiency: New York Analysis of Residential Heat Pump Potential and Economics," NYSERDA, Albany, 2019.

[5] Y. A. Çengel, M. A. Boles and M. Kanoğlu, Thermodynamics: An Engineering Approach, New York: McGraw-Hill Education, 2019.